



Title	Network Design and Performance Evaluation Considering Traffic Growth and Users' Behavior for Optical and Mobile Wireless Networks
Author(s)	金田, 茂
Citation	大阪大学, 2014, 博士論文
Version Type	VoR
URL	<a href="https://doi.org/10.18910/34555">https://doi.org/10.18910/34555</a>
rights	
Note	

*The University of Osaka Institutional Knowledge Archive : OUKA*

<https://ir.library.osaka-u.ac.jp/>

The University of Osaka

Network Design and Performance  
Evaluation Considering Traffic Growth and  
Users' Behavior for Optical and Mobile  
Wireless Networks

Submitted to  
Graduate School of Information Science and  
Technology  
Osaka University

January 2014

Shigeru Kaneda

# List of Publications

## Journal Papers Corresponding to Thesis

1. Shigeru Kaneda, Tomohiko Uyematsu, Naohide Nagatsu, and Ken-ichi Sato, "Network Design and Cost Optimization for Label Switched Multi-Layer Photonic IP Networks", *IEEE J. on Selected Areas in Commun.*, vol.23, no.8, pp.1612-1619, Aug. 2005.
2. Shigeru Kaneda, Tomohiko Uyematsu, Naohide Nagatsu, and Ken-ichi Sato, "Network Design for Multi-Layered Photonic IP Networks Considering IP Traffic Growth", *IEICE Trans. Commun.*, E87-B, no.2, pp.302-309, Feb. 2004.
3. Shigeru Kaneda, Taka Maeno, Mineo Takai, Hirozumi Yamaguchi, and Teruo Higashino, "A Performance Improvement of Large-Scale ITS Wireless System Simulations by Abstract Interference Model", *IPSSJ Journal*, vol. 55, no. 1, Jan. 2014. (in Japanese)

## Conference Papers Corresponding to Thesis

1. Shigeru Kaneda, Tomohiko Uyematsu, Naohide Nagatsu, and Ken-ichi Sato, "Network Dimensioning of Electrical/Optical Label Switched Multi-Layer Photonic IP Networks", in *Proc. 7th European Conference on Network and Optical Communications 2002*, pp. 14-21, 2002.
2. Shigeru Kaneda, Yoshikazu Akinaga, Noriteru Shinagawa, Akira Miura, and Mineo Takai, "Integrated User and Network Simulation for Traffic Control by Influencing User Behavior", in *Proc. 2nd ACM International Workshop on Performance Evaluation of Wireless Ad Hoc, Sensor, and Ubiquitous Networks 2005 (PE-WASUN 2005)*, pp. 99-105, 2005.
3. Shigeru Kaneda, Yoshikazu Akinaga, Noriteru Shinagawa, Akira Miura, "Traffic Control by Influencing Users' Behavior in Mobile Networks", in *Proc. 19th International Teletraffic Congress (ITC19)*, 6a, pp. 583-592, 2005.
4. Shigeru Kaneda, Akihito Hiromori, Yoshikazu Akinaga, Noriteru Shinagawa, Kazuo Sugiyama, and Mineo Takai, "Performance Evaluation

of Network Systems Accounting for User Behaviors”, in *Proc. IEEE International Conference on Communications 2007 (ICC2007)*, pp. 57-64, 2007.

# Abstract

Our society heavily relies on the Internet and the other network services. We use mobile phones all the day, communicate and do businesses by using email and video conferences, and enjoy audio and video streaming services. Also, machine to machine communications play a role on measurements, sensing, or other purposes. All these services are provided through the Internet and the other network systems and services. To handle the expanding demands of communications, network systems need to be built effectively and reliably. Network design and performance evaluation is significantly important to sustain reliable network systems and enrich our society through communications. In this thesis, we focus on how to design and evaluate photonic networks and mobile wireless networks.

Firstly, we propose network design algorithms that minimize the network cost for electrical and optical label switched multilayer Photonic IP networks. Using the developed algorithms, the cost-effectiveness of multilayered photonic IP networks has been evaluated. In fact, compared with LSP networks with point-to-point WDM transmission systems, the benefit of multilayer photonic IP networks is obtained even if the average LSP demand between pairs of nodes is less than the OLSP capacity. The proposed algorithms comprise two steps and the first step provides multiple different optimization start points (initial networks). The optimal result is the best result chosen among the obtained results after multiple optimization procedures. We have verified that most of the results obtained through the multiple different optimization procedures applying different scenarios and subcases converge to almost the same value. This implies that the heuristics developed here could effectively avoid the local minima, and the validity of the obtained results is very high.

Secondly, we newly propose a new network design algorithm that minimizes the network cost considering IP traffic growth for multi-layered photonic IP networks that comprise electrical label switched paths (LSPs) and optical LSPs. We have evaluated the network cost obtained from the developed network design algorithm that considers IP traffic growth and compare it to the results obtained from a static zero-based algorithm. The static zero-based algorithm does not take into account the history of progressive past IP traffic changes/growth until that time. The results show that our proposed algorithm is very effective; the cost increase from the cost obtained using the zero-based algorithm is marginal. The algorithm developed herein enables effective multi-layered photonic IP network design that can be

applied to practical networks where IP traffic changes/increases progressively and that can be used for long term network provisioning.

Thirdly, we propose a traffic control by influencing users, and a user and network integrated simulation which is able to represent individual user behavior in a realistic situation. We also have implemented a real map loading function, pedestrian mobility, and a user behavior model to meet the requirements. We also evaluate the simulation capability, and show that the simulator has high functionality and it is able to represent the effect of individual user behavior (mobility and communication). The results show that the use of a mobility model and communication model which can take account for the different behavior of users does influence the simulation results, and that it is both important and effective to take detailed user behavior into consideration for accurate simulation.

Fourthly, we propose abstraction methods of pathloss and fading calculations to improve simulation runtime for large-scale ITS wireless system simulations. In abstracted pathloss calculation model, we use more of cached pathloss values to improve runtime when a received signal power is less than a threshold. In abstracted fading calculation model, we neglect fading calculation when a received signal power is less than a threshold. We have implemented our proposed methods to network simulator and have evaluated simulation runtime and simulation accuracies with two-ray ground reflection and ITU-R P.1411 models. The evaluation shows that regardless of propagation models about 55% to 70% simulation runtime improvements are achieved with the very limited degradation of simulation accuracies.

In summary, we have proposed multi-layered photonic network design algorithms for a given traffic demand and a growing traffic demand to minimize network cost. Also, we have proposed a mobile traffic control scheme and an evaluation and optimization methods for mobile wireless networks. All proposed methods have been verified through simulation experiments with realistic scenarios. The obtained results show that our proposed methods contribute to design and evaluate photonic and mobile wireless networks, and eventually to enrich our society through communication systems and services.

# Contents

1	Introduction.....	8
2	Related Work .....	13
2.1	Multi-Layered Photonic Network Design.....	13
2.2	Mobile Traffic and System Evaluation .....	14
3	Network Design and Cost Optimization for Label Switched Multilayer Photonic IP Networks .....	16
3.1	Introduction.....	16
3.2	Network Model .....	16
3.3	Design Algorithm.....	18
3.4	Simulations .....	23
3.4.1	Different OLSP Setup Policies .....	23
3.4.2	Further Optimization and Its Validity.....	26
3.4.3	Impact of Physical Network Topology Scale on Cost Reduction...	31
3.5	Conclusion .....	33
4	Network Design for Multi-Layered Photonic IP Networks Considering IP Traffic Growth .....	35
4.1	Introduction.....	35
4.2	Network Model .....	35
4.3	Network Design Algorithm.....	38
4.3.1	Static Design .....	39
4.3.2	Dynamic Design.....	40

4.4	Simulations .....	43
4.4.1	Comparison between static and dynamic design .....	44
4.4.2	Impact of parameter values on the network cost: traffic increase rate, traffic distribution, and network topology .....	46
4.5	Conclusion .....	49
5	Performance Evaluation of Network Systems Accounting for User Behaviors 50	
5.1	Introduction.....	50
5.2	Traffic Control by Influencing User Behavior.....	50
5.2.1	Concept .....	50
5.2.2	Control Scheme.....	52
5.3	User and Network Simulator.....	53
5.3.1	Concept .....	53
5.3.2	Functional Requirements .....	54
5.4	Implemented Functions.....	55
5.4.1	Real Map Loading Function .....	55
5.4.2	Pedestrian Mobility Model.....	56
5.4.3	User Behavior Model.....	59
5.5	Evaluation and Validation of the Simulator.....	61
5.5.1	Evaluation of the Mobility Models .....	62
5.5.2	Evaluation of Communication Behavior Model .....	66
5.6	Conclusion .....	72
6	A Performance Improvement of Large-Scale ITS Wireless System Simulations by Abstract Interference Model .....	73

6.1	Introduction.....	73
6.2	Simulation of an ITS wireless system.....	74
6.3	Abstract model .....	77
6.3.1	Speeding up pathloss calculations.....	77
6.3.2	Speeding up fading calculations.....	79
6.4	Performance evaluation.....	81
6.4.1	Simulation scenario.....	81
6.4.2	Effect of the pathloss calculation optimization.....	84
6.4.3	Effect of the fading calculation optimization.....	88
6.4.4	Effects of applying both the pathloss calculation and fading calculation optimizations .....	91
6.5	Conclusion .....	98
7	Conclusions.....	100
	Appendix.....	102
	Acknowledgement .....	104
	Bibliography .....	105

# 1 Introduction

Our society heavily relies on the Internet and the other network systems and services. We use mobile phones all the day, communicate and do businesses by using email and video conferences, and enjoy audio and video streaming services. Also, machine to machine communications play a role on measurements, sensing, or other purposes. All these services are provided through the Internet and the other network systems and services. To handle the expanding demands of communications, network systems need to be built effectively and reliably. Network design and performance evaluation is significantly important to sustain reliable network systems and enrich our society through communications. Furthermore, network systems are basically comprised of backbone networks and access networks. Backbone networks are mainly built with photonic networks which provide huge bandwidth and less latency. On the other hand, access networks are mainly provided by wireless networks which can avoid limitation of mobility and wiring. In this thesis, we focus on how to design and evaluate photonic networks and mobile wireless networks. We propose design and evaluation methods for multi-layered photonic networks as well as mobile wireless networks.

Firstly, we describe a multi-layered photonic network design for a given traffic demand. An explosive increase in the amount of Internet traffic has been evident spurred by the increased penetration of broadband access to date. To cope with this, how the most effective future Internet protocol (IP) backbone networks should be created is a key topic that must be resolved [1], [2], [3], [4]. Looking at existing IP backbone networks, wavelength-division-multiplexing (WDM) technology is used in order to better utilize the transmission capability of an optical fiber. Current commercially available WDM systems allow for the multiplexing of several dozens of wavelengths. Such WDM transmission systems are denoted as point-to-point WDM systems in the sense that all the wavelengths are terminated link-by-link and the required electrical signal processing is performed utilizing an electrical switching element at each intermediate node. Rather expensive optical/electrical conversions are, therefore, necessary at each node. With regard to IP packet transmission, packets are encapsulated using a data link protocol such as PPP/HDLC-over-SONET/SDH (POS) [5]. Since each IP packet is routed at each intermediate node based on the information in its header, this will cause severe header processing bottlenecks in the IP backbone network nodes, which must process more than several hundreds of gigabits of data.

In order to mitigate the processing bottlenecks and to realize effective traffic engineering, multiprotocol label switching (MPLS) [6] has been proposed as a viable transport mechanism. This can provide cut-through of Layer 3 routing, i.e., a label switched path (LSP) is introduced, by adding a fixed-size label to each IP packet. The label provides a routing identifier recognized by high-speed electrical switches, e.g., label switches such as an asynchronous transfer mode (ATM) switch. Many of the state-of-the-art IP backbones employ label switch routers (LSRs) that are equipped with this label switching capability. However, the forwarding processing is still based on electrical processing, i.e., LSP level routing, at each intermediate node. As such, when the traffic volume to be processed becomes much larger, electrical bottlenecks will become increasingly tangible.

In order to solve this problem, the introduction of optical cross-connects (OXC) that employ wavelength routing has been widely discussed [1], [7], [8], [21]. Furthermore, the extension of the control mechanisms of MPLS and generalized MPLS (GMPLS) [9] to OXC control has also been studied to integrate an IP and optical control mechanism [10], rather than to use separate controls for the IP and optical layers. The optical LSP (OLSP) discussed herein is an optical path in which connection setup/release is controlled by using the GMPLS mechanism. In this thesis, the IP backbone network is denoted as the photonic IP network, which employs wavelength routing achieved through the capability of OLSPs. We clarify the benefits of the Photonic IP network through quantitative evaluations regarding the transport network cost.

We present a newly developed multilayered (LSP/OLSP) network design method that minimizes the network cost, i.e., the optimal network design for a given LSP traffic demand. Other purposes of this thesis are to elucidate the potential benefits of the multilayered photonic IP network employing OLSPs, and to estimate the impact on the network cost reduction toward physical network topologies and traffic volumes. The particular point of the algorithms proposed in this thesis is that they adopt different cost minimization scenarios in accordance with different OLSP provisioning conditions, which are chosen as the first step in the design stage. This approach effectively removes local minima and enhances the reliability of the obtained results in terms of the optimization. In other words, the validity of the obtained results can be judged as quite reliable when the best achievable cost among different scenarios and their subcases are very close to each other.

Secondly, we describe a new network design considering IP traffic growth for multi-layered photonic IP networks. As traffic demands are expanding, network operators need to upgrade their network systems to handle traffic growth. For instance, at a certain point of the year, for example every quarter, we evaluate the

traffic growth until the end of the next quarter, and add the necessary equipment to the working network based on the dynamic network design. The design method directly affects network cost because the deployed equipment may not be used. Therefore, we propose a new network design algorithm that minimizes the network cost considering IP traffic growth for multi-layered photonic IP networks. We evaluated the network cost obtained from the developed network design algorithm that considers different IP traffic growth patterns and volumes. The obtained results are compared with those obtained from the static zero-based algorithm that we proposed. It was shown that the presented algorithm is effective; the cost increase from that cost obtained with the static algorithm was marginal. Furthermore, under various conditions (physical network topology, traffic demand, and the traffic increase rate), the proposed algorithm was confirmed to produce excellent results.

Thirdly, we describe a traffic control method and an evaluation method. In mobile networks, users carry mobile terminals, and make or receive calls whenever they want. Therefore, the generation of communication traffic is heavily dependent on user behavior. Also, user mobility and communication behavior are strongly influenced by environmental factors associated with the user (street layout, weather, and special events, such as fireworks displays or football matches). For instance, when a user walks in a crowded area like a fireworks display, he or she may not take the shortest route to the destination, but rather may select a route which is less busy, to avoid the crowds. In the case where many people are gathered in a small area causing network congestion, they may reattempt calls repeatedly at short intervals until they are successful [43], [48], [49]. Moreover, even if different people are in the same environmental situation, their communication behavior, such as interval between retries, differs according to certain attributes (gender, age and so on). Therefore, in mobile networks, we can state two issues: 1) the traffic that flows into a mobile network is heavily dependent on user behavior and the quality of service resulting from the condition of the network greatly influences user behavior, 2) individual users may behave differently according to certain attributes, such as age.

In order to evaluate the performance of mobile networks, network simulation is widely used. For example, we have proposed a traffic control method that guides users, to alleviate congestion by giving them information about the network [55], [56]. In this method, the network sends users one of three guidance messages according to the state of the network congestion. These messages are A) to encourage users to wait, to achieve time balancing, B) to encourage user to change communication medium (for instance, from phone call to text messaging), and C) to encourage users to move, to achieve geographical balance. This traffic control method aims to improve not only network performance but also the quality of

service users perceive, and so ultimately to increase customer satisfaction. It is quite difficult to evaluate the performance of such a method in the field and therefore evaluation by means of simulation is useful. To evaluate such a control method through simulation, it is necessary for the simulator to represent both the behavior of individual users and the degree of customer satisfaction with the network service provided.

In this thesis, we describe the development a simulator as a platform for performance evaluation corresponding to various applications and services. We have developed a large-scale simulator which can more faithfully represent the network (which offers communication services), users (who are the source of traffic), and the environment (which influences user behavior). Using the simulator we developed, we also evaluate the network systems by the communication logs and a survey of cellular phone customers. The simulation results obtained show that the developed simulator has high functionality and it is able to represent detailed individual user behavior (mobility and communication) and evaluate performance in a realistic situation.

Fourthly, we describe a performance improvement method for large scale wireless networks. In recent years, research and development is underway on wireless communication systems for the Intelligent Transport System (ITS), which aims to realize safe driving support, platoons, and information delivery to vehicles. In this R&D, it is necessary to evaluate the performance of a large-scale system under a variety of scenarios. Simulation-based evaluation is effective in the early stage of research. Later, in the development stage in which a realistic system is in sight, it is more effective evaluate system performance using a prototype system or a combination of a prototype system and a simulator which are linked via a virtual network and operate in an integrated manner.

There are a large number of simulators, both commercial and non-commercial, for evaluating performance of a wireless communication system. It is reported that how a system is modelled has a great impact on the accuracy of simulation [68], [69]. Assumptions are made to model the target system. In particular, in simulation of wireless communication, how radio propagation and the physical layer are modelled greatly affects evaluation of system performance [70], [71]. In an IEEE802.11 wireless LAN system, all nodes that share an identical channel monitor the state of the channel, and avoid collision using carrier sense multiple access/collision avoidance (CSMA/CA). In the ITS, SAE J2735 [72] specifies a mechanism in which each vehicle broadcast its information every 100 milliseconds to let surrounding vehicles know its presence. When a node transmits a frame in an ITS wireless system that uses such a wireless LAN system, all the surrounding

nodes, including those that are not destinations of the frame, process the frame received. In simulation of a large system of this kind, the processing of received frames requires a huge amount of computation. To simulate such a system efficiently, it is important to use a system model that strikes a good balance between the amount of computation required and simulation accuracy [73]. Therefore, we propose a performance improvement method for large scale wireless networks and evaluate the proposed methods in several situations.

The rest of this thesis is organized as follows. In Chapter 2, we address the related work and contributions of our study. In Chapter 3, we describe the network design and cost optimization method. In Chapter 4, we propose a network design algorithms considering IP traffic growth. In Chapter 5, we describe mobile traffic control scheme and system evaluation method. In Chapter 6, we propose performance optimization method for wireless communication system evaluation. Chapter 7 concludes this thesis.

## 2 Related Work

### 2.1 Multi-Layered Photonic Network Design

In this section, we describe related works and our contributions on multi-layered photonic network design. The design of the networks we are considering requires solving both routing and wavelength assignment optimization problems [4], [8]. Most of the previous studies that deal with OXC-related network design were aimed at optimization of the optical layer by taking into account optical path routing and the wavelength assignment [11], [12] [13], [14], [15]. They deal with single-layer network optimization, whereas this thesis resolves multilayer network optimization, where an OLSP accommodates multiple (electrical) LSPs. In other words, the traffic to be accommodated within the network is given by the LSP demand matrix rather than the OLSP demand matrix. Although the study area of this thesis is dedicated to hierarchical LSP networks where the  $n:1$  relationship between LSP and OLSP is considered, other types of hierarchical networks have been extensively studied in, e.g., [16] [17], [18], [26], [27], [28]. The objective of [16] and the network conditions are different from this work; to improve the network throughput under given optical network resources, while enforcing constraints on one pair of fibers between nodes. Other papers [17], [18] assumed multilayer networks comprising waveband and wavelength multiplexing. Each waveband can accommodate a fixed set of wavelengths, which set more restrictions on the wavelength assignment. Our objective is to minimize the network cost for a given amount of LSP traffic for the photonic IP networks consisting of LSP and OLSP layers. Our study, thus, focuses on different objective functions under different network conditions.

Regarding the optimization of a network that includes routing and wavelength assignment, the problem is known to be NP-complete [19]. An approach using integer linear programming (ILP) [16], [41] is only applicable to small networks due to the large calculation time required; hence, the application of the ILP is rather limited. Therefore, an approach employing heuristic algorithms is widely considered for designing practically sized networks.

There are some previous studies that deal with dynamic design of photonic networks [23], [24] They, however, assume a single optical layer network aimed at optimization of the optical layer by taking into account optical path routing and wavelength assignment. In this thesis, instead, the traffic to be accommodated within the network is given by the LSP demand matrix rather than the OLSP

demand matrix. Some studies include quasi-dynamic design for multi-layered photonic networks [29], [30], [31]. They are considering service holding time to design and expand network system. These works extends our works and are basically done based on our primary work in the thesis.

Some related works consider restoration or sustainability for multi-layer photonic networks [32], [33]. They introduce extra demands for restoration of optical paths. The studies in [34], [35], [36], [41], [45], [46] deal with waveband switching and assignments. Other studies in [37], [38], [39], [42], [44] deal with network design for multi-layered photonic network. However, they rely on our previous work as fundamental design method and extend or add new limitation for design. Therefore, we could significantly contribute our work to the field of multi-layer network design and facilitate the research activities.

## 2.2 Mobile Traffic and System Evaluation

Recently there have been some studies on simulation techniques which consider user mobility for mobile networks, such as the verification of the random waypoint model, which is often used to evaluate network performance, and the development of realistic mobility models [57], [58], [59], [60]. However, there have been few reports that consider detailed network simulation to deal with both issues 1) the traffic that flows into a mobile network is heavily dependent on user behavior and the quality of service resulting from the condition of the network greatly influences user behavior, and issue 2) individual users may behavior differently according to certain attributes such as gender and age. For the performance evaluation of mobile networks, we have proposed the concept of a user and network integrated simulation capable of dealing with both issues 1) and 2) and showed the importance of such a simulation [56].

Regarding wireless network simulation, network simulators have been compared and monitored in terms of runtime performance and required memory size [74], [75], [76]. There have been proposals [77], [78], [79] to speed up simulation of a wireless network by focusing on MAC of IEEE802.11. The technical area targeted by these papers differs from the area addressed by this thesis, which focuses on pathloss and fading calculations. Therefore, the methods proposed by these papers can be combined with the method proposed in this thesis. References [80] and [81] discuss simulation of a Long Term Evolution (LTE) system and a mechanism to speed up simulation. They aim to reduce fading calculations in a cellular system that is based on orthogonal frequency division multiple access (OFDMA). The wireless system assumed in these papers differs from the one assumed in this thesis.

The interference from a fixed base station assumed by these papers also differs from the one assumed in this thesis, which assumes that all communication nodes are mobile. Therefore, the mechanism proposed in these papers cannot be applied to the environment addressed in this thesis. There are studies on making simulation faster at the radio propagation layer [82], [83], [84]. Their results have been implemented in some commercial and non-commercial simulators. A basic approach to reducing the computational load is to use an abstract model. One method is not to register a reception event to a node in cases where the power of the received signal is lower than a specified threshold or where the receiving node is located farther than a specified threshold distance from the transmitting node. Another method is to use the signal to interference plus noise ratio (SINR) estimated from past data, in processing a reception event. Both of these approaches reduce computation time by omitting to process some reception events. Since determination of whether to process a reception event or not depending on the SINR, the impact of the SINR value on simulation result is not insignificant.

Since the use of an abstract model impacts simulation accuracy, there is a tradeoff between speed and accuracy. In this thesis, we propose an abstract model that focuses on pathloss calculations and fading calculations in order to speed up simulation with a minimum impact on simulation accuracy. The number of pathloss calculations is reduced by using cached pathloss values when the received signal power is below a threshold. Similarly, the number of fading calculations is reduced by omitting the calculation when the received signal power is below a threshold.

# 3 Network Design and Cost Optimization for Label Switched Multilayer Photonic IP Networks

## 3.1 Introduction

An explosive increase in the amount of Internet traffic has been evident spurred by the increased penetration of broadband access to date. To cope with this, how the most effective future Internet protocol (IP) backbone networks should be created is a key topic that must be resolved. In this chapter, we clarify the benefits of the Photonic IP network through quantitative evaluations regarding the transport network cost. In this chapter, we present a newly developed multilayered (LSP/OLSP) network design method that minimizes the network cost, i.e., the optimal network design for a given LSP traffic demand. Other purposes of this chapter are to elucidate the potential benefits of the multilayered photonic IP network employing OLSPs, and to estimate the impact on the network cost reduction toward physical network topologies and traffic volumes. In the following sections, we first present the optimal network design algorithms of multilayered photonic IP networks using two layers of paths, LSP and OLSP. The network cost of the LSP network (single layer) is then compared with that of the designed photonic IP network (multilayer, i.e., LSP and OLSP) to demonstrate the benefits of introducing OLSPs.

## 3.2 Network Model

Figure 3-1 illustrates the photonic IP network and the node structure discussed in this chapter. The node consists of three functional elements: the OXC, OLSP terminator, and LSR. The LSR consists of an IP router controlled by the MPLS mechanism. At the ingress of the OXC, WDM signals from adjacent nodes are demultiplexed into each wavelength (optical path). Some of the optical paths (OLSPs) that must be terminated at the node will be delivered to the OLSP terminator and the corresponding OLSPs are converted into electrical signals. The LSPs accommodated within the terminated OLSPs are switched by a LSR, where packet-by-packet forwarding is done based on the LSP label information. The other

OLSPs are cross-connected at the optical level at the OXC. At the egress of the OXC, OLSPs are wavelength multiplexed and launched into the outgoing fibers.

The relationships among the IP packets, LSP, OLSP, and optical fiber are shown in Figure 3-2. LSPs are logical paths with a variable bandwidth identified by a label attached to each IP packet. An OLSP is an optical path that has a fixed bandwidth and is identified by the wavelength. An OLSP accommodates a number of LSPs, and such a relationship is the same as that of higher order and lower order paths in the SDH networks [20]. The optical fiber accommodates a fixed number of OLSPs.

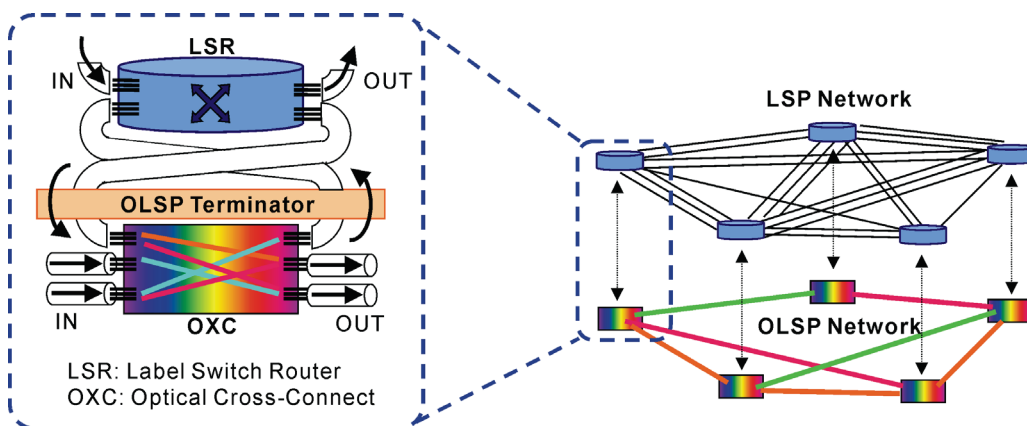


Figure 3-1. Photonic IP network and node structure.

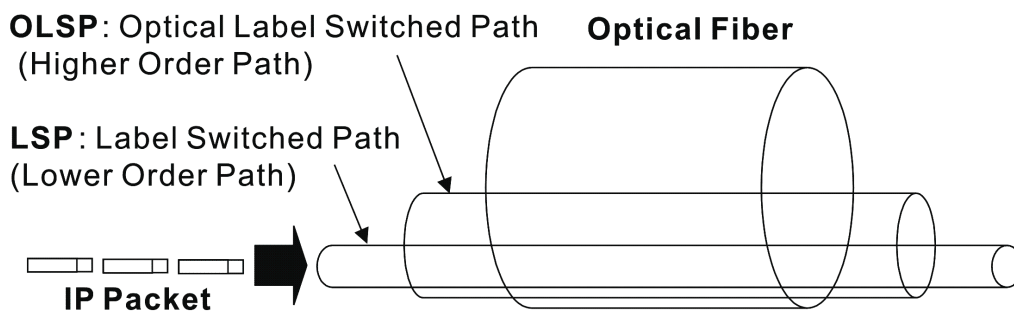


Figure 3-2. Relationships among IP packets, LSP, OLSP, and optical fiber.

### 3.3 Design Algorithm

The developed algorithm comprises two steps as described next.

Step 1) Set up direct OLSPs as per the given policy (given later) without regard for LSP level grooming at intermediate nodes.

Step 2) Reconfigure the network developed in Step 1 allowing for LSP level grooming at intermediate nodes.

Step 1) creates initial networks that should be optimized in Step 2). In Step 1), different policies to set up direct OLSPs are, as mentioned before, introduced so that multiple initial networks are developed. Each initial network, created with a different policy (represented by parameter  $X$ , as explained later), is optimized by Step 2), where different cost minimization scenarios in accordance with different OLSP provisioning policies in Step 1) are chosen. The best result among the results from Step 2) is selected as optimal. Through this process, the criterion of the OLSP setup policy according to the network conditions is obtained. This approach can effectively remove the local minima and enhances the reliability of the obtained results in terms of the optimization, since multiple different starting points are used to attain the goal. For these two steps, heuristic algorithms were developed. The outline of the design algorithm is given below.

Here, we assume the following.

- No wavelength conversion capability at intermediate nodes (wavelength path [1]).
- An OLSP shall be set up as per various OLSP setup policies.
- The data traffic distribution pattern is asymmetrical.

When the traffic pattern is symmetrical, the algorithms described next can also be applicable. For symmetrical traffic, the calculation time can be reduced with a slight modification to the calculation process.

Each step is described as follows.

Step 1:

1) Given a defined LSP demand, search the shortest LSP routes (Dijkstra algorithm), supposing a weighted link and node cost.

2) Add an OXC at each node.

- 3) Select a node pair to examine the possible provisioning of a direct OLSP, based on the selection criterion, explained below.
- 4) Establish a direct OLSP along the route of the bundle of LSPs and assign a wavelength to it according to different policies. The policies are represented by parameter. The total bandwidth of the LSPs to be accommodated within the OLSP exceeds  $X\%$  of the OLSP capacity.
- 5) Iterate 3 and 4 so long as non-accommodated LSPs exist that meet the above criterion.
- 6) Accommodate the remaining LSPs within point-to-point OLSPs.

In 3 above, we adopt a simple rule [14] that determines the priority for the OLSP provisioning. The highest priority is given to a node pair that is determined by the value  $\max\{H_{ij} \times P_{ij}\}$ , where  $H_{ij}$  is the number of hops between node  $i$  and node  $j$ , and  $P_{ij}$  is the number of LSPs from node  $i$  to node  $j$ . The procedures included in Step 1 are explained in Table 3-1 and Figure 3-3.

**Table 3-1. Parameters incorporated in design algorithm.**

Input	Physical network topology, LSP traffic demand
Parameters	OLSP setup policy, node/link cost, etc.
Output	Total network cost, LSP route, OLSP routes, OLSP wavelengths

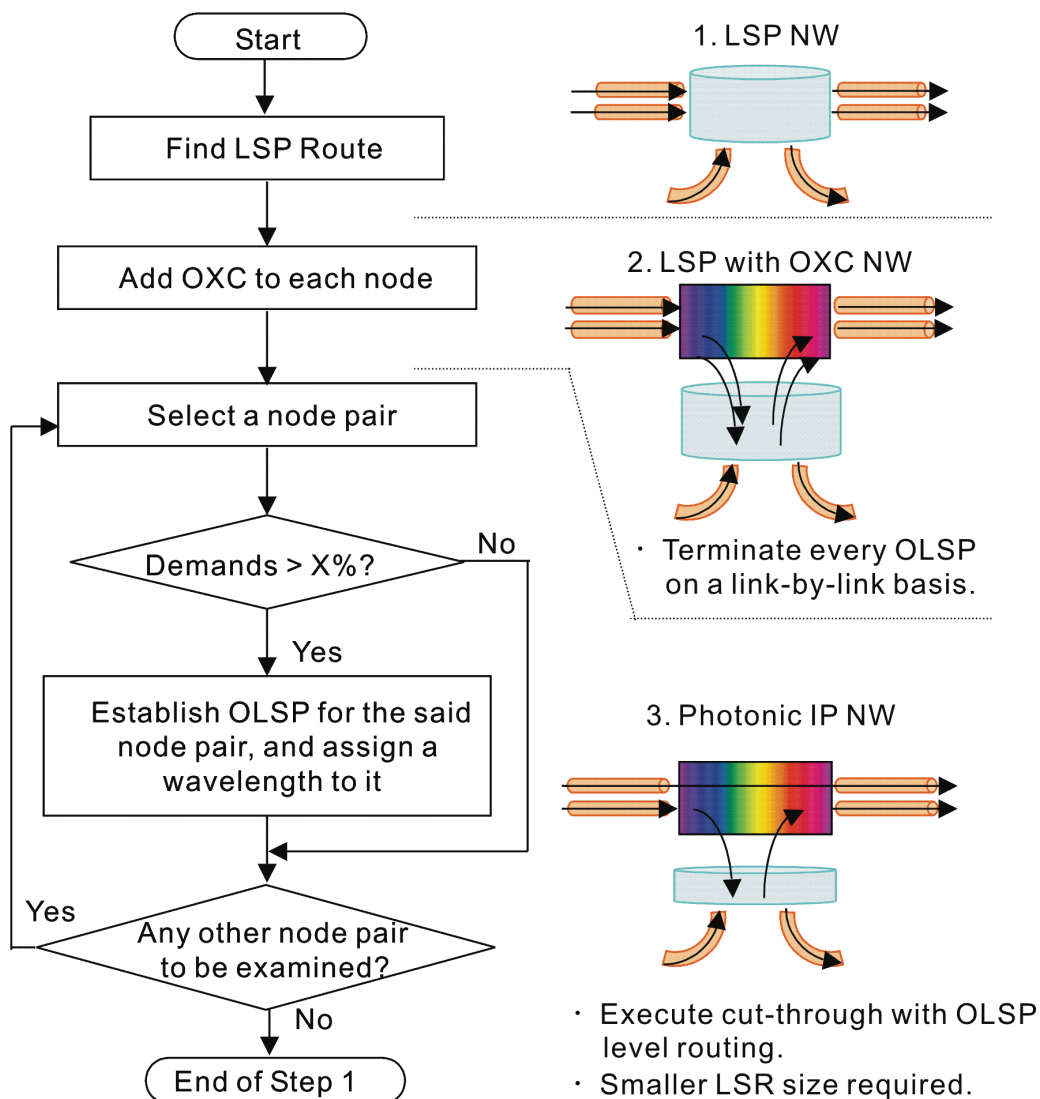
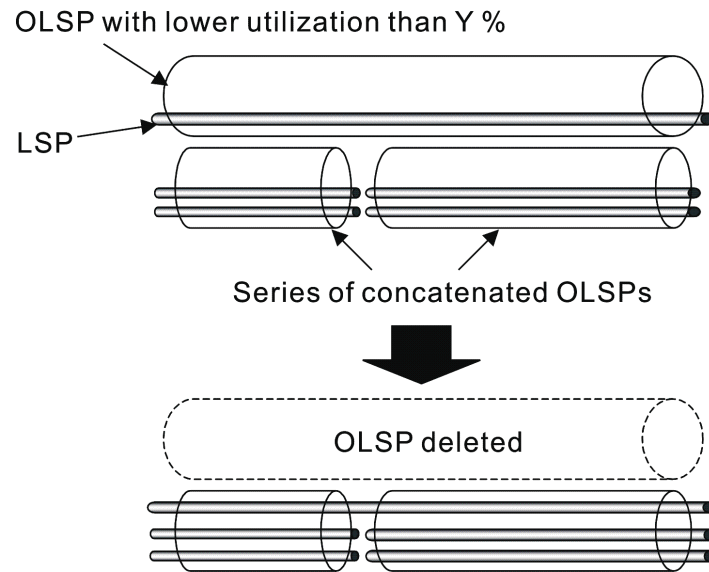


Figure 3-3. Outline of Step 1 design algorithm.

Step 2: Step 2 is a further optimization process that is taken after Step 1. Since some of the LSPs are accommodated within point-to-point OLSPs and some of the established direct OLSPs may have spare bandwidth irrespective of the chosen policies, further cost reduction can be expected by rearranging LSPs. These are detailed as Scenario A and Scenario B below, selected according to the value of  $X$ . Taking this approach, the spare OLSP bandwidth is effectively used by allowing for LSP level grooming at intermediate nodes. The LSPs can be accommodated using more than two OLSPs, and the LSPs may take a different route from the

original one, if the total cost can be reduced. According to the value of  $X$  in Step 1, two different scenarios are developed to achieve further cost reduction, i.e., Scenario A and Scenario B. These two scenarios are outlined as follows, and are depicted in Figure 3-4 and Figure 3-5.



**Figure 3-4. Procedure in Scenario A.**

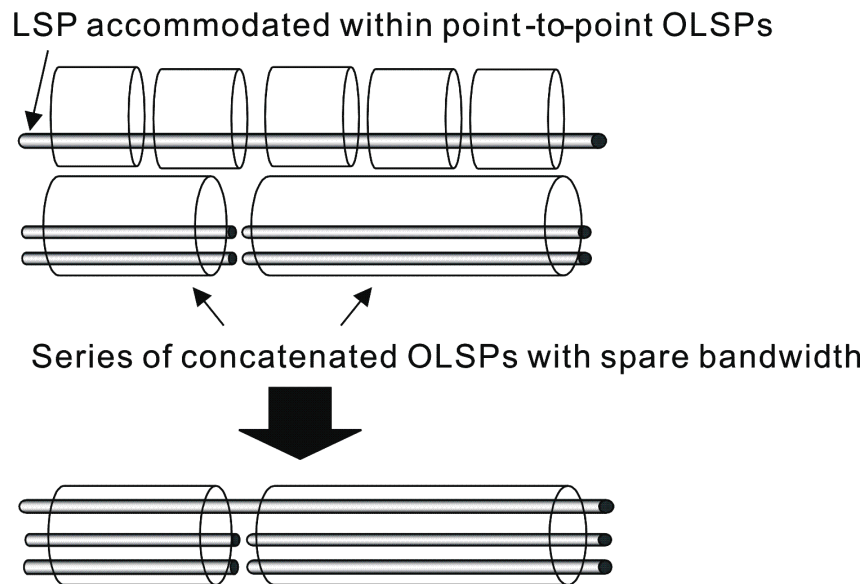


**Figure 3-5. Procedure in Scenario B.**

Scenario A: Establish OLSPs for  $X = 0$  in Step 1, and then reconfigure the OLSP network by executing Step 2, the procedure for which is given next.

- 1) Extract OLSPs with a bandwidth utilization lower than  $Y\%$  (parameter).
- 2) Reaccommodate the LSPs that are accommodated within such extracted OLSPs using the spare bandwidth of the remaining consecutive two or more OLSPs.

This procedure causes changes in the network element resource requirements, as shown in Table 3-2.

Scenario B: Establish OLSPs for nonzero  $X$  in Step 1, and then reconfigure the OLSP network by executing Step 2, the procedure for which is given next.

- 1) Find LSPs accommodated within concatenated multiple point-to-point OLSPs with three hops or more. Alternatively, find a series of established OLSPs that can afford to accommodate more LSPs.
- 2) Accommodate such LSPs within the existing OLSPs by using their available spare bandwidth.

This procedure causes changes in the network element requirements, as shown in Table 3-3.

The range of  $X$  in Step 1 is from 0 to 1. Then, Scenario A covers all cases for  $X=0$  and Scenario B covers all cases for  $X \neq 0$ . Therefore, Scenario A and Scenario B are adequate further optimizations for our Step 1 design.

**Table 3-2. Changes in network element resource requirements in Scenario A.**

OXC	Number of required ports	↓
LSR	Number of required ports	↑
Optical fiber	Number of required wavelength	(↓)

↓ : Decrease, ↑ : Increase, (↓) : Occasionally decrease.

**Table 3-3. Changes in network element resource requirements in Scenario B.**

OXC	Number of required ports	(↓)
LSR	Number of required ports	↓
Optical fiber	Number of required wavelength	(↓)

↓ : Decrease, (↓) : Occasionally decrease.

## 3.4 Simulations

The cost-effectiveness of the multilayered photonic IP network was evaluated by simulation using the developed algorithms. We generated a network cost model that consists of node and link costs on the basis of state-of-the-art technologies. The details are provided in the Appendix.

### 3.4.1 Different OLSP Setup Policies

In order to evaluate roughly the benefits of the photonic IP networks against LSP networks and to determine the relationship between the traffic volume and the appropriate policy, a basic cost comparison was done where only Step 1 was run for the dimensioning of the photonic IP network. We here used the regular grid topology for the simulations. The reason we adopted this was to remove the influence of a particular topology and to obtain more general results. The grid topology is commonly used in many papers for evaluation.

In this simulation, the following network models are assumed.

- Physical network topology: Polygrid (3×3, 5×5, 7×7, etc.).

- LSP demand: Random pattern.
- Average one-way traffic intensity: 0.5–7.5 Gb/s (changed in 0.5-Gb/s increments) per node pair.

Three OLSP setup policies were examined: establish an OLSP: 1) if any LSP demand exists,  $X = 0$ ; 2) if the LSP demand exceeds 50% of the OLSP capacity,  $X = 50$ ; or 3) if the LSP demands exceeds 100% of the OLSP capacity,  $X = 100$ . We examined 30 random traffic patterns for each traffic intensity level. At each level, the cost ratio of the photonic IP network to the LSP network is calculated over the 30 traffic patterns, and the average ratios are plotted. The results obtained for  $5 \times 5$  network is shown in Figure 3-6.

The obtained results are summarized next.

- The photonic IP network is less expensive than the LSP network at higher traffic intensity levels, such as more than approximately 2.0 Gb/s, and its effectiveness becomes more significant as the traffic intensity increases.
- There is a trend change point around 2.5 Gb/s and 3.0 Gb/s. That is because we assume that OLSP capacity is set to be 2.5 Gb/s and related port costs are calculated per 2.5 Gbps. The network cost trend varies whether an OLSP is established or not.
- For instance, if the traffic intensity is 5.0 Gb/s and 7.5 G/s, then 30% and 45% cost reductions are achieved using the photonic IP network, respectively.
- $X = 50\%$  is the most cost-effective, whereas  $X = 0\%$  and  $X = 100\%$  are more expensive by a few percent and more than 10%, respectively.

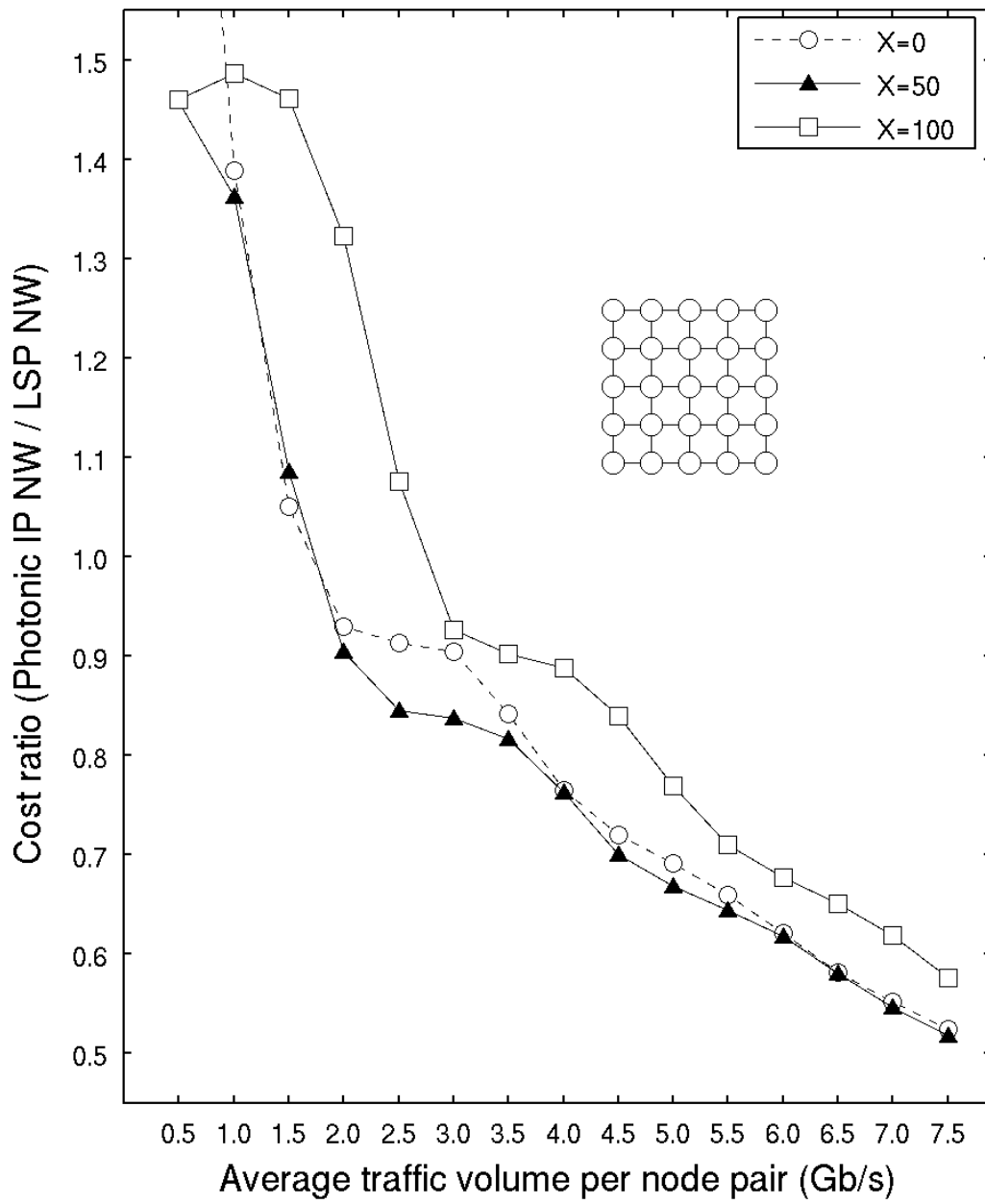


Figure 3-6. Network cost obtained from Step 1.

### 3.4.2 Further Optimization and Its Validity

The following discusses further cost reduction, which is attainable through Step 2 procedures. All simulation parameters except OLSP setup policies are the same as those in the previous section.

As mentioned previously, two scenarios were tested. A variety of design parameters, such as  $X$  in Step 1 and  $Y$  in Step 2 of Scenario A, or different algorithms of Scenario B, were tested. The reason for this is to obtain confidence in the obtained results, if the best achievable cost for each scenario is almost equal, then the validity of the results can be assured.

In Scenario A, we select two values for  $Y$  in Step 2, namely,  $Y = 25$  and  $50\%$ . In addition, we assumed two cases in terms of routing restrictions.

A1) A LSP route contained in a removed OLSP cannot be changed.

A2) A LSP route contained in a removed OLSP can be changed.

In all, we tested four cases in Scenario A.

In Scenario B, we selected two OLSP setup criteria in Step 1, i.e.,  $X = 25$  and  $50\%$ . In addition, we examined four different algorithms for the OLSP network reconfiguration in Step 2.

They are given next.

B1) Choose a direct OLSP with spare bandwidth and find LSPs accommodated within a series of point-to-point OLSPs that share partially or entirely the same route as the said OLSP.

B2) In the above, give higher priority to the LSPs that have the same ingress or egress node as that of the candidate, and then try to reroute using the candidate OLSP.

B3) Choose the LSPs accommodated within point-to-point OLSPs, and find two concatenated OLSPs that span the same route as that of the said LSP.

B4) In the above, find two concatenated OLSPs, the route of which is not necessarily the same as that of the said LSP.

After the simulations of the four cases in Scenario A and eight cases in Scenario B, as shown in Figure 3-7, Figure 3-8 and Figure 3-9 (these are for a  $5 \times 5$  network), assuming the same network model, the following results were obtained

- The best achievable cost of Scenario A is almost the same as that of Scenario B.
- For instance, if the traffic intensity is 5.0 Gb/s and 7.5 G/s, then the cost reductions of 35% and 49% are achieved with the photonic IP network, respectively.
- Among various simulation results, the best one for each simulation point is selected as the optimal; the result as the optimal is expected to be very reliable, since results from different optimization strategies based on various scenarios (Figure 3-7, Figure 3-8 and Figure 3-9) converge.
- The algorithm developed here is based on heuristics, and as a result, the calculation time needed is acceptably short. It takes in the order of a minute for each traffic intensity value to reach the optimal value which is the one selected from results of the multiple different optimization procedures for a network with 50 nodes or more. (OS: Linux, CPU clock: 1.5 GHz).

By testing different scenarios and their subcases described above, the confidence in the obtained results is enhanced; the local minima can be removed and the validity and the generality of the obtained results are significantly improved.

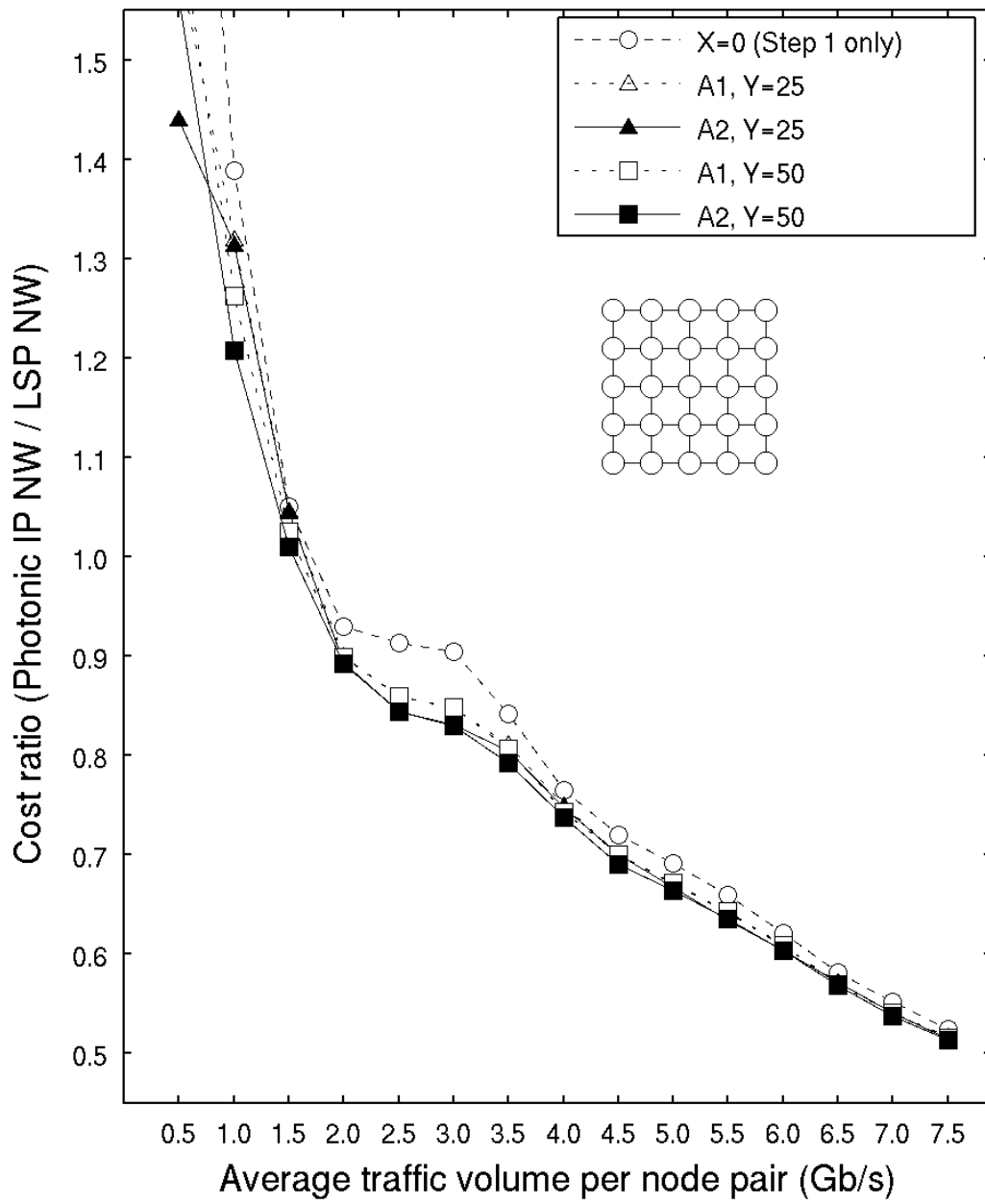


Figure 3-7. Network cost obtained from Scenario A.

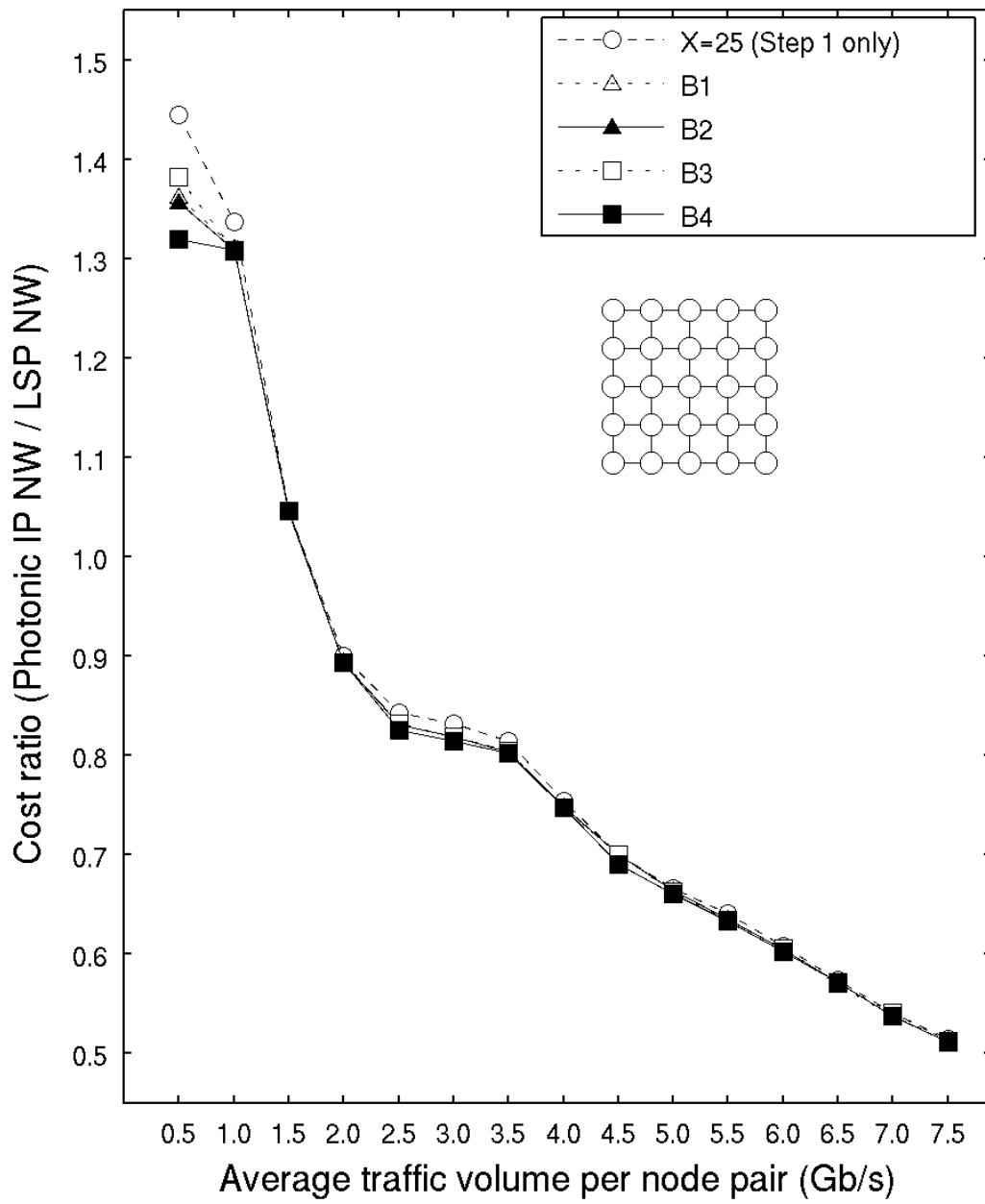


Figure 3-8. Network cost obtained from Scenario B (X = 25).

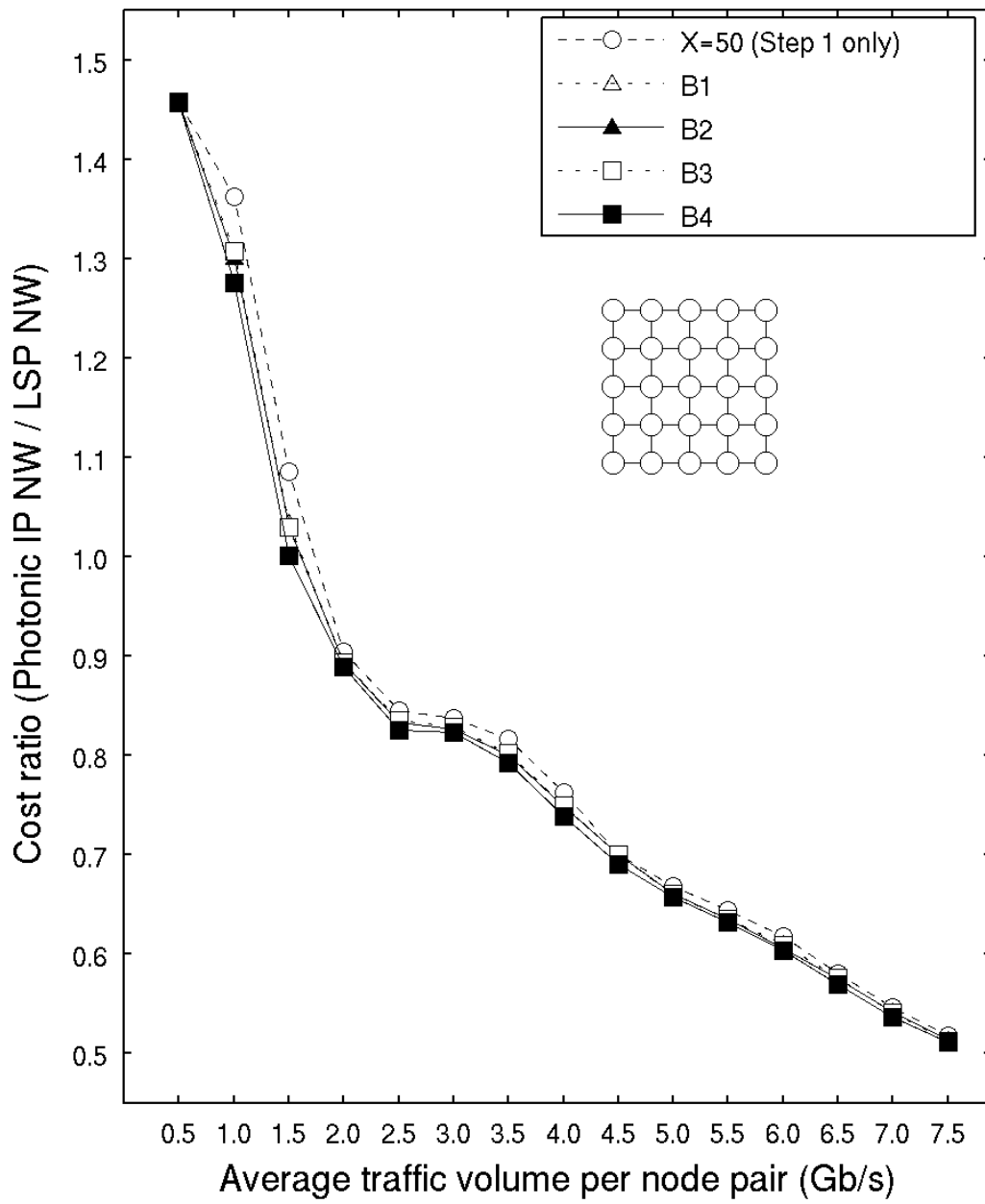


Figure 3-9. Network cost obtained from Scenario B (X = 50).

### 3.4.3 Impact of Physical Network Topology Scale on Cost Reduction

The previous simulations assumed a certain physical topology, i.e., an  $N \times N$  polygrid network. This section examines the impact of the network scale on network cost comparison.

For this simulation, the following network models were assumed.

- Physical network topology:  $3 \times N$  Polygrid ( $N = 3, \dots, 10$ ) and  $N \times N$  Polygrid ( $N = 3, \dots, 7$ ).
- LSP demand: Random pattern.
- Average one-way traffic intensity: 2.5, 5.0, and 7.5 Gb/s per node pair.
- Scenarios: Scenario A (A2,  $X = 0$ ,  $Y = 50$ ) and Scenario B (B4,  $X = 50$ ). These scenario and parameter values are chosen since they provided good results.

Other parameters are the same as those mentioned previously. The simulation results are plotted in Figure 3-10 and Figure 3-11. The average hop number of LSPs is also shown in parenthesis on the  $X$  axis, wherein the hop number is defined as the number of links that will be passed through by a LSP between its source and destination pair.

The obtained results are summarized next.

- The degree of cost reduction becomes more significant as the size of the physical topology becomes larger. In other words, the impact on cost reduction, attained by a hierarchical LSP network as studied here, becomes more significant as the average number of hops between source and destination pair increases, which makes the effect of cut-through in the OLSP domain more significant.

The magnitude of cost reduction, attained by the LSP/OLSP network, according to the average traffic increase, i.e., 2.5 Gb/s  $\rightarrow$  5.0 Gb/s  $\rightarrow$  7.5 Gb/s per node pair, becomes larger as the size of physical topology becomes larger.

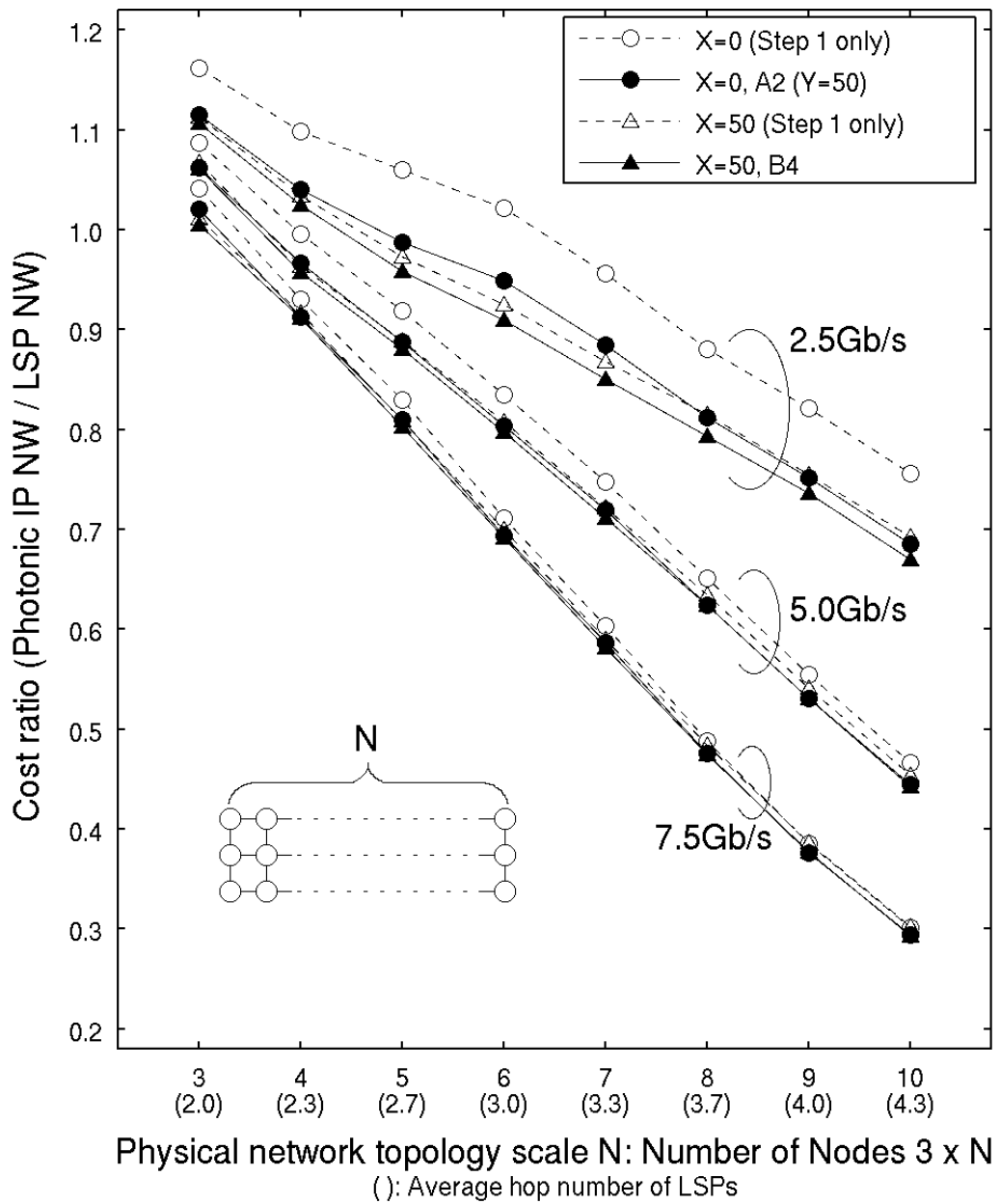


Figure 3-10. Network cost obtained from 3xN network.

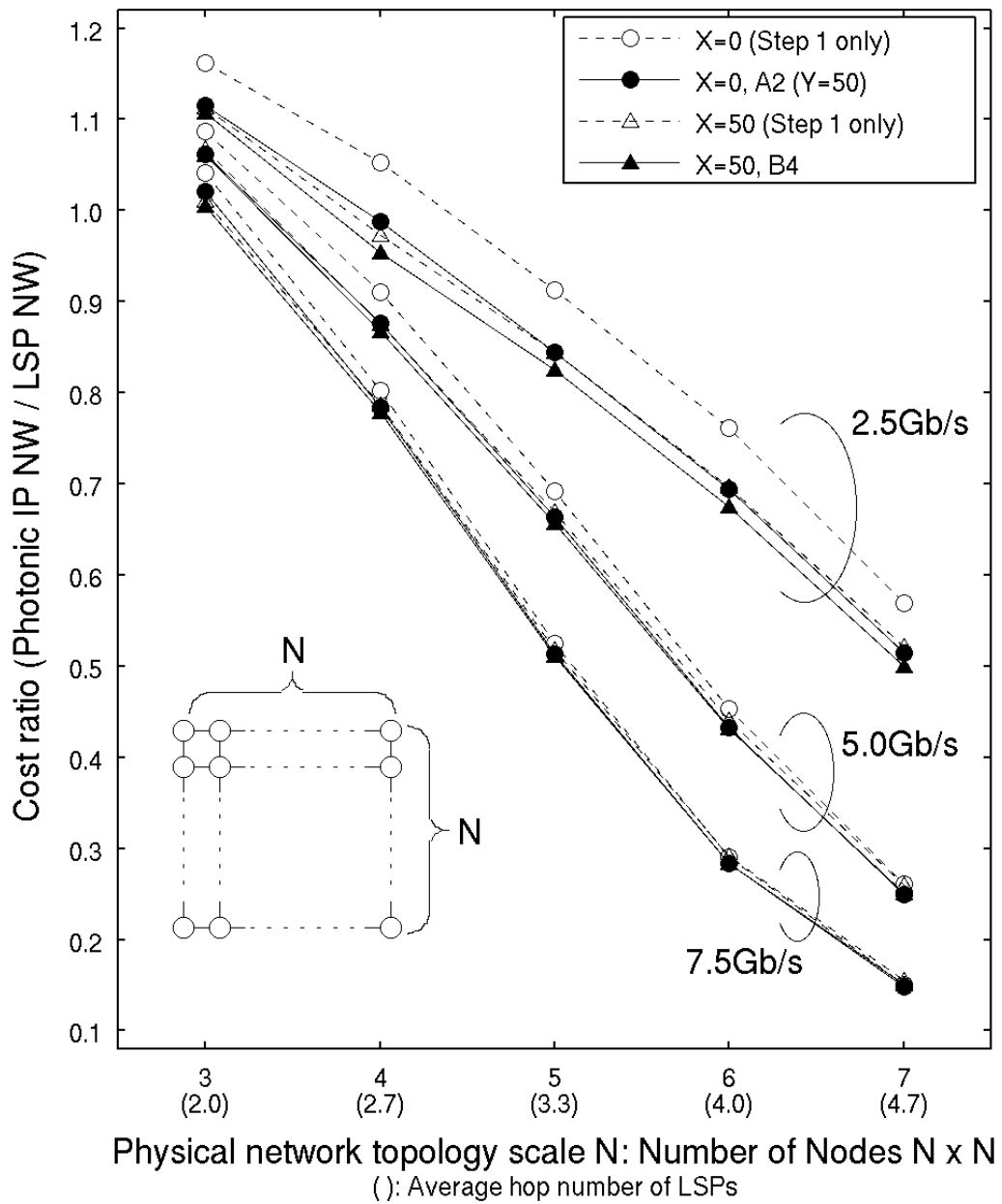


Figure 3-11. Network cost obtained from  $N \times N$  network.

### 3.5 Conclusion

We proposed network design algorithms that minimize the network cost for electrical and optical label switched multilayer Photonic IP networks. Using the

developed algorithms, the cost-effectiveness of multilayered photonic IP networks was evaluated.

In fact, compared with LSP networks with point-to-point WDM transmission systems, the benefit of multilayer photonic IP networks was obtained even if the average LSP demand between pairs of nodes was less than the OLSP capacity. The proposed algorithms comprise two steps and the first step provides multiple different optimization start points (initial networks). The optimal result was the best result chosen among the obtained results after multiple optimization procedures. We verified that most of the results obtained through the multiple different optimization procedures applying different scenarios and subcases converge to almost the same value. This implies that the heuristics developed here could effectively avoid the local minima, and the validity of the obtained results is very high. Each algorithm is based on heuristics and so the total calculation time required after multiple procedures was not excessively long. The network design algorithm proposed here can be easily extended to other type of multilayered networks such as SONET/SDH over OLSP and ATM over OLSP networks.

# 4 Network Design for Multi-Layered Photonic IP Networks Considering IP Traffic Growth

## 4.1 Introduction

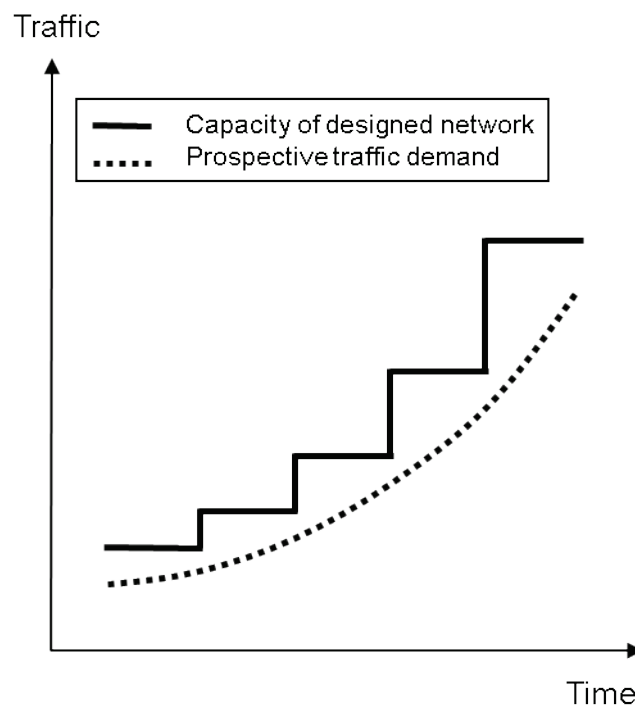
The amount of IP traffic is explosively increasing due to the increase in the number of Internet users and the penetration of wired and wireless broadband access using FTTH, LTE, and Wireless LAN. In order to expand genuine broadband services in the future, IP transport network capabilities must be enhanced. Photonic network technologies explained below are expected to provide the solution. In this chapter, we propose a new network design algorithm that minimizes the network cost considering IP traffic growth (denoted as “dynamic design” herein) for multi-layered photonic IP networks.

We first discuss a new dynamic network design algorithm that minimizes the network cost. We then evaluate the network cost obtained from the developed dynamic network design algorithm and compare it with the results obtained from the static zero-based algorithm which does not take into account the history of the progressive past IP traffic changes/growth until that time. It is shown that our proposed algorithm is very effective; the cost increase from the cost obtained with zero-based algorithm is marginal. The algorithm developed here enable effective multi-layered photonic IP network design that can be applied to practical networks where IP traffic changes/increases progressively and that can be used for long term network provisioning.

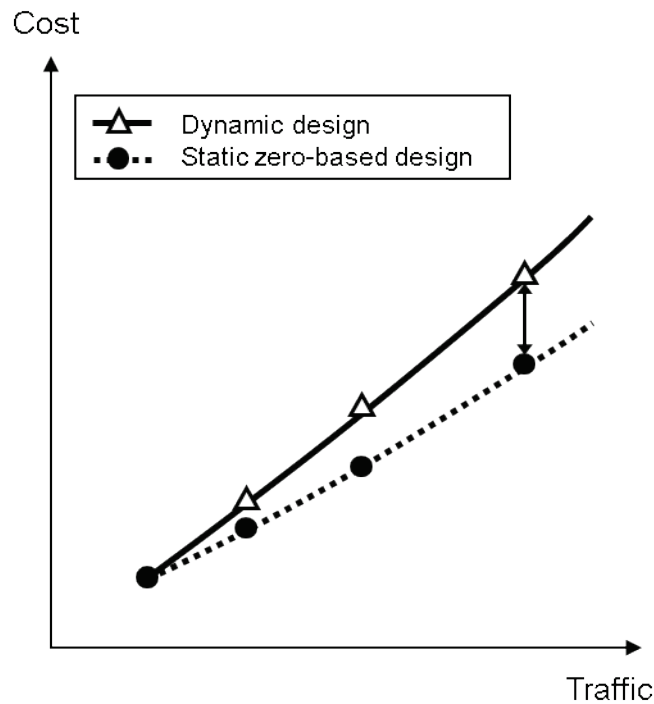
## 4.2 Network Model

Figure 4-1 is a schematic of the relation between the prospective traffic demand that increases as time passes and the capacity of the designed network based on it at every provisioning time. The necessary network equipment should be added to (and removed from) the network to support the prospective traffic demand periodically. In practically, network operators predict traffic demand and extend

their network equipment every quarter of a year, every half year, or every year. If we can statically design and provision the network under given traffic conditions, the designed network is then almost optimal at all times. This will not always be possible, however. Practically, we may have to extend the working network a couple of times a year or so according to changes in traffic demand, and the increased (decreased) traffic will be accommodated (removed) using newly provisioned network resources such as node equipment and optical fibers. In this process, existing traffic (LSPs and OLSPs) will not be rerouted. This is usually the case in a network that accommodates real-time or delay sensitive services, lambda leased line services, and so on. By repeating the network resource changes several times, network resource utilization may deteriorate compared to a network that is designed using the zero-based design (static design), as shown in Figure 4-2. The network design algorithm developed in this thesis minimizes the additional equipment required for the dynamic design.



**Figure 4-1. Traffic model of designed network and prospective.**



**Figure 4-2. Cost model obtained from dynamic and static design.**

Regarding the optimization of a network that includes routing and wavelength assignment, the problem is known as NP-complete [19]. An approach using integer linear programming [16] can be used, but this approach is only applicable to small networks. The application is very limited. Therefore, an approach employing heuristic algorithms is widely considered for designing practically-sized networks.

Figure 4-3 illustrates the Photonic IP network and the node structure discussed in this chapter. The node consists of three functional elements: the OXC, OLSP terminator, and LSR. The LSR consists of an IP router controlled by the MPLS mechanism. At the ingress of the OXC, WDM signals from adjacent nodes are demultiplexed into each wavelength (optical path). Some of the optical paths (OLSPs) that need to be terminated at the node will be delivered to the OLSP terminator and the corresponding OLSPs are converted into electrical signals. The LSPs accommodated within the terminated OLSPs are switched by an LSR where packet-by-packet forwarding is done based on the LSP label information. The other OLSPs are cross-connected at the optical level at the OXC. At the egress of the OXC, OLSPs are wavelength multiplexed and launched into the outgoing fibers.

The relationships among the IP packets, LSP, OLSP, and optical fiber are shown in Figure 4-4. LSPs are logical paths with a variable bandwidth identified by a label attached to each IP packet. An OLSP is an optical path that has a fixed bandwidth and is identified by the wavelength. An OLSP accommodates a number of LSPs and the optical fiber accommodates a fixed number of OLSPs.

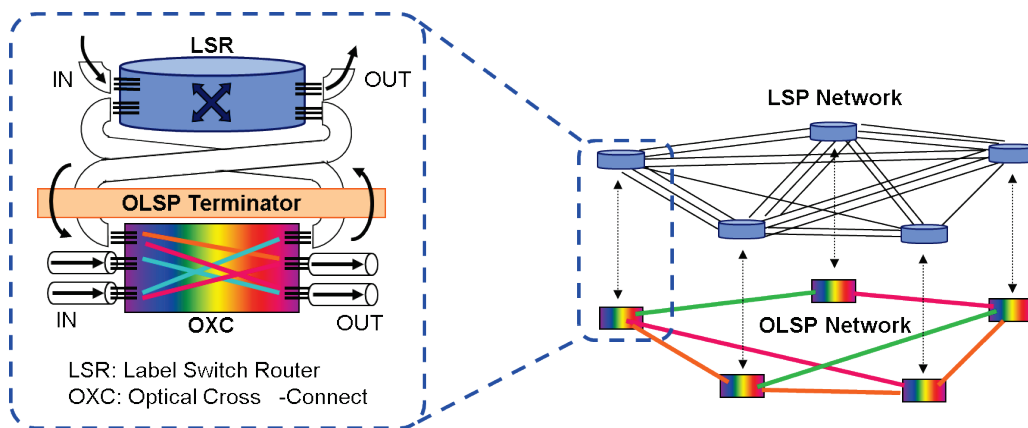


Figure 4-3. Photonic IP network and node structure.

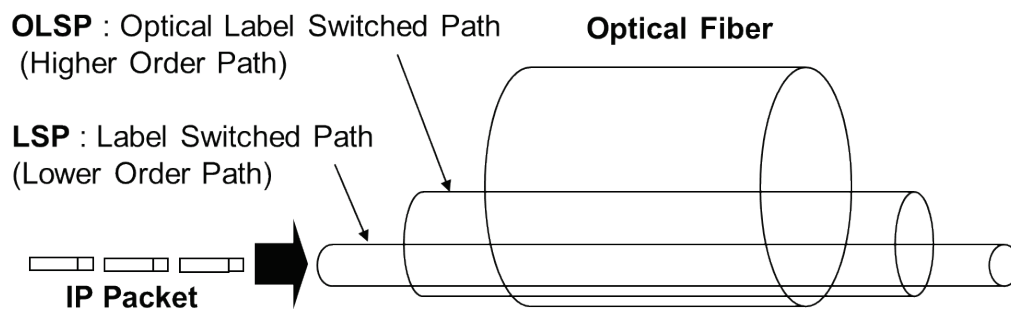


Figure 4-4. Relationships among IP packets, LSP, OLSP, and optical fiber.

### 4.3 Network Design Algorithm

There are two types of network design for photonic IP networks as mentioned in the previous section. One is the static zero-based design on a given traffic that will

be used for the initial network design. The other is the dynamic network design considering IP traffic growth.

In this study, we make the following assumptions.

- There is no wavelength conversion capability at intermediate nodes.
- An OLSP should be established as per various OLSP setup policies
- The data traffic distribution pattern is asymmetrical.

#### 4.3.1 Static Design

The static zero-based design algorithm is used for initial network design and used as a reference to evaluate the results obtained from the dynamic design. The static zero-based design has been shown to provide a nearly optimal network for a given amount of IP traffic [22]. The algorithm we adopt here is that previously proposed [25] and the effectiveness has been verified on several network scales and under different network conditions. The particular point of the algorithm is that it has two optimization stages (explained below) and at the first stage it adopts different cost minimization scenarios in accordance with different OLSP provisioning conditions that are chosen to accommodate a given LSP traffic demand. This approach was shown to remove effectively the local minima, which are attained by introducing different first stages, and to enhance the reliability of the obtained results in terms of the optimization [25]. Here, we explain only the points of the algorithm.

The developed algorithm comprises two steps. Step 1: Establish direct OLSPs as per the given policy without LSP level grooming at intermediate nodes. Step 2: Reconfigure the network developed in Step 1 allowing for LSP level grooming at intermediate nodes.

The algorithm introduces parameter  $X$  as an OLSP setup policy in Step 1. This OLSP setup policy is the decision regarding whether to establish a direct end-to-end OLSP or to establish point-to-point OLSPs for the LSP traffic demand to be accommodated. When the LSP traffic demand between a certain node pair is above  $X\%$  of the OLSP capacity, the LSP traffic is accommodated within a direct end-to-end OLSP. If it is below  $X\%$ , the LSP traffic is accommodated within point-to-point OLSPs (Step 1). Figure 4-5 compares a direct end-to-end OLSP and a point-to-point OLSP. LSP 1 is accommodated within point-to-point OLSPs, OLSP 1 and OLSP 2. LSP 2 is accommodated within a direct end-to-end OLSP 3. In regard to LSP 1, ingress, transit and egress routers correspond to LSR 1, LSR 2 and LSR 3,

respectively. Regarding LSP 2, ingress and egress routers correspond to LSR 1 and LSR 3, respectively. When  $X = 0$ , many OLSPs will have much spare bandwidth since all LSP traffic is accommodated within direct OLSPs. Then, in Step 2, LSPs accommodated within such OLSPs are reconfigured and accommodated within two concatenated OLSPs. On the other hand, when  $X$  is between 0 and 100, some LSPs are accommodated within concatenated point-to-point OLSPs. Such LSPs are reconfigured and accommodated within two concatenated OLSPs (Step 2). These procedures effectively reduce the required wavelengths and optimize the network [25].

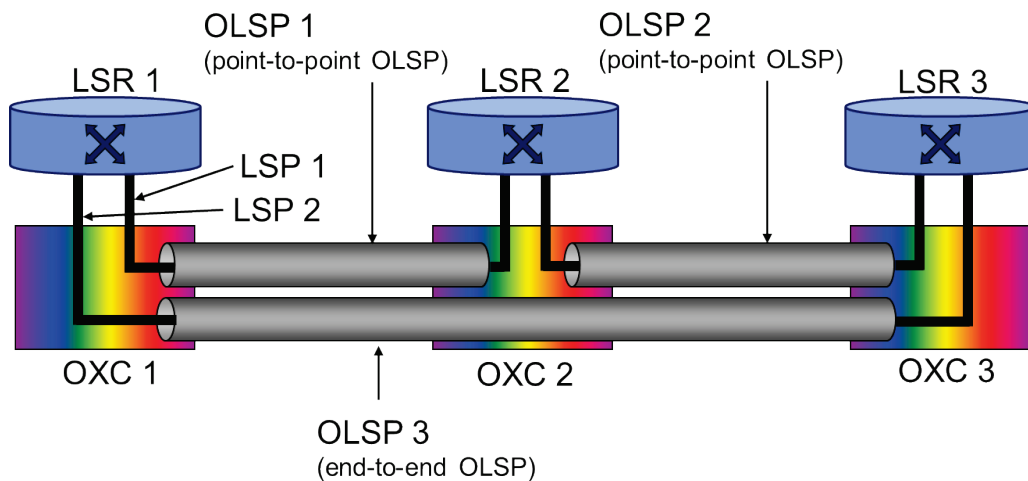


**Figure 4-5. Direct end-to-end OLSP and a point-to-point OLSP.**

### 4.3.2 Dynamic Design

In practical networks, we extend the working network according to the IP traffic changes/growth a few times a year. At a certain point of the year, for example every quarter, we evaluate the traffic growth until the end of the next quarter, and add the necessary equipment to the working network based on the dynamic network design.

The network design algorithm to minimize the network cost considering IP traffic growth is described below and summarized in Figure 4-6. Here, we employ the algorithm explained Section 4.3.1 in order to design a network for the initial traffic demand. We assume here that IP traffic change during the next term consists of

increasing and decreasing segments, and the total amount is increasing. We also assume that the equipment for the decreased LSPs can be removed and the working LSPs should not be rearranged. In practice, the equipment that becomes unused will not be removed from the network, since the traffic increases rapidly and the equipment will become utilized soon. This depends on the network provisioning policy of the network providers. Parameters incorporated in the design algorithm are summarized in Table 4-1.

**Table 4-1. Parameters Incorporated in the Design Algorithm.**

Input	Physical network topology, LSP traffic demand
Parameters	OLSP setup policy, node/link cost, etc.
Output	Total network cost, LSP route, OLSP routes, OLSP wavelengths

#### Dynamic design algorithm

1. Design the initial network [25].
2. Delete the decreased LSPs from the developed network. (OLSPs with no LSP and optical fibers with no OLSP should then be deleted. The remaining LSPs are not rearranged.)
3. Accommodate some of the increased LSPs that have the same ingress and egress node as that of the existing OLSPs when there are available OLSP capacities.
4. Search for the shortest LSP routes (Dijkstra algorithm) for the rest of the increased LSPs, employing a weighted link and node cost.
5. Select a node pair to establish residual new OLSPs, based on the selection criterion, explained below.
6. Establish a direct end-to-end OLSP along the route of the bundled LSPs and assign a wavelength to it if the total bandwidth of the LSPs exceeds  $X\%$  of the OLSP capacity.
7. Iterate 5 and 6 as long as there are candidates to establish a direct end-to-end OLSP.
8. Accommodate the remaining LSPs within point-to-point OLSPs.

9. Optimize the network allowing for LSP level grooming at intermediate nodes.

In 5 above, we adopted a simple rule [14] that determines the priority for the OLSP provisioning. The highest priority is given to a node pair that is determined by the value  $\max\{D_{ij} \times P_{ij}\}$ , when  $D_{ij}$  is the distance between node  $i$  and node  $j$ , and  $P_{ij}$  is the number of LSPs from node  $i$  to node  $j$ .

In 9 above, the optimization procedure is the same as that performed in Step 2 of the static design (see Section 4.3.1) [25]. This process reduces the required wavelengths (OLSPs) and fibers, and thus decreases the network cost.

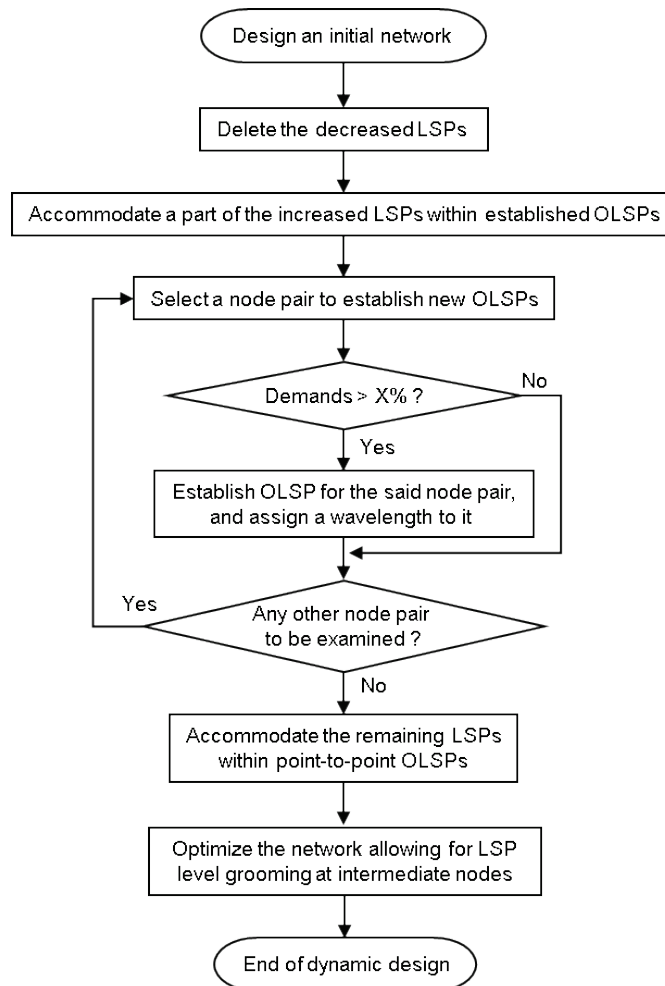


**Figure 4-6. Outline of dynamic design algorithm.**

## 4.4 Simulations

We evaluated the network cost obtained from the developed dynamic network design and compared it with that obtained from the static zero-based algorithm.

We generated a network cost model that comprises node and link costs on the basis of state-of-the-art technologies. The details are provided in the Appendix. We used Japan's national network model comprising 18 nodes (see Figure 4-7) and a 5×5 polygrid network as the physical network topologies.

LSP traffic demands are generated by selecting randomly a node pair (ingress node and egress node) per LSP. In regard to IP traffic distribution, we adopted two types of traffic models. One is a random uniform distribution where all node pairs have the same probability to be selected as LSP endpoints. The other takes into account the population density of the city (region) where the node is located. A model in which a node pair that has a large population has a higher probability to be selected than does a node pair in the city (region) with a small population. Here, we adopted the criterion where the probability to select a node pair is proportional to the product of the population of the two cities (regions) where the ingress and egress node is located.

An initial LSP demand is set to be equal to 0.5 Gbps per node pair on average. We tested three different net traffic increase rates for the next prospective period: 25% (50% increase, 25% decrease), 50% (100% increase, 50% decrease), and 100% (150% increase, 50% decrease). Three OLSP set-up policies (X) were examined: X = 0, 25, and 50.

We, therefore, evaluated nine different conditions as shown in Table 4-2. In order to obtain reliable results, we examined 30 random traffic patterns for each traffic increase rate. The cost ratio is calculated over the 30 traffic patterns, and the average ratios are plotted.

**Table 4-2. Simulation conditions.**

Network topology	Demand distribution	Traffic net increase; 25% / 50%/100%
Japan's national network	Consider population density	(1) / (2) / (3)
Japan's national network	Uniform and random	(4) / (5) / (6)
5×5 polygrid	Uniform and random	(7) / (8) / (9)

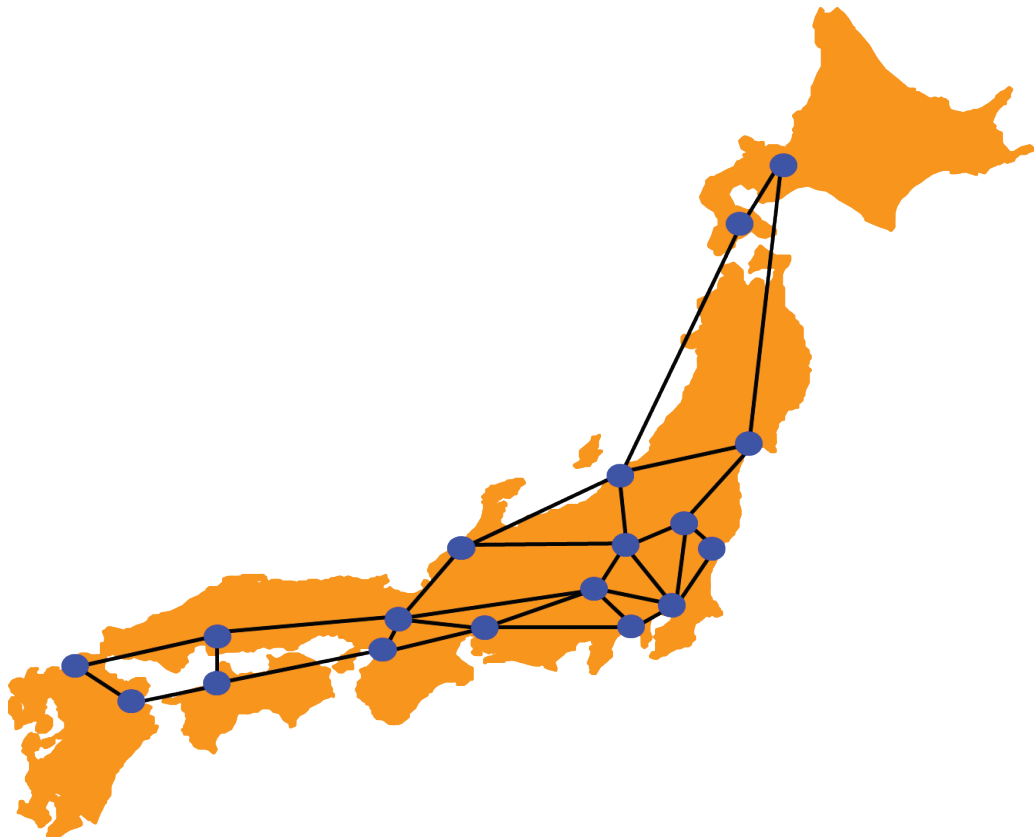


**Figure 4-7. Japan's national network.**

#### 4.4.1 Comparison between static and dynamic design

Figure 4-8 shows the cost ratios of a photonic IP network compared to a single layer LSP network that does not use OLSPs in the case of Condition (2) (Japan's national network, consider population density, rate of net traffic increase is 50%; see Table 4-2). The LSP network is a present network architecture that uses IP routes at every node to route IP traffic and does not use OXCs. The figure shows that the cost difference between static design (dotted lines) and dynamic design (solid lines) is slightly different according to parameter  $X$ . Figure 4-9 shows the cost ratios of the developed dynamic design algorithm to static zero-based design algorithm for different  $X$ . Figure 4-9 indicates that when  $X = 0$ , the cost increase from the cost obtained with the zero-based algorithm is very small, about less than

1%. When  $X = 25$  or  $50$ , then it is larger, from a few percent to 10%. Irrespective of  $X$ , the cost increase becomes marginal as the traffic intensity increases.

In static zero-based design, it is shown that the impact of the difference of value  $X$  on cost is very small [25]. In dynamic design, however, the impact is slightly enhanced, and when  $X = 0$ , as shown in Figure 4-8, the minimum network cost is attained when the average traffic exceeds about 2 Gbps (OLSP capacity is set to be 2.5 Gbps in this chapter), and when  $X = 50$  is the worst. When  $X = 0$ , in particular in the beginning (where traffic volume is low, less than about 2 Gbps) there are relatively many unused OLSPs (OLSPs with much spare capacity), however, as the traffic increases over time, such OLSPs are well occupied and this scenario ( $X = 0$ ) imposes minimum inefficiency (see Figure 4-9). In other words, LSPs are accommodated in OLSPs almost optimally. We confirmed these tendencies under all the conditions shown in Table 4-2.

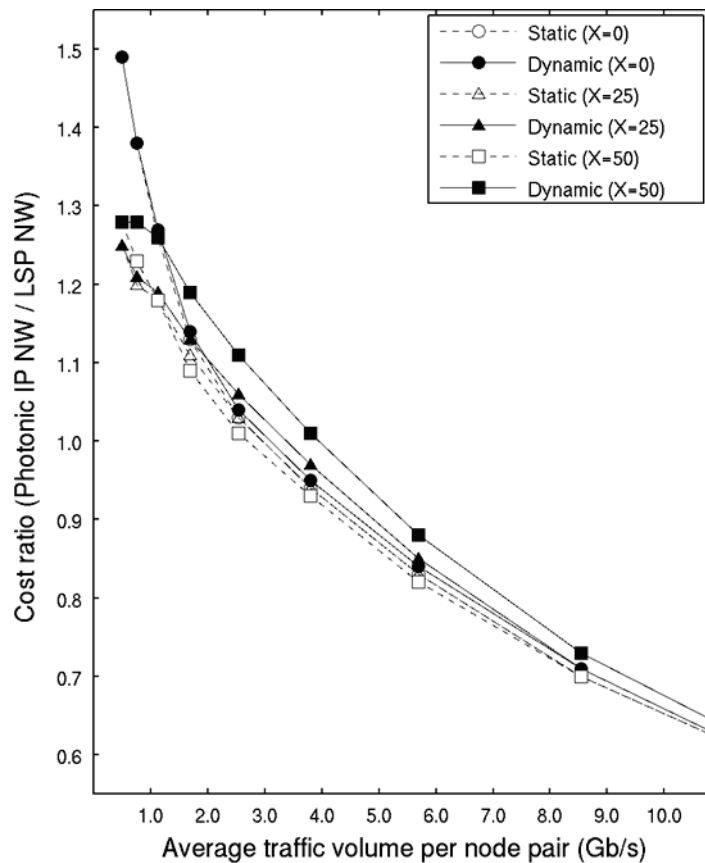


Figure 4-8. Network cost compared to LSP network.

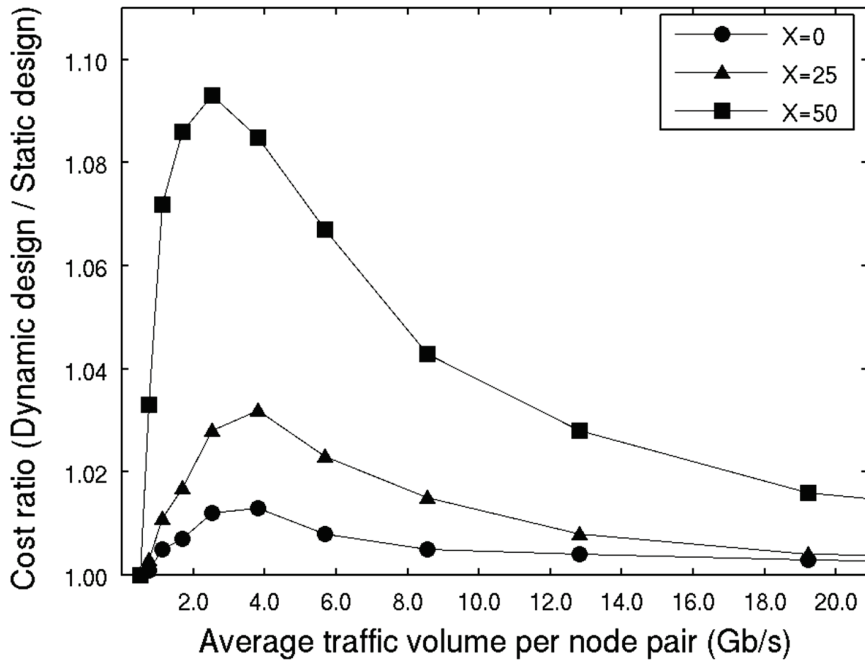


Figure 4-9. Network cost obtained from dynamic design.

#### 4.4.2 Impact of parameter values on the network cost: traffic increase rate, traffic distribution, and network topology

We investigate here the impact of the traffic increase rate (25%, 50%, and 100%) in each term on the network cost. The variation of the traffic increase rate corresponds to the frequency of the network provisioning or the traffic increase rate in the fixed term. Figure 4-10 (a)-(c) show the cost ratios of dynamic design algorithm to static zero-based design algorithm; (a)-(c) are for Conditions (1)-(3), (4)-(6), (7)-(9) in Table 4-2, respectively. The results for the OLSP setup policy,  $X = 0$ , are shown.

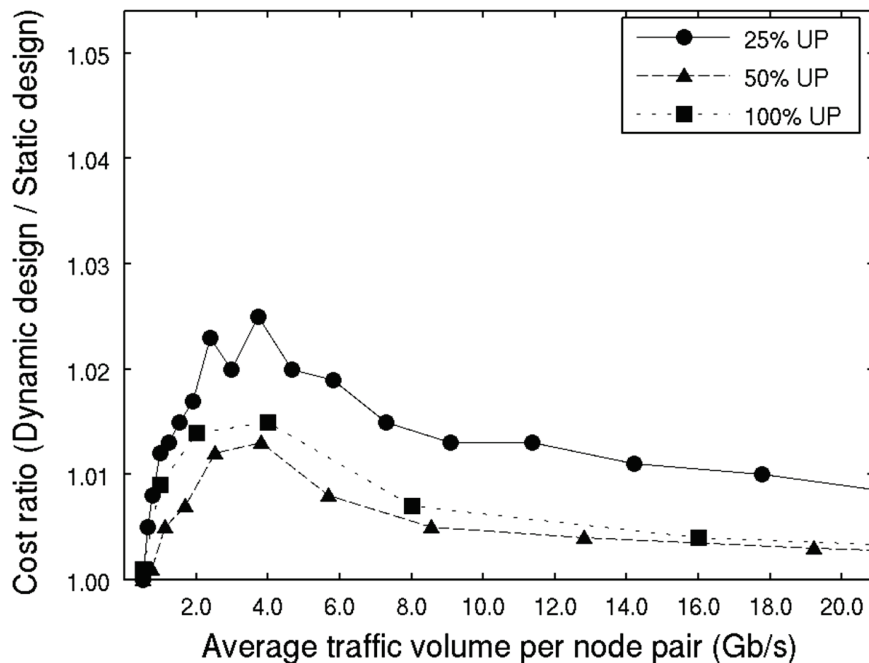
Figure 4-10(a) indicates that when the traffic increase rate is 25%, the cost increase from the static design is the largest, although the value is small, i.e., less than 3%. The smallest increase occurs when the rate is 50%, however, the differences between 50% and 100% are marginal. For the other conditions (Figure 4-10 (b) and Figure 4-10 (c)), the largest increase also occurred when the traffic increase ratio is 25% and differences between 50% and 100% are marginal also. The small traffic increase rate means that the term for network provisioning is shorter when the

traffic increasing rate is constant. Then the degree of inefficiency increases until the average traffic intensities reach a certain traffic volume that is around the OLSP capacity. After that point, the degree of inefficiency decreases as the traffic increases. Generally, as a result, too frequent provisioning should be avoided until the average traffic volume reaches a point around twice the OLSP capacity.

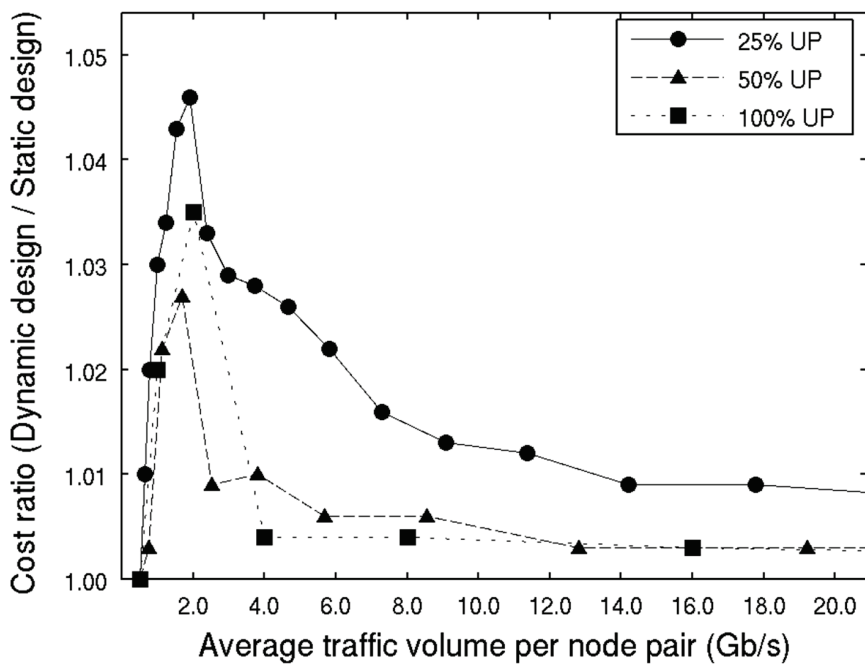
There is little influence exerted by the different traffic distributions (compare Figure 4-10 (a) and Figure 4-10 (b)). A higher cost ratio (higher peak) is obtained for random and uniform distributions than that for traffic distribution considering population density. This tendency is well predicted, since when population density is considered, the traffic change/ increase is the focus and occurs more for node pairs in large cities, and the absolute traffic increase is larger between particular nodes. As a result, the degree of inefficiency decreases; degree of inefficiency decreases as traffic increases (see Figure 4-9 and Figure 4-10).

A comparison between Figure 4-10 (b) and Figure 4-10 (c) demonstrates the difference in network topology. The difference was found to be very marginal.

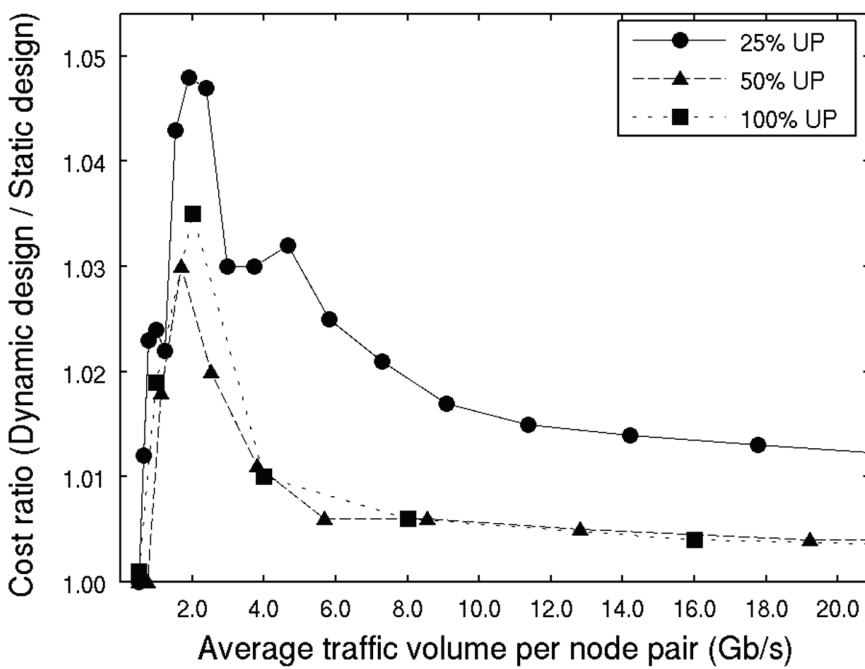
In any case tested, it can be said that the inefficiency is marginal when the average traffic volumes between nodes are a couple of times the OLSP capacity.



(a) Conditions (1)-(3); Japan's network, considering population density.



(b) Conditions (4)-(6); Japan's network, random and uniform.



(c) Conditions (7)-(9); 5x5 polygrid, random and uniform.

Figure 4-10. Network cost obtained from dynamic design.

## 4.5 Conclusion

We newly proposed a network design algorithm that minimizes the network cost considering IP traffic growth for multi-layer photonic IP networks that consist of electrical LSPs and optical LSPs. We evaluated the network cost obtained from the developed network design algorithm that considers different IP traffic growth patterns and volumes. The obtained results are compared with those obtained from the static zero-based algorithm that we proposed previously. It was shown that the presented algorithm is effective; the cost increase from that cost obtained with the static algorithm was marginal. Furthermore, under various conditions (physical network topology, traffic demand, and the traffic increase rate), the proposed algorithm was confirmed to produce excellent results.

In practice, traffic projections will be done every quarter or every half year, and generally speaking, the estimation accuracy will not be so good as an order of percentage. Furthermore, the network will be provisioned so that some amount of margin is taken from the provisioned traffic volume. Thus, the algorithm presented here is considered to be very effective and practical in particular when we consider the wide applicability to various conditions. In other words, if traffic engineering of IP layers and traffic estimation, which are out of the scope of this thesis, are done properly the designed supporting optical layer will cause no QoS degradation that can stem from network resource scarcity.

# 5 Performance Evaluation of Network Systems Accounting for User Behaviors

## 5.1 Introduction

In mobile networks, users carry mobile terminals, and make or receive calls whenever they wish. Therefore, the generation of communication traffic is heavily dependent on user behavior. Therefore, we propose a traffic control method that guides users, to alleviate congestion by giving them information about the network. This traffic control method aims to improve not only network performance but also the quality of service users perceive, and so ultimately to increase customer satisfaction. It is quite difficult to evaluate the performance of such a method in the field and therefore evaluation by means of simulation is useful. To evaluate such a control method through simulation, it is necessary for the simulator to represent both the behavior of individual users and the degree of customer satisfaction with the network service provided. In this chapter, we describe the development a simulator as a platform for performance evaluation corresponding to various applications and services. We have developed a large-scale simulator which can more faithfully represent the network (which provides communication services), users (who are the source of traffic), and the environment (which influences user behavior). Using the simulator we developed, we also evaluate the network systems by the communication logs and a survey of cellular phone customers. The rest of this chapter is organized as follows. First, we describe proposed traffic control method. Then, we show the concept of, and the requirements for, the proposed simulator. The functions of the developed simulator are then explained. The results of performance evaluation of network systems are shown.

## 5.2 Traffic Control by Influencing User Behavior

### 5.2.1 Concept

Traffic control by influencing user behavior is a method of controlling traffic by dynamically influencing user behavior according to the situation applying to the network, the users and the environment that surrounds the users when there is a

massive number of connection requests to a cellular network system [55]. We can consider three ways of controlling traffic: 1) balancing the distribution of traffic inflow between locations in the network (geographical balancing), 2) balancing the time that traffic flows into the network (time balancing), and 3) reducing the volume of traffic. We have studied three ways to influence users that correspond to the above: A) changing the communication place (move), B) changing the communication time (wait), and C) changing the communication method (i.e., the communication medium). The relationship between traffic control and influencing the users is shown in Figure 1. Each influencing method is described below.

1. Changing the communication place (move); the network system encourages the users to move to a location where there is spare capacity. This balances traffic geographically.
2. Changing the communication time (wait); the network system encourages the users to wait for a while until the network has spare capacity. This balances traffic in time.
3. Changing the communication medium (change media); the network system encourages the users to switch to a different communication medium, for example, from phone to SMS (Short Message Service). This reduces the volume of traffic.

We assume that a network system that provides this traffic control sends messages only to advise the users, and the users are free to decide whether to follow the guidance. The information in the guidance messages can include the present and future network conditions such as the resource usage rate or the recommended place, time or media which the users can adopt as an alternative. It is naturally expected that the network system should provide services to satisfy all the users' requests in any situation. However, it is financially difficult for the operator to construct and maintain the network capacity that is necessary if temporary, exceptional communication demands are to be met. Therefore, this traffic control scheme is one of the possible methods of using the limited resources efficiently. It may be necessary to give the user some incentives so that users will behave in the way the operator expects. Incentives can be achieved by pricing [65], [66], [67], quality control, etc.

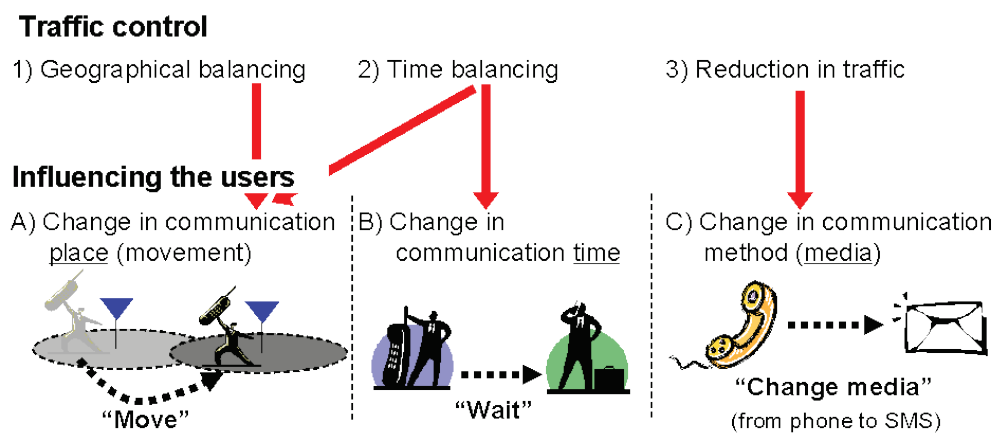


**Figure 5-1. Type of traffic control and corresponding influence on user behavior.**

### 5.2.2 Control Scheme

Figure 2 shows the sequence of events when implementing traffic control by influencing the users. The sequence is explained below. First, the network system judges whether it is necessary to guide the users or not when it receives a connection request. When the system guides the users, it sends the users a message to encourage a certain action, such as changing the communication place, time or media. The threshold of whether or not to send a message can be determined according to the radio resource usage, etc. When the system doesn't send a message, the connection request is processed as usual. Depending on the availability of spare resources, a call request may be accepted, resulting in a connection set up to the network or may be rejected, resulting in a blocked call.

When the system sends a message, the user can judge whether or not to follow the guidance in the message. When the user follows the guidance, the user behaves as recommended (move, wait or change media), and requests a connection again. When the user doesn't follow the guidance, the request is connected immediately or blocked depending on the availability of spare resources.

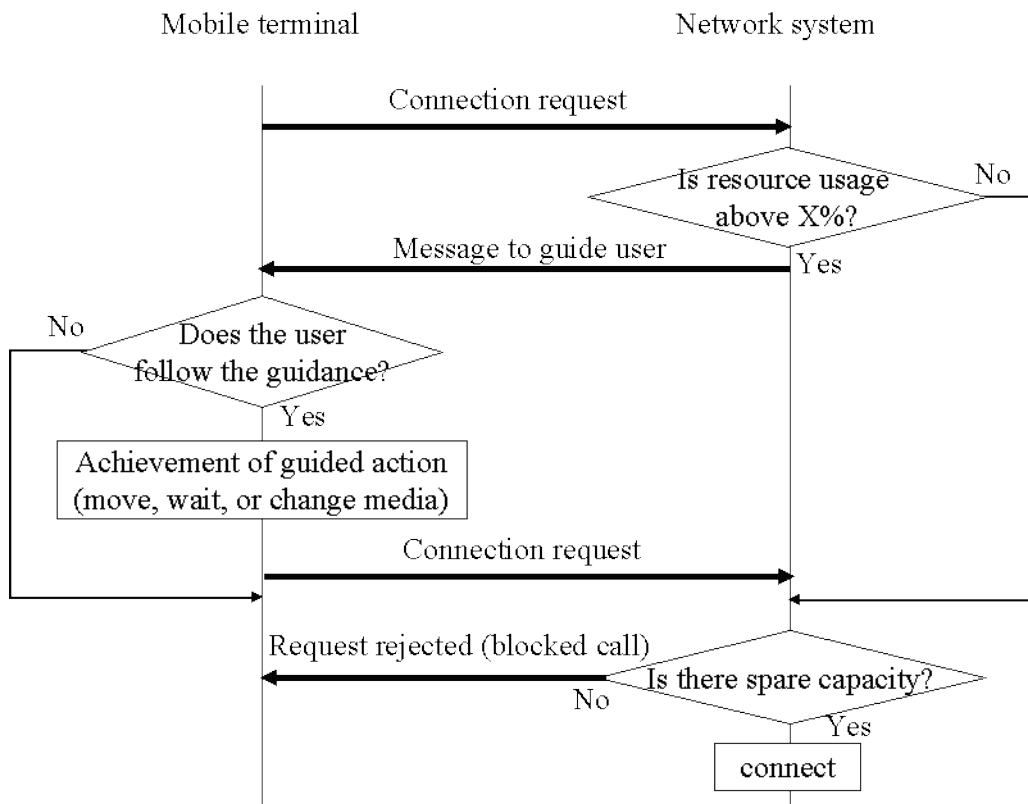


Figure 5-2. Sequence of events in influencing the users.

## 5.3 User and Network Simulator

### 5.3.1 Concept

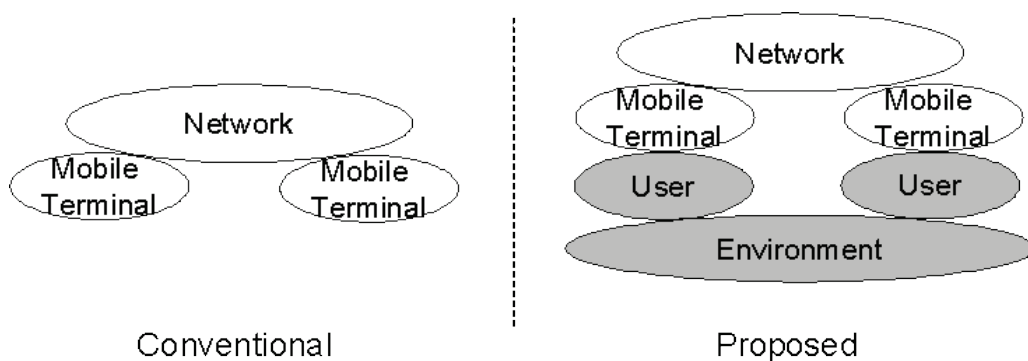
The proposed user and network integrated simulation can represent individual user behavior (communication behavior and mobility) and user satisfaction (or dissatisfaction) with the quality of service provided, in addition to providing the functionality of a conventional network simulator. Therefore, it also has a mechanism to incorporate feedback from user behavior to traffic, from traffic to quality of service, and from quality of service to user behavior [56].

Figure 5-3 shows the simulation targets of conventional network simulators and the proposed simulator. Conventional simulators cover only network elements and mobile terminals. In contrast, our simulator covers not only the network per se (which provides network services), but also users (who are the source of traffic) and the environment (which influences users and the network). Here, the

environment includes the geographical situation, such as streets and traffic lights, the weather, and events, such as football matches and fireworks displays.

The proposed simulator can model traffic based on realistic user behavior and the user environment rather than assuming simple traffic based on Poisson distribution and so on. This simulator makes it possible to:

- 1) analyze the mechanism of traffic generation for modeling mobile traffic in both usual and unusual conditions such as congestions or equipment failures,
- 2) evaluate new traffic control methods which take account of individual user satisfaction, including “traffic control by influencing user behavior” [55], and
- 3) improve the simulation accuracy by using realistic traffic inputs.



**Figure 5-3. Simulation targets.**

### 5.3.2 Functional Requirements

This section describes the key functions required to realize the concept described in Section 5.3. The user and network simulator needs to represent realistic individual user mobility and communication behavior. For modeling realistic user mobility, users in the simulation should walk along streets laid out according to real geographical information. In order to utilize real geographical information in simulations, the function of loading real map data into the simulator is required.

For modeling realistic user communication behavior, it is necessary to use not just a uniform models but detailed models which can be defined by user attributes.

Thus, the main functional requirements for the simulator to meet these conditions are as follows:

- Real map loading function
- Pedestrian mobility model
- User behavior model.

## 5.4 Implemented Functions

A variety of commercial and non-commercial network simulators are used for network research, such as ns-2 [61], OPNET [62] and QualNet [63]. In developing our simulator, we chose to make use of an existing network simulator, and selected QualNet for our simulation engine on account of its scalability and high simulation speed. To build the proposed simulator, we added the required functions described in Section 5.3.2 to QualNet as add-ons and also made some customization. Each function is explained in the following sections.

### 5.4.1 Real Map Loading Function

The real map loading function loads the map information of a specified area for use in simulation scenarios. We adopted digital maps that conform to the Japan Profile for Geographic Information Standards (JPGIS) issued by Japan Geographical Survey Institute (JGSI). We developed a converter, which extracts the required information relating to a specified area and converts it into an XML format suitable for simulation scenarios. Although the maps issued by JGSI include information about streets, intersections, and park areas, they do not include all the information needed for our simulation. We therefore developed a mechanism to add the necessary information which is absent from these maps. In the default setting, train station areas, connections between station areas and streets, entrances to parks, street widths, and traffic lights are added from the other geographic information. We also developed an add-on function for loading the XML-format maps required for simulation scenarios. The XML format which we defined allows an easy description of streets, intersections, parks, train stations etc. By uniformly basing data on this format, it is possible to use original geographic feature data in simulation scenarios.

## 5.4.2 Pedestrian Mobility Model

The pedestrian mobility model represents users walking along the streets on the maps loaded by the real map loading function. This model assumes that each user has a definite destination and walks independently of others. It allows users to change their walking speed and destination dynamically depending on the state of the surrounding environment, such as a crowded street.

We divided the mobility model into three parts (streets, intersections, and parks). Each part is explained below.

### 1) Mobility model for Streets

It would be more realistic to consider how users adjust their walking speed to the conditions in the street. When there are a large number of people in the street, the walking speed is generally reduced. We defined population density as the number of users divided by the street area (street width  $\times$  street length), as shown in Figure 5-4. The street length is divided into segments:  $\Delta$  (Figure 5-4), and users move segment by segment. The population density of a street is calculated every time a user moves, and is reflected in the walking speed. Figure 5-5 shows how walking speed is assumed to vary with population density. This model provides for more realistic mobility whereby users reduce their walking speed when the street gets crowded and increase it when the situation is alleviated.

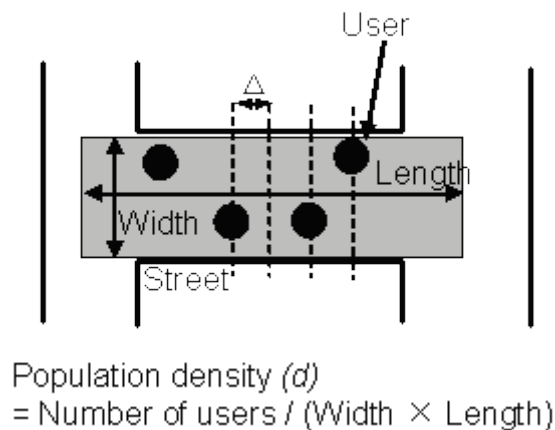
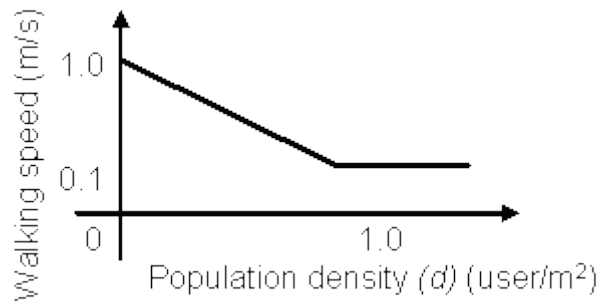


Figure 5-4. Population density in streets.



**Figure 5-5. Variation of walking speed with population density.**

## 2) Mobility Model for Intersections

When a user arrives at an intersection, he or she selects one of the streets connected to the intersection. In general, the user selects the street that leads to the shortest path to the destination. This would uniquely determine which street the user will select. However, in a real situation, users may avoid a crowded street even if it is the shortest route to the destination. In our model, the user selects a street connected to the intersection on the basis of parameter value  $w$ , which is defined by Formula 5-1. When a user arrives at an intersection,  $w$  is calculated for every street connected to it. Here,  $\theta$  is an angle between the direction to the destination and the direction of the street in question, as shown in Figure 5-6.  $f(d)$  is a function of population density ( $d$ ), as mentioned in previous subsection. We defined this function as shown in Figure 5-7.

$$w = (\cos \theta + 1)^2 \times f(d) \quad \dots \text{Formula 5-1}$$

When this algorithm is applied to the selection of the street to take, users tend to select a street which is less crowded but still provides a reasonably short path to the destination. When the population density is above a certain value, the value of  $f(d)$  is set to 0. This prevents the user from selecting a street whose population density is above the threshold, a realistic situation in crowded conditions.

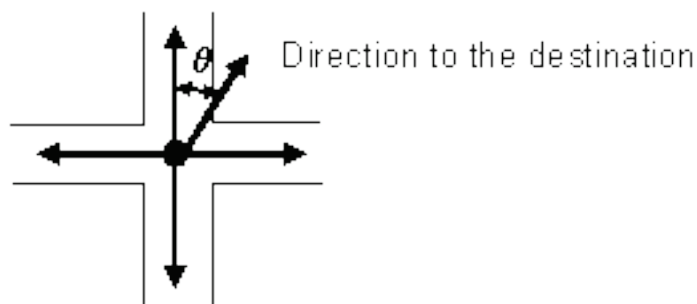


Figure 5-6. Definition of  $\theta$  at an intersection.

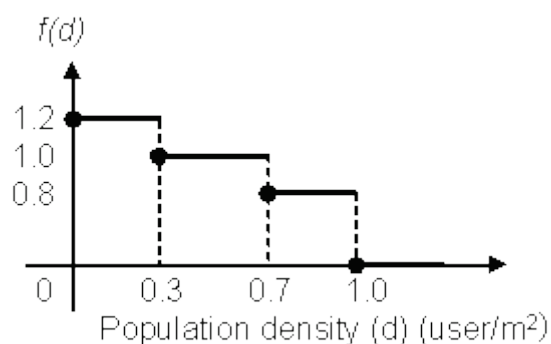


Figure 5-7. Definition of  $f(d)$ .

### 3) Mobility Model for Parks

In a park, user movement is not constrained by streets, and users can move in any direction. They tend to move in a direction which is not too crowded but still provides a reasonably short route to the destination. In order to simulate such behavior, we defined a model similar to the mobility model for intersections. That is, the direction is selected based on the angle to the destination and Formula 5-1. We assumed that a user in the park can move in one of the four directions: north, south, east, and west, as shown in Figure 5-8. The user selects the direction based on  $w$ . The population density ( $d$ ) is calculated for four each directions from the number of users in the area in front of the user. The area size is  $n \times 2n+1$  as shown in Figure 5-8, where we assume  $n$  to be two meters  $\theta$  is the angle formed between one of the four directions and the direction to the destination, as shown in Figure 5-9. As in the mobility model for intersections, we use  $f(d)$ , as shown in Figure 5-7. As in the mobility model for streets, the walking speed is assumed to change

dynamically depending on the population density. Thus, the mobility model for parks can represent the case where users in the park move to a place which is less crowded but is still on a reasonably short route to the destination.

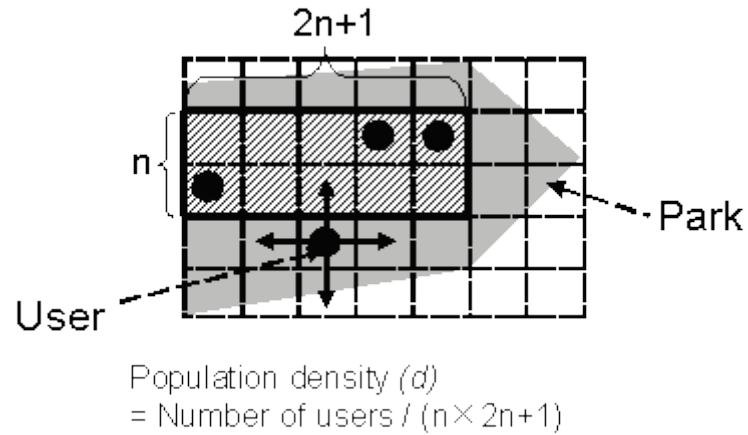


Figure 5-8. Population density ( $d$ ) in a park.

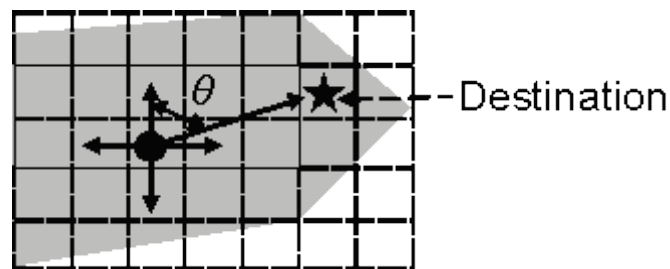


Figure 5-9. Definition of for  $\theta$  movement in a park.

### 5.4.3 User Behavior Model

User behavior (for example, communication behavior and mobility) is strongly influenced by the surrounding environment and the time of day. For example, many calls are generated in downtown regions and near train stations in the evening, and users move slowly in a crowded street. In addition, people with different attributes (age, gender etc.) behave differently [64]. Therefore, we developed a mechanism representing the facts that the communication and movement patterns change dynamically depending on the user attributes and the

user environment. Specifically, we introduced a “User Layer” that controls the “Application Layer”, as shown in Figure 5-10.

Figure 5-11 shows a part of the structure of user layer which provides the communication behavior description. The communication behavior description is defined by “User”, “Profile”, and “Traffic pattern”. N in “User” is the number of users in simulations, and M in “Profile” is the number of profiles ( $1 \leq M \leq N$ ). Each user is assigned attributes such as gender and age, and a profile which characterizes his or her communication behavior. We can also configure the traffic pattern according to the required situation as part of the profile. A profile can be applied not only to an individual user but also to a group of users who exhibit similar user behavior. For example, one profile can be defined for younger persons, another for middle-aged persons and yet another for elderly persons. Specifically, the traffic pattern in the profile defines the following items, some of which are expressed in the form of distributions.

#### Traffic Patterns

- Communication interval
- Communication methods
- Probability of selecting each communication method
- Probability of making repeated attempts (retries) for each communication method
- Interval of retries for each communication method
- Maximum number of retries for each communication method
- Types of persons called using each communication method
- Communication duration for each communication method

Using these parameters, it is possible to specify a variety of service applications (voice calls, text mail, and videophone etc.) in detail. Traffic patterns can be changed flexibly depending on the time of day or the specific user environment. This way, changes in user behavior resulting from changes in the user environment can be well represented.

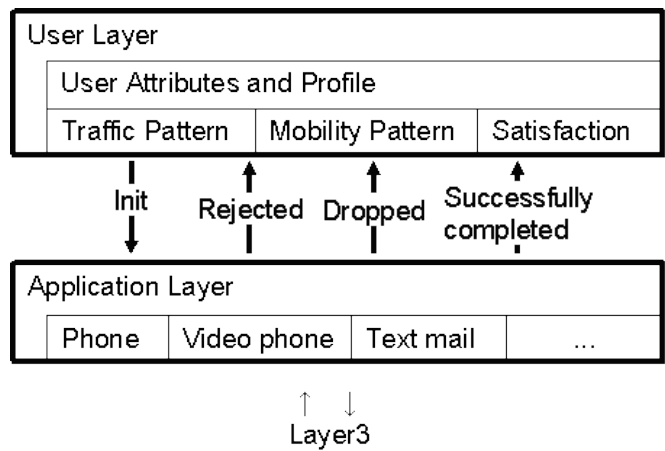


Figure 5-10. User layer.

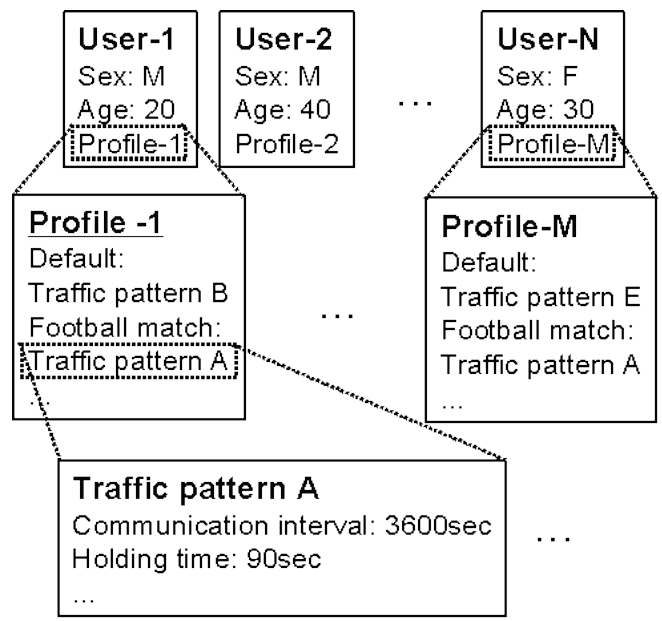


Figure 5-11. Communication behavior description.

### 5.5 Evaluation and Validation of the Simulator

We implemented the three functions described in Section 5.4 in the user and network simulator, and conducted some experiments to evaluate the network systems.

### 5.5.1 Evaluation of the Mobility Models

First, we demonstrated the functionality and the effectiveness of the real map loading function and the pedestrian mobility model described in Sections 5.4.1 and 5.4.2, respectively. To confirm the influence of the pedestrian mobility model on the simulation result, we compared our model with the random waypoint model, which is used widely for the performance evaluation of mobile communication networks.

We measured the amount of the resource used at each base station in two models: one where the random waypoint model was applied and the other where the pedestrian mobility model was applied. In the latter case, users chose the route they walked along based on the geographical information. We used the map shown in Figure 5-12, which represents a part of one of the largest cities in Japan and covers an area of 1.5 kilometers square. The shaded areas on the map are parks, and applied the park mobility was applied to users in these areas. The simulation conditions are as follows.

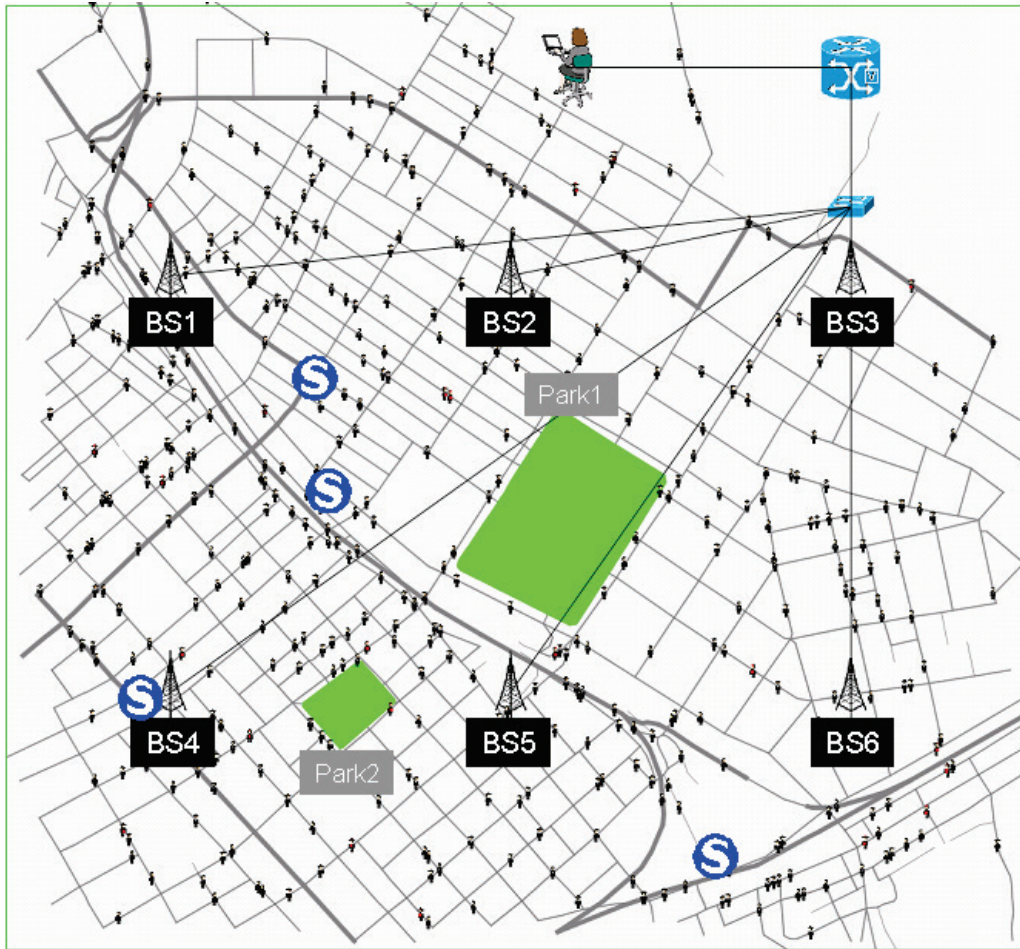


**Figure 5-12. Map of area used in simulation.**

**Simulation conditions**

- Simulation Area: 1.5 km × 1.5 km, as shown in Figure 5-12
- Number of users: 500
- Number of base stations: 6
- Number of sectors in each base station: 6
- Cannel bandwidth in each sector: 1024kbps
- Mobility model: random waypoint model, pedestrian mobility model.

- Communication model: One call occupies a bandwidth of 64 kbps. The average call origination interval is 1,800 seconds, and the average communication duration is 90 seconds.
- Call destination: a randomly selected user in the simulation
- Simulation duration: 3,600 seconds.

We considered five cases for the mobility scenario as shown in Table 5-1. Case 1 uses the random way point model and the other cases use the pedestrian mobility model described in Section 5.4.2. “Random intersection” in Initial location of Table 5-1 means that each user starts from a randomly selected intersection and “Station” means that each user starts from a station selected randomly from the four train stations on the map. “Random intersection” in Destination of Table 5-1 means that the destination of each user is a randomly selected intersection, and when a user arrives at the destination, he or she heads toward the next destination which is again selected randomly. “Park” in Destination means that users first move to randomly selected intersections for 600 seconds and then move to their respective parks, and when 2400 seconds has passed, they move out of the park and go to the nearest train station. Therefore, in Cases 2-5 which use the pedestrian mobility model, Case 2 has the highest randomness and is the most similar to the random waypoint of Case 1. In contrast, Case 5 represents the most realistic situation of a fireworks display.

We ran 20 simulations under these conditions and measured the average resource usage in each simulation. Figure 5-13 shows the average amount of resource used at each base station. The horizontal axis identifies the base stations, and the vertical axis indicates the average usage of bandwidth. In Case 1, the bandwidth usage of base stations 2 and 5, which are located nearest the center of the area, is higher than that of other base stations, and the others all used more or less the same amount of resource because the users with random waypoint mobility tend to congregate in the center of the area [58]. In Cases 2, 3, 4 and 5 where the pedestrian mobility model is used, the differences in resource usage among base stations are larger than those in Case 1 where the random waypoint model is used. The resource usage of base station 3 in Cases 2-5 is rather small because there are few roads around it and so users rarely used this base station. Moreover, the initial locations and the destinations are the key factors in the mobility model and strongly influenced the simulation results. In Case 4 and 5, as there is a park near base station 5, users gathered in the areas covered by this base station, resulting in higher resource

usages than those in Cases 1, 2 and 3. The simulation results quantitatively show that when we set realistic parameters for the mobility model, initial locations and destinations, the results are closer to the result reflecting the most realistic situation of Case 5. Conversely, when the randomness of the parameters increases, the results are closer to those in Case 1, the random waypoint model.

The above indicates that the results of the simulation using the pedestrian mobility model match what we would normally expect from the geographical information. In other words, the simulation using the pedestrian mobility model reflects the real world better than the simulation using the random waypoint model. When evaluating the design and traffic control techniques of a real network, it is necessary to consider user movement that takes account of the actual geography. Our pedestrian mobility model is effective for such an evaluation.

**Table 5-1. Mobility scenarios.**

	Mobility Model	Initial location	Destination
Case 1	Random waypoint	Random	Random
Case 2	Pedestrian	Random intersection	Random intersection
Case 3	Pedestrian	Station	Random intersection
Case 4	Pedestrian	Random intersection	Park
Case 5	Pedestrian	Station	Park

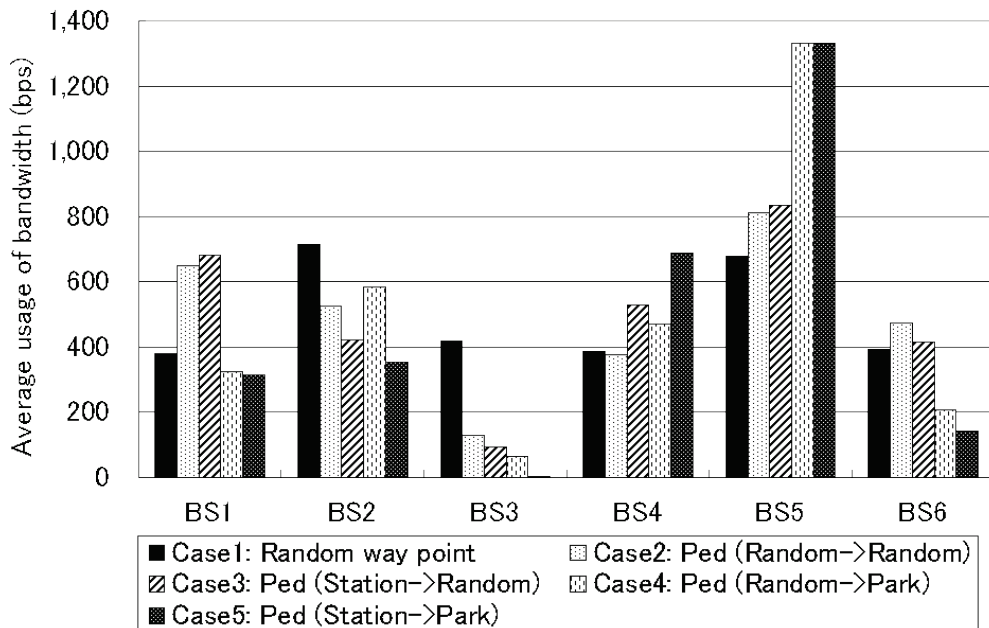


Figure 5-13. Average usage of bandwidth.

### 5.5.2 Evaluation of Communication Behavior Model

We show an example of the simulation applying the communication behavior model described in Section 5.4.3 and demonstrate the effectiveness and significance of the function. First, we indicate the difference in the real traffic between users with different attribute values. Figure 5-14 shows the differences in the communication patterns for twelve combinations of attributes (gender and age) based on the communication logs and a survey of cellular phone customers. Figure 5-14 (a) and Figure 5-14 (b) show the mean values of the number of phone calls and the holding time per call for users with different attributes based on the communication logs of about 16 million cellular phone customers. Figure 5-14 (c) and Figure 5-14 (d) show the mean value of the interval between retries and maximum number of retries during network congestion. The values result from the survey of 2339 cellular phone customers because these values cannot be obtained from the communication logs. The numbers of survey respondents for each combination of attribute values are shown in Table 5-2. These four figures show the normalized values when the mean value for a male in his teens is one. We can see that there are significant differences in the communication trends according to age and gender. The communication behavior model we developed can take into account such a difference in the communication behavior among users with

different attributes in the simulation. Then, we ran more simulations in order to clarify whether there is a difference in the simulation results between the conventional case in which the simulation parameters are set by using only the average value of the total set of users (scenario 1) and the case in which parameters are set using the values which account for the differences between users with different attributes (scenario 2). We generated the following two simulation scenarios applicable to the communication behavior model described in Section 5.4.3.

1) Scenario 1 (using 1 profile)

- All users are assigned the same profile.
- Simulation parameters for the communication behavior (number of phone calls, holding time, interval between retries, and maximum number of retries): mean value of all simulation users (exponential distribution).

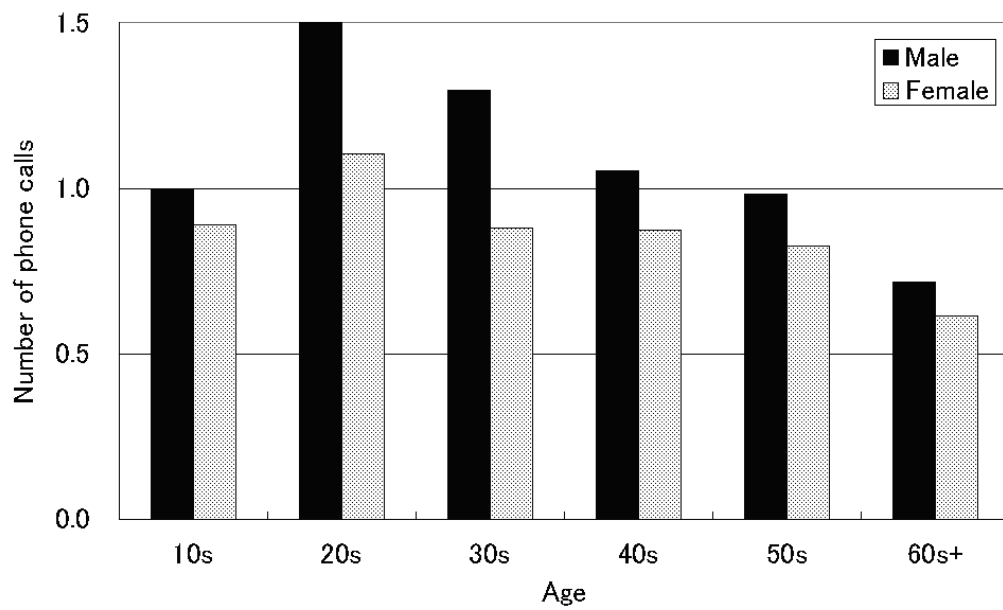
2) Scenario 2 (using 12 profiles)

- Each user is assigned a profile corresponding to his or her attributes (gender and age).
- Simulation parameters for the communication behavior: mean value of the users grouped by their attributes (refer to Figure 5-14).

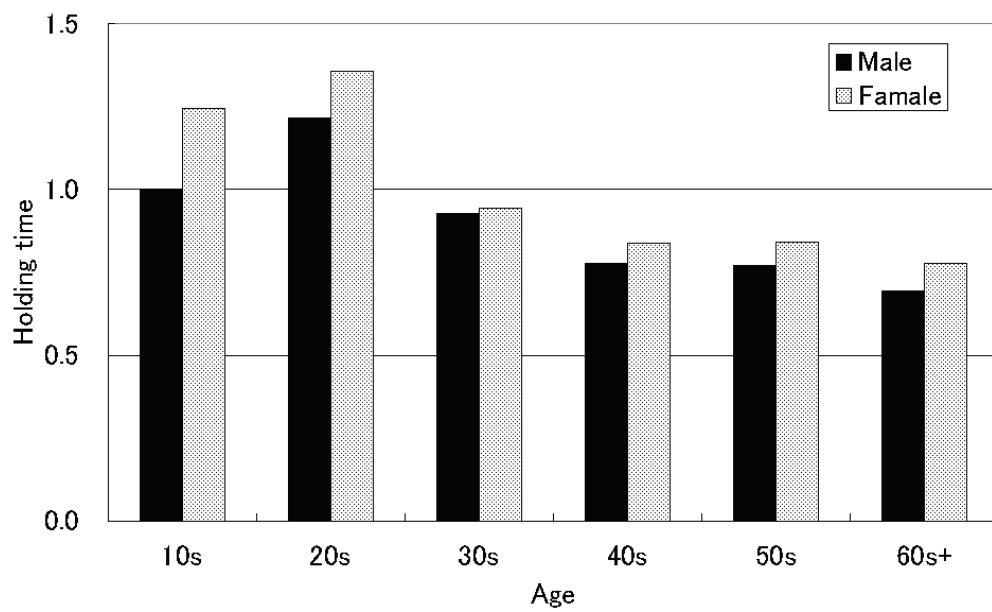
We assumed the number of simulation users to be 2339, which is same as the number of respondents to the survey shown in Figure 5-14 (c) and Figure 5-14 (d). Also, we utilized the same attribute distribution as existed for the respondents, as shown in Table 5-2. Other simulation parameters were the same as those of the experiment described in Section 5.5.1 and the mobility model was assumed to be that of Case 5, which applies to the pedestrian mobility model in the situation of a fireworks display.

**Table 5-2. Number of survey respondents.**

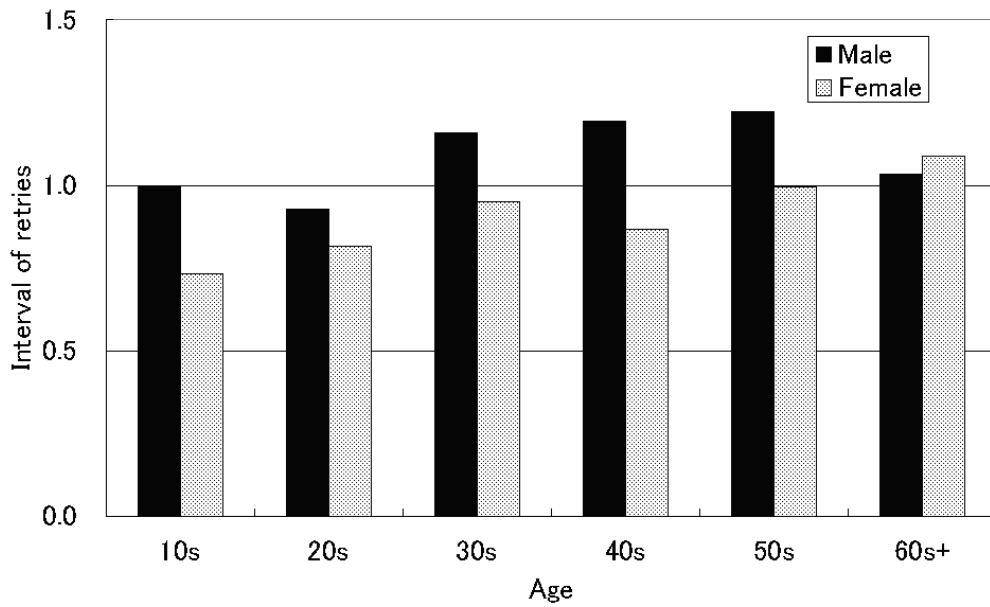
	10s	20s	30s	40s	50s	60s+
Male	149	266	232	221	210	112
Female	151	227	216	225	220	110



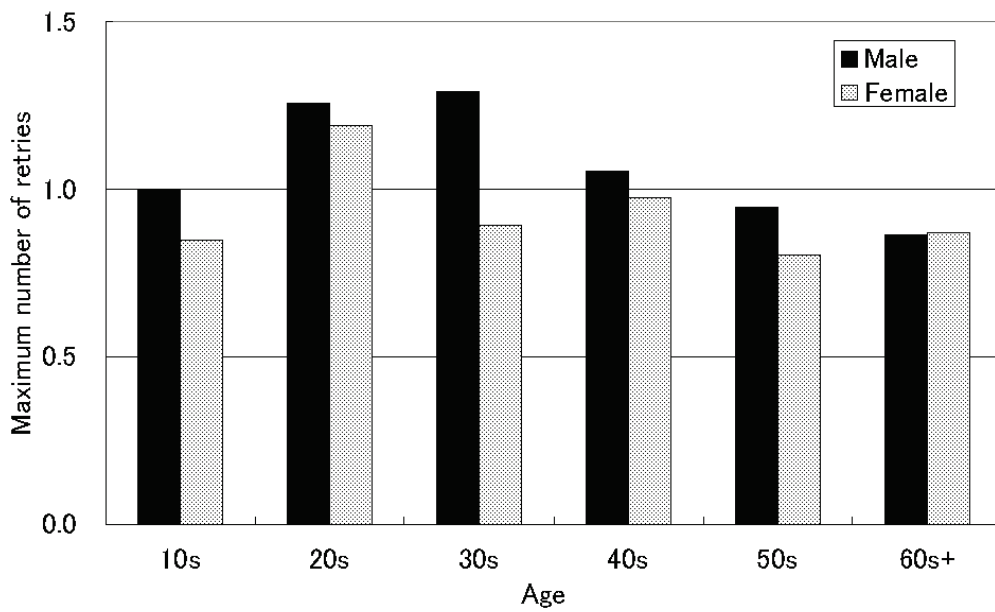
(a) Number of phone calls



(b) Holding time



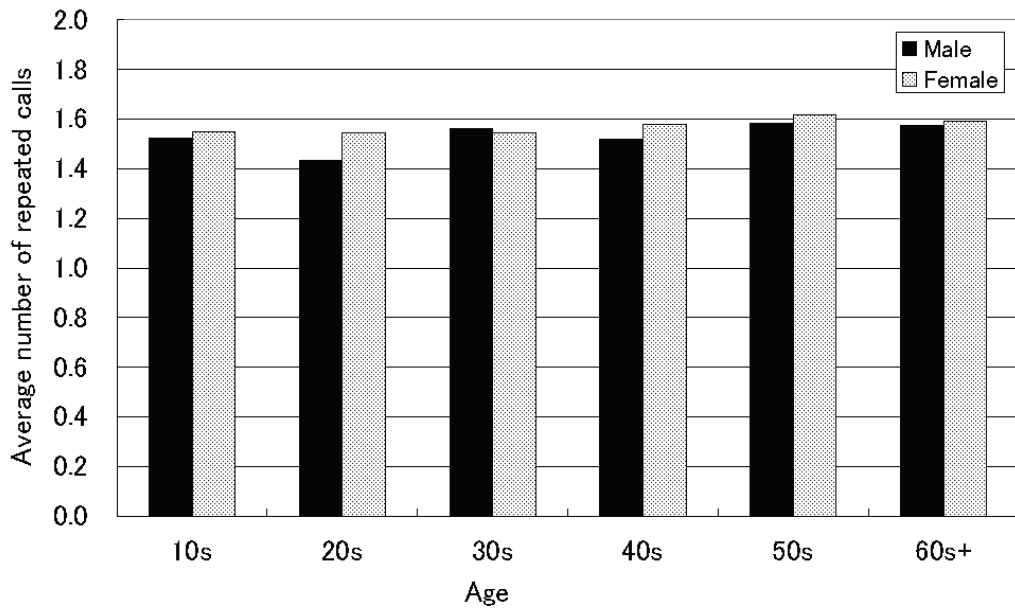
(c) Interval of retries



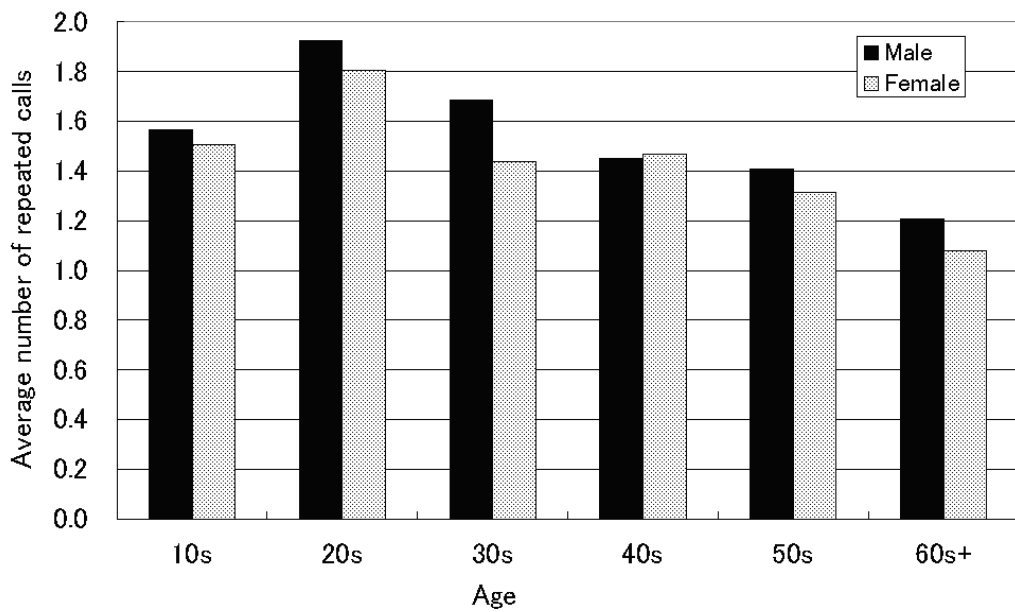
(d) Maximum number of retries

Figure 5-14. Communication behavior trend on attributes (gender, age).

Figure 5-15 shows the mean values of the number of retries per call for users with different attributes. The number of retries is one of the evaluation metrics resulting from a variety of types of communication behavior by the user, and is influenced by the various parameters, that is the number of phone calls, holding time, interval between retries, and maximum number of retries, defined in the simulation scenarios. The horizontal axis of the figure indicates age and the vertical axis indicates mean value of number of retries. Figure 5-15 (a) shows the results of scenario 1, using the common profile, while Figure 5-15 (b) shows the results of scenario 2, using the twelve profiles which depended on the attributes of gender and age. The results in scenario 1 show that there is no difference in the number of retries for users with different attributes. This means that this simulation in scenario 1 cannot reflect the diversity of communication behavior which depends on user attributes. On the other hand, the results in scenario 2 using 12 profiles which differ according to users' attributes show that there is a significant difference in number of retries for users of different genders and ages. Therefore, the developed communication behavior description enables simulations to represent the detailed communication behavior of different categories or users with different attributes, as opposed to the conventional method of treating all users uniformly. In other words, we can simulate realistic communication behavior by directly using traffic logs of real customers, and improve the simulation validity. Moreover, as it is possible to represent each individual user, we can evaluate new metrics which may vary for each user, such as customer satisfaction.



(a) Scenario 1 (1 profile)



(b) Scenario 2 (12 profiles)

Figure 5-15. Average number of repeated calls vs. user attributes.

## 5.6 Conclusion

We have investigated the functional requirements for achieving an evaluation platform based on our proposed concept of a user and network integrated simulation which is able to represent individual user behavior in a realistic situation. We also have implemented a real map loading function, pedestrian mobility, and a user behavior model to meet the requirements. In addition, we have evaluated the simulator that includes the developed functions, and shown that differences in the mobility model and in the communication model definitely influence the simulation results. This means that in evaluations of the performance of mobile networks it is both important and effective to take realistic and detailed user mobility and communication behavior into consideration.

# 6 A Performance Improvement of Large-Scale ITS Wireless System Simulations by Abstract Interference Model

## 6.1 Introduction

Research and development is underway on wireless communication systems for the Intelligent Transport System (ITS), which aims to realize safe driving support, platoons, and information delivery to vehicles. In this R&D, it is necessary to evaluate the performance of a large-scale system under a variety of scenarios. Simulation-based evaluation is effective in the early stage of research. Later, in the development stage in which a realistic system is in sight, it is more effective evaluate system performance using a prototype system or a combination of a prototype system and a simulator which are linked via a virtual network and operate in an integrated manner. Since the use of an abstract model impacts simulation accuracy, there is a tradeoff between speed and accuracy. The required accuracies basically depend on target systems and metrics to be evaluated. For example, if we evaluate satisfactions for individuals, we need to simulate each users described in the Chapter 5. However, if we evaluate total system usages, we may not need to simulate each uses. In this chapter, we propose an abstract model that focuses on pathloss calculations and fading calculations in order to speed up simulation with a minimum impact on simulation accuracy. The number of pathloss calculations is reduced by using cached pathloss values when the received signal power is below a threshold. Similarly, the number of fading calculations is reduced by omitting the calculation when the received signal power is below a threshold.

We first describe how a received frame is processed in simulating a wireless network, and factors that increase simulation time. We then propose a method of reducing simulation time by reducing the number of pathloss calculations and fading calculations. The proposed method has been implemented in a network simulator. Finally, how the method affects simulation time and simulation result is discussed.

## 6.2 Simulation of an ITS wireless system

In an ITS wireless system that uses a wireless LAN, a packet transmitted by a node is received by all the surrounding nodes. If each of  $n$  nodes transmits a packet,  $n \times (n-1)$  packet reception events occur. In the Basic Safety Message (BSM) [72], which is applicable to ITS safe driving support systems, a frame is broadcast by each vehicle every 100 milliseconds. If there are 1,000 vehicles equipped with the BSM capability, a simulation over a period of one second needs to handle about 10 million frame reception events. Since the number of calculations in simulation is proportional to the number of packet reception events, simulation time is proportional to the square of the number of nodes.

A packet reception in a wireless LAN system is processed in the following manner in commonly used wireless network simulators, such as Scenargie [85] and QualNet [62]:

1. The transmitting node processes its transmission event from the physical layer to the application layer.
2. It registers a frame reception start event and a frame reception end event with surrounding receiving nodes.
3. Each receiving node determines whether to receive a frame, based on the probability of bit errors for the current SINR over a period from the reception start to the reception end.
4. If a frame is received correctly, the receiving node processes the reception event at the MAC and upper layers.

In 3 above, it is necessary to calculate the SINR, which is defined by Formula 6-1. The value is calculated from the received power of both the target and interfering signals and the noise power.

$$SINR = \frac{P_R}{N + \sum P_I} \quad \dots \text{Formula 6-1}$$

where  $P_R$  is the received power of the target wave (mW),  $P_I$  is the received power of the interfering signal (mW), and  $N$  is the power of noise (mW).

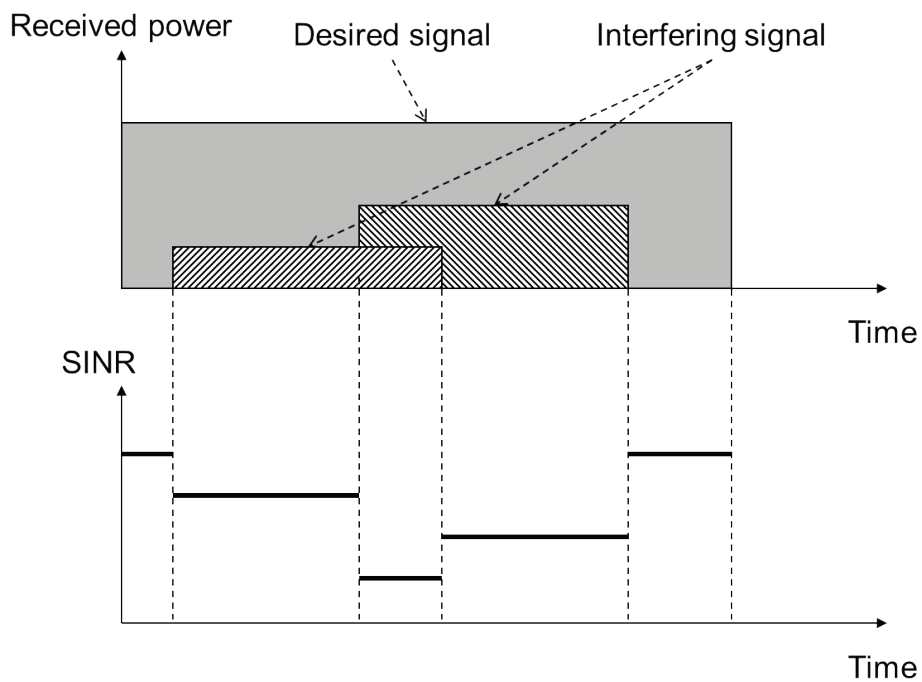


**Figure 6-1. Arrivals of interfering signals and change in SINR.**

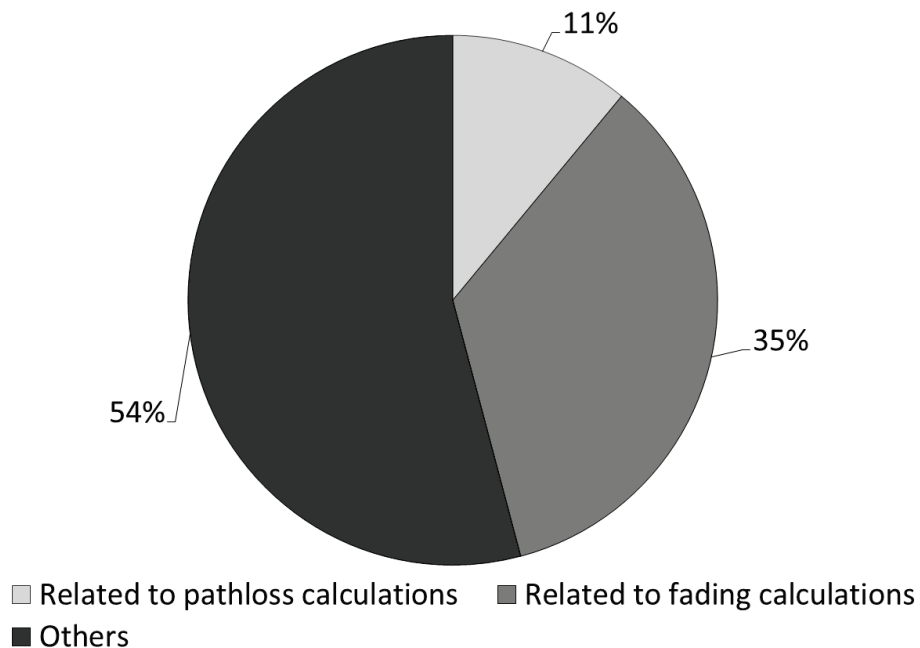
Figure 6-1 shows a conceptual diagram of how the SINR changes when multiple interfering signals have arrived. While a frame is being received, the SINR varies depending on the received power of interfering signals. Consequently, the probability of correct reception also varies. To determine whether a frame can be received or not, it is necessary to know not only the received power of the target wave but also those of interfering signals. The received power is defined by Formula 6-2. The propagation loss is determined by the path attenuation (pathloss) due to distance and shielding objects and by instantaneous variations in attenuation due to the presence of multiple paths.

$$P_R[\text{mW}] = \frac{P_T}{L} \quad \dots \text{Formula 6-2.}$$

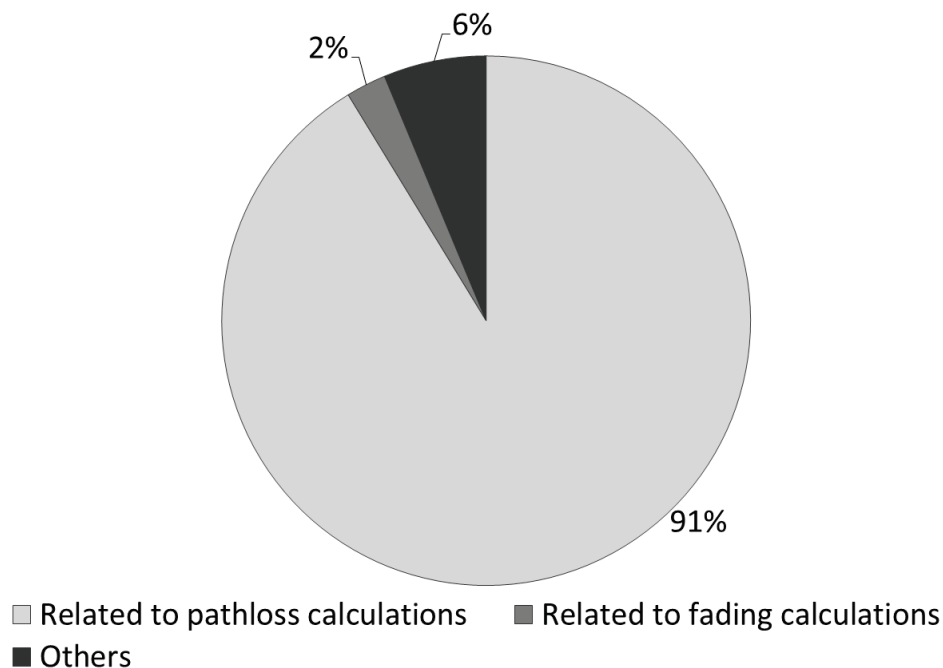
where  $P_T$  is the transmission power (mW), and  $L$  is the propagation loss.

Figure 6-2 shows a breakdown of simulation runtime when a system simulator, Scenargie, is used to simulate an ITS scenario, in which 200 vehicles broadcast packets periodically. In this chapter, we use two radio propagation models: a 2-ray model [86] and a model defined in ITU-R P.1411 [87]. (Other parameters used in our simulation are described in Section 6.4.1.) Figure 6-2 indicates that pathloss calculations and fading calculations account for the major part of the calculation time. Therefore, reducing the number of these calculations is high effective in reducing simulation runtime.

As is discussed above, to speed up the simulation of an ITS wireless system, it is important to reduce the number of calculations related to the processing of frame reception events, in particular, the number of pathloss calculations and fading calculations. The result of pathloss and fading calculations is directly associated with the SINR, and has an impact on determining whether a frame should be received or not. It is necessary to develop an abstract model that minimizes the effect of this on simulation result.



(1) In the case of two-ray ground reflection model



(2) In the case of ITUR-R P.1411

**Figure 6-2. Proportions of simulation runtime.**

### 6.3 Abstract model

As mentioned above, a key to speeding up simulation of an ITS wireless system is to reduce the amount of calculations related to radio propagation. For this purpose, we propose an abstract model for pathloss calculations and fading calculations.

#### 6.3.1 Speeding up pathloss calculations

A way to speed up pathloss calculations is not to calculate pathloss values for every frame broadcast, but reuse cached pathloss values when the change in the location of the transmitting node or the receiving node is small. The pathloss value is calculated based on the distance between the transmitting and receiving nodes. If the change in the distance between the two nodes is small, the change in the pathloss value is also small. It is important to select the right granularity in node location data. This method is used in an existing network simulator [85]. We propose to enhance this method by dynamically changing the granularity of change in the inter-node distance that causes update of location data, in accordance with

the level of the received power. For example, when the radio propagation model used is the 2-ray model [86], and when the transmitting power is 20 dBm, the receiving power decreases with the distance as shown in Figure 6-3. It is assumed that the antennas of both the transmitting and receiving nodes are 1.5 m high. In the 2-ray model, the pathloss value can be expressed in the following approximate equation. It is approximately proportional to the 4-th power of the distance.

$$L_P[\text{dB}] = 40\text{Log}(d) - 20\text{Log}(h_T) - 20\text{Log}(h_R) \quad \dots \text{Formula 6-3.}$$

where  $L_P$  is pathloss,  $d$  is the distance [m] between the transmitting and receiving nodes,  $h_T$  and  $h_R$  are the heights of antennas of the transmitting and receiving nodes, respectively.

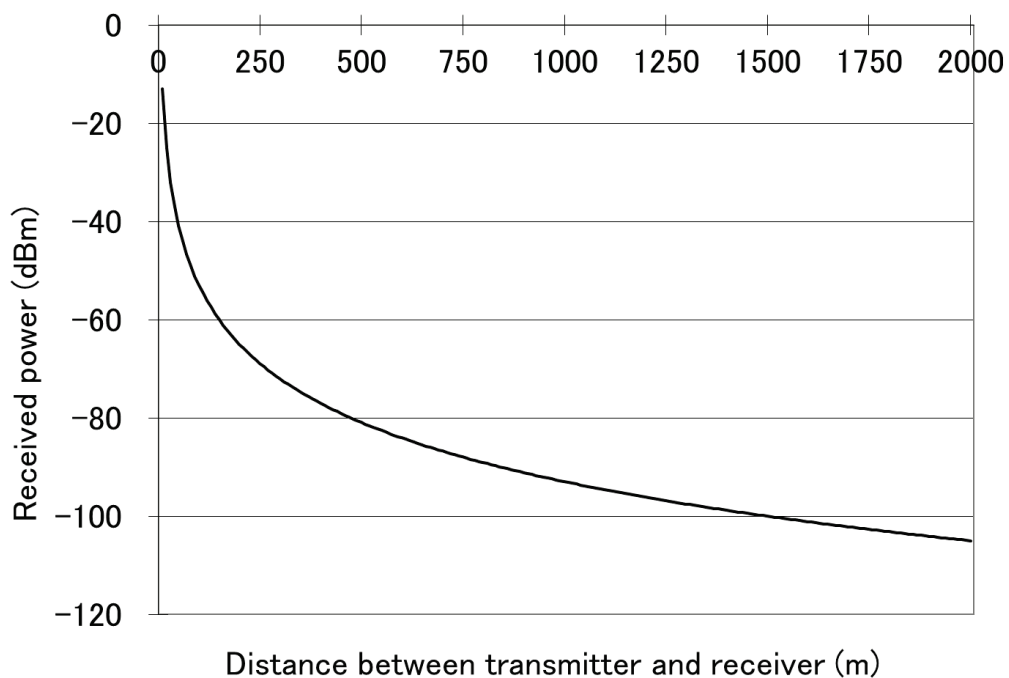


**Figure 6-3** Received power calculated with two-ray ground reflection model.

When the distance between the two nodes changes by 20 m, from 100 m to 120 m, the received power changes by 3.17 dB. However, when the distance between the

two nodes also changes by 20 m, but from 1,000 m to 1,020 m, the received power changes only by 0.34 dB. In other words, in a case where the distance between the two nodes is short, the impact of the change in the distance on the received power is large, but when the distance is long, the impact is small. In this chapter, we also use the ITU-R P.1411 model [87] as a radio propagation model. This model takes account of shielding effects, and is often used in simulating inter-vehicle communication in the ITS. Although the equation used for line-of-sight (LOS) communication is different from that used for non-line-of-sight (NLOS) communication in this model, the pathloss value in both of these equations are functions of the inter-node distance, and thus the trend of how the pathloss changes with the inter-node distance is the same as that of the 2-ray model.

Therefore, we propose to reduce the frequency of calculating pathloss by using the normal granularity (e.g., 1 m) of the change in distance that causes update of the location data in cases where the distance between the transmitting and receiving nodes is relatively small, and the received power is no lower than a certain threshold, and by using a larger granularity (e.g., 10 m) in cases where this distance is relatively long, and the received power is lower than the threshold. In either case, the receiving power is that before taking account of fading.

In this method, we can reduce the number of pathloss calculations by reusing cached pathloss values in cases where the impact of the distance on the received power is small (i.e., the received power is lower than the threshold). The normal pathloss calculation is carried out in cases where the change in the distance has a great impact on the received power (i.e., the received power is no lower than a threshold). The frequent use of cached data can an adverse impact on simulation accuracy but this impact is limited because the change in the received power is relatively small. Since only the latest pathloss data (8 Bytes) is cached for each node pair, the cache size is limited. The cache memory size is extremely small compared to the memory size used in the entire simulation. Hereinafter, the method proposed above to speed up pathloss calculations is referred to as the “pathloss calculation optimization.”

### 6.3.2 Speeding up fading calculations

In addition to the pathloss value, which depends on the inter-node distance, fading, which arises from the presence of multiple propagation paths, greatly affects the received power in a radio propagation environment. Figure 6-4 shows short-term variations of the received power, assuming Rayleigh fading that arises in accordance with the Jakes model [88]. While it is important to take account of the effect of fading if we are to simulate a wireless network accurately, fading

calculations require a relatively large amount of computation as mentioned in Section 6.2. We have studied how to speed up fading calculations. Consider a case where the levels of the received power of the target wave, interfering signal 1, and interfering signal 2 are -50 dBm, -70 dBm, and -90 dBm, respectively, and the thermal noise is -94dBm (assuming a noise figure of 10 dB, a channel bandwidth of 10MHz, and temperature at 290 °K). When the received power of inference wave 1 changes from -70 dBm to -65 dBm, the SINR changes from 19.9 dB to 15.0 dB. However, when the received power of interfering signal 2 changes from -90 dBm to -85 dBm, the SINR changes by only 0.1 dB, from 19.9 dB to 19.8 dB. In other words, while a change in the received power of a relatively strong interfering signal has a great impact on the SINR, a change in the received power of a relative weak interfering signal has only a small impact on the SINR. In addition, when the noise is large, the impact of a change in the received power of an interfering signal on the SINR is small.

So, we propose a method in which fading calculations are carried out when the received power is no lower than a certain threshold but are omitted when the received power is lower than the threshold.

When a node receives a frame, it measures the received power of the frame. If the power is high, the frame affects the SINR greatly and consequently is likely to have a great impact on the determination of whether to process the frame. For such a frame, fading is calculated as usual. However, if the received power of a frame received is low, its fading calculation is omitted, thereby reducing the amount of computation. Although such omission has an adverse impact on simulation accuracy, the impact is limited because fading calculations are carried out for frames whose received power is high. Hereinafter, the method proposed above to speed up fading calculations is referred to as the “fading calculation optimization.”

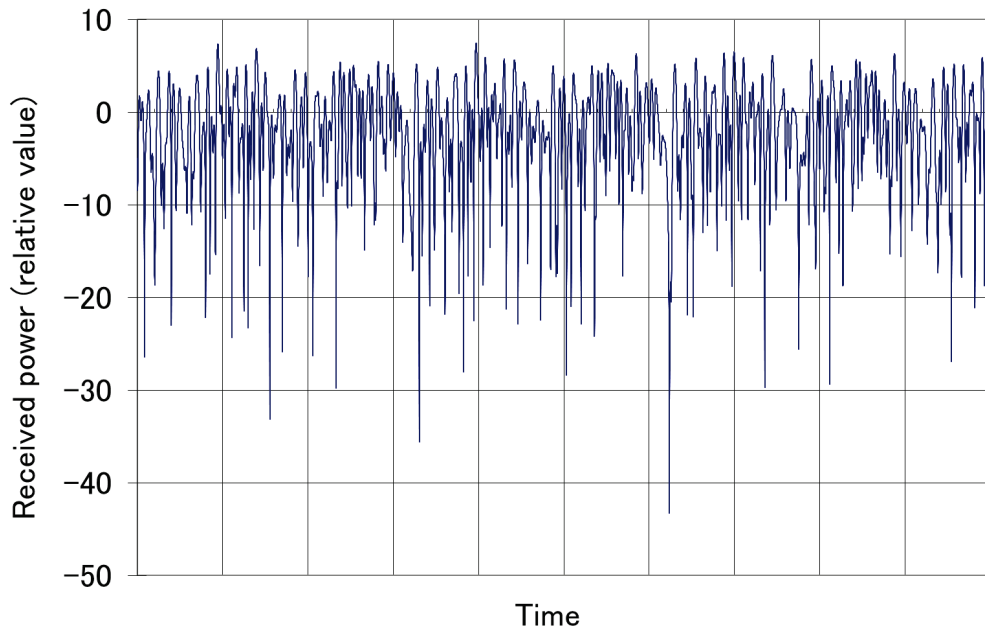


**Figure 6-4 Short-term fluctuation of received power by fading.**

## 6.4 Performance evaluation

To verify how effective the above-proposed method of speeding up pathloss and fading calculations is, we have implemented the method in a system simulator, Scenargie [85], and evaluated simulation runtime and simulation accuracy.

### 6.4.1 Simulation scenario

We have developed a simulation scenario of an ITS wireless system that uses inter-vehicle communication, as shown in Table 6-2. Targeting simulation of a large-scale network, we considered five different numbers of vehicles equipped with communication capability: 200, 400, 600, 800, and 1000. The scenario assumed a safe driving support system. Specifically, each vehicle transmits its vehicle information to surrounding vehicles every 100 milliseconds using CBR broadcast. The communication system used is IEEE802.11p, which is used in ITS wireless systems for inter-vehicle communication. UDP/IP is used at the upper layer. IEEE802.11p is an IEEE802.11 system with its channel bandwidth and parameters of EDCA (Enhanced Distributed Channel Access) expanded for the purpose of ITS wireless communication. As do other wireless LAN systems, such as IEEE802.11a/b/g/n, it uses CSMA/CA for access control. Therefore, the method

proposed in this thesis is applicable even when other wireless LAN systems are applied. Two radio propagation models were considered: a 2-ray model and the model specified in ITU-R P.1411. The 2-ray model assumes an ideal environment in which there are no shielding effects of buildings. Its pathloss value is determined based on the channel frequency and the distance between the transmitting and receiving nodes. The ITU-R P.1411 model is more realistic and takes the shielding effects of buildings into consideration. Its pathloss value is determined based not only on the distance between the transmitting and receiving points but also on whether there is a line of sight. We assumed a road network of a 2-km square, shown in Figure 6-5. There is one lane (with a width of 7.5 m) each way. The roads form a grid with intervals of 200 m. It is assumed that 10-m-high buildings stand outside the roads. The mobility model used is the Gis-Based Random Waypoint model, in which vehicles move along roads. With the scenario shown in Table 6-2, the longest distance that packets can reach is 632 m if there is no interference. Therefore, irrespective of where a packet transmitting vehicle is, there are always vehicles that are located at points that can be reached by packets transmitted and vehicles that are located at points that cannot be reached by the packets. Thus, evaluation can be conducted without being affected by an uneven distribution of vehicles. The pathloss value is determined by the distance between the transmitting and receiving nodes in the case of the 2-ray model, and by this distance and the presence or absence of a line of sight in the case of the ITU-R P.1411 model. The proposed method can be applied to other topologies because the principle of pathloss calculation is not affected by the topology of the road network.

Under this scenario, 3.98 million pathloss and fading calculations occur in the case where the number of vehicles is 200, and 99.9 million calculations in the case where the number of vehicles is 1,000. The simulation runtime and simulation accuracy have been evaluated for three cases: a case with the pathloss calculation optimization, a case with the fading calculation optimization, and a case with the optimization of both the pathloss and fading calculations. The simulation runtime was evaluated using a computer that satisfies the specification shown in Table 6-1. We used the packet reception ratio at the application layer to evaluate simulation accuracy. The packet reception ratio of node  $i$  is defined by Formula 6-4. When a packet transmitted by a node is successfully received by all the other nodes, the packet reception ratio is 1 (or 100%). (Hereinafter the ratio is expressed in a percentage.) The average and variance of packet reception ratios are those of the packet reception ratio of each node for all the nodes when a certain initial location is given. We evaluated not only the average but also the variance of packet reception ratios in order to examine the effect of the optimizations on simulation accuracy closely.

Packet reception ratio at node  $i$  = number of packets received by node  $i$  divided by number of packets received by any of the nodes other than node  $i$

...Formula 6-4.

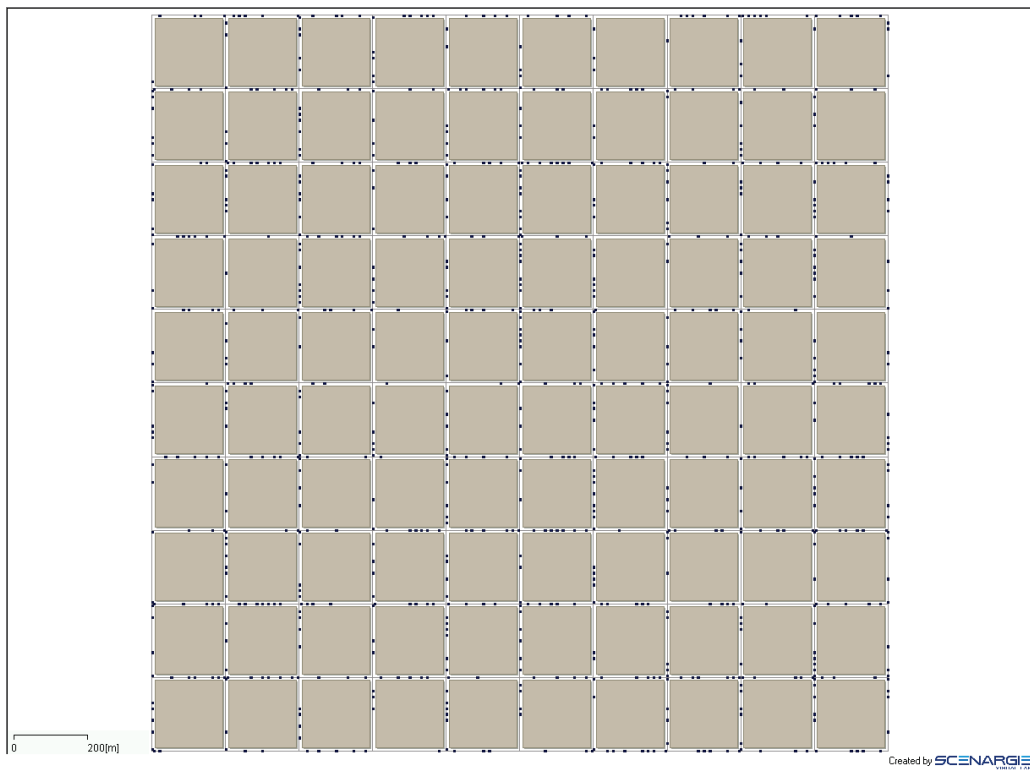


**Figure 6-5. Simulation topology.**

**Table 6-1. Computer specification.**

OS	CentOS 5.8 64bit
CPU	i7-2770k Quad Core 3.5 GHz
Memory	32 GB (DDR3-1333)

**Table 6-2. Scenario.**

Number of vehicles	200/400/600/800/1000
Application	CBR broadcast (transmission interval: 100 milliseconds; data payload: 128 Bytes)
System model	UDP/IP, IEEE802.11p
Data rate	3 Mbps (BPSK 1/2)
Transmission power	20 dBm
Carrier sensing level	-85 dBm
Channel frequency	5.9 GHz
Mobility model	Gis-Based Mobility Model [85] (Minimum speed: 15 m/s; maximum speed:20 m/s)
Propagation model	Two-ray ground reflection model [86] and ITU-R P.1411 [86]
Thermal noise	Noise figure: 10dB; temperature: 290 K
Simulation time	10 seconds

#### 6.4.2 Effect of the pathloss calculation optimization

This section evaluates the effect of the pathloss calculation optimization.

We start with the 2-ray model. Figure 6-6 shows simulation runtime for cases where the received power threshold was varied from -105 dBm to -85 dBm at intervals of 5 dB and where the number of vehicles involved was varied from 200 to 1,000. The simulation runtime is expressed as a relative value with the runtime of the conventional method being 100%. The simulation runtime (absolute time) of the conventional method was 23 seconds (with 200 vehicles), 98 seconds (with 400 vehicles), 234 seconds (with 600 vehicles), 433 seconds (with 800 vehicles), and 699 seconds (with 1,000 vehicles). The granularity of the distance triggering location data update was 1 m when the received power was no lower than the threshold, and 10 m when it was lower than the threshold. As shown in Figure 6-6, the pathloss calculation optimization can reduce simulation runtime by up to 8%. The effect of the optimization can be increased by raising the threshold, which causes cached pathloss data to be used more frequently. While only 20% of pathloss calculations used cached data in the conventional method, up to 64% of calculations used cached data in the proposed method when the received power threshold was -85 dBm. To examine the effect of the optimization on simulation accuracy, the average and variance of packet reception ratios (%) are compared as shown in Table 6-3. Neither the average nor the variance of the packet reception

ratios varied greatly irrespective of whether the number of vehicles was 200 or 1,000 (the maximum difference is less than 0.5%). So, the impact of the optimization on the simulation accuracy is very limited.

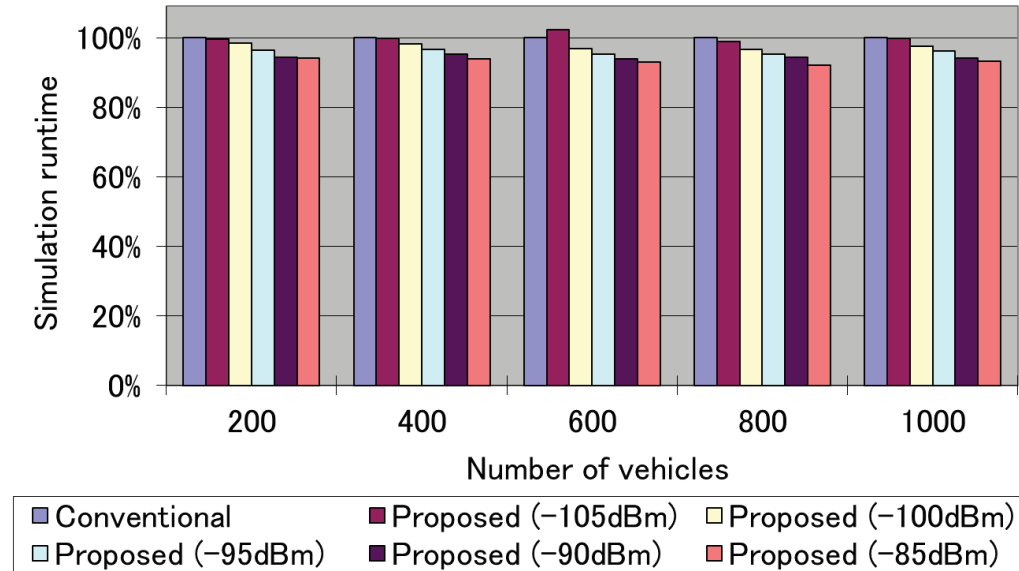


Figure 6-6. Runtime performance with the pathloss calculation optimization (Two-ray ground reflection model).

Table 6-3. Average and variance of packet reception ratios (%) (Two-ray ground reflection model).

(1) 200 vehicles

	Conventional	Proposed (-105dBm)	Proposed (-100dBm)	Proposed (-95dBm)	Proposed (-90dBm)	Proposed (-85dBm)
Average	12.76	12.76	12.78	12.78	12.75	12.76
Variance	6.27	6.27	6.27	6.28	6.25	6.26

(2) 1000 vehicles

	Conventional	Proposed (-105dBm)	Proposed (-100dBm)	Proposed (-95dBm)	Proposed (-90dBm)	Proposed (-85dBm)
Average	2.60	2.61	2.60	2.60	2.61	2.61
Variance	0.39	0.39	0.39	0.38	0.40	0.39

Figure 6-7 and Table 6-4 show simulation results for cases where the ITU-R P.1411 model was used. With the conventional method, the simulation runtime was 117 seconds (with 200 vehicles), 478 seconds (with 400 vehicles), 1,094 seconds (with 600 vehicles), 1,932 seconds (with 800 vehicles), and 3,052 seconds (with 1,000 vehicles). Figure 6-7 shows that the pathloss calculation optimization reduced simulation runtime by 60% or more. Unlike the 2-ray model, the ITU-R P.1411 model takes the presence/absence of a line of sight between buildings and diffraction into consideration. Therefore, this model requires more calculations than the 2-ray model, in which the amount of calculations depends only on the distance between the transmitting and receiving nodes and antenna heights. In addition, since the proportion of the pathloss calculations in the entire simulation runtime in this model is greater than that of the 2-ray model, the benefit of the optimization is also greater. As shown in Table 6-4, the percentage of the maximum error of the average packet reception ratio was as low as less than 1% (variance: 0.54 with 200 vehicles, and 0.13 with 1,000 vehicles). In other words, simulation runtime can be reduced dramatically while maintaining the accuracy of the simulation result. The simulation runtime and packet reception ratios varied little even when the received power threshold was changed. This is because the transmitting and receiving nodes had no line of sight in many cases in the ITU-R P.1411 model. In fact, 97% of the transmitting and receiving node pairs had no line of sight when the received power threshold was -85 dBm, and 90% when it was -105 dBm. This percentage varied by only up to 7% in cases where the received power threshold was between these two extreme cases. Cached data were used only 20% of calculations in the conventional method, but was used 75% of calculations in the proposed method. This explains why the number of pathloss calculations was reduced dramatically.

In summary, when the proposed optimization is applied in proportion to the percentage of pathloss calculations in the entire simulation, it can reduce simulation runtime by several percent to 60% with a minimum impact on simulation accuracy.

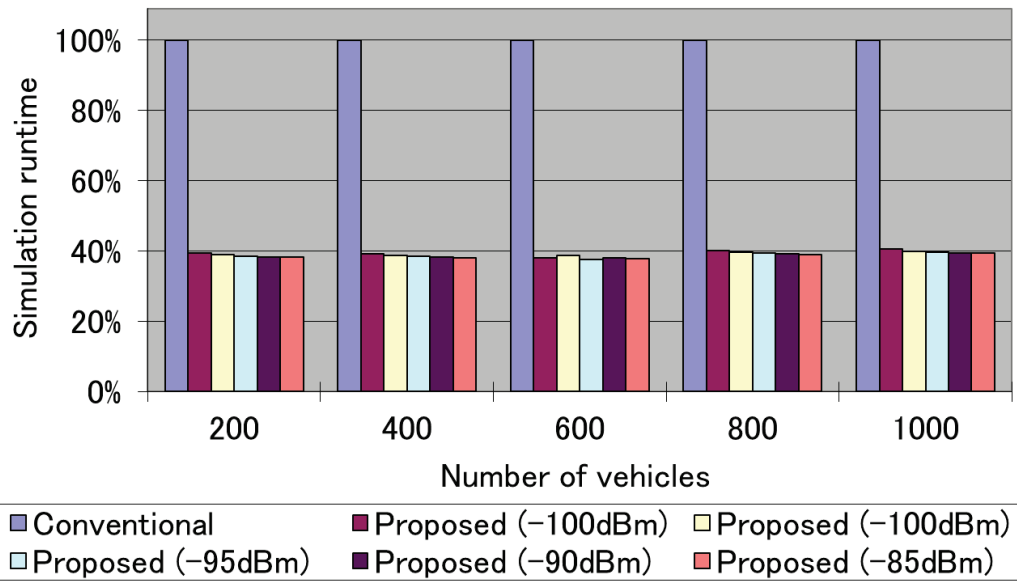


Figure 6-7. Runtime performance with the pathloss calculation optimization (ITU-R P.1411).

Table 6-4. Average and variance of packet reception ratios (%) (ITU-R P.1411).

(1) 200 vehicles

	Conventional	Proposed (-105dBm)	Proposed (-100dBm)	Proposed (-95dBm)	Proposed (-90dBm)	Proposed (-85dBm)
Average	1.80	1.78	1.78	1.78	1.78	1.78
Variance	0.54	0.53	0.53	0.53	0.53	0.53

(2) 1000 vehicles

	Conventional	Proposed (-105dBm)	Proposed (-100dBm)	Proposed (-95dBm)	Proposed (-90dBm)	Proposed (-85dBm)
Average	1.62	1.61	1.61	1.61	1.60	1.60
Variance	0.13	0.13	0.13	0.13	0.13	0.13

### 6.4.3 Effect of the fading calculation optimization

This section examines how effective the fading calculation optimization is. The scenario described in Section 6.4.1 was used as with the pathloss calculation optimization, and the two radio propagations models were also used.

We will first discuss the case where the 2-ray model was used. Figure 6-8 shows simulation runtime in cases where the received power threshold was varied from -105 dBm to -85 dBm in the intervals of 5 dB and where the number of vehicles was varied from 200 to 400, 600, 800 and 1,000 vehicles. The simulation runtime is expressed as a relative value with the runtime of the conventional method, which uses no abstract model, being 100%. Table 6-5 compares the average and variance of packet reception ratios (%) for a case where the number of vehicles was 200 with those of a case where the number of vehicles was 1,000. As shown in Figure 6-8, simulation runtime can be reduced by as much as 50% depending on the threshold for triggering a fading calculation. In the 2-ray model, the proportion of the pathloss calculation in the entire simulation runtime is much smaller than that of the fading calculation. Therefore, unlike the case of the pathloss calculation optimization described in Section 6.4.2, simulation runtime can be reduced significantly. The number of fading calculations can be reduced by 4% in the case where the received power threshold was -105 dBm, and by 77% in the case where the threshold was -85 dBm. As shown in Table 6-5, changes in the average and variance of the packet reception ratios were small if the threshold was -90 dBm or lower, but the average packet reception ratio changed by 10% when the threshold was -85 dBm. This means that the impact of the fading calculation optimization on simulation accuracy is not negligible. A close analysis of the simulation result reveals that some of the signals that were received as the target signals in the conventional method cannot be received in the proposed method because their preambles cannot be detected as a result of a reduction in the received power or because reception errors occurred as a result of the deterioration in the SINR. Consequently, the number of received frames decreased, and the packet reception ratio decreased by 10% or more. There can be two reasons why this happened. One is that signals that can be received in the conventional method were not subjected to fading calculations because the signal detection level was set to -85 dBm in our scenario. The other reason is that, as a result, the average received power decreased, making it difficult to receive these signals. Therefore, to minimize the impact on simulation accuracy, it is necessary to set the received power threshold to -90 dBm or lower. This adverse impact was not present with the pathloss calculation optimization because, in the abstract model, factors that treat the received power higher than the actual value and factors that treat the received power lower than the actual value balanced out each other, leaving little effect on packet reception.

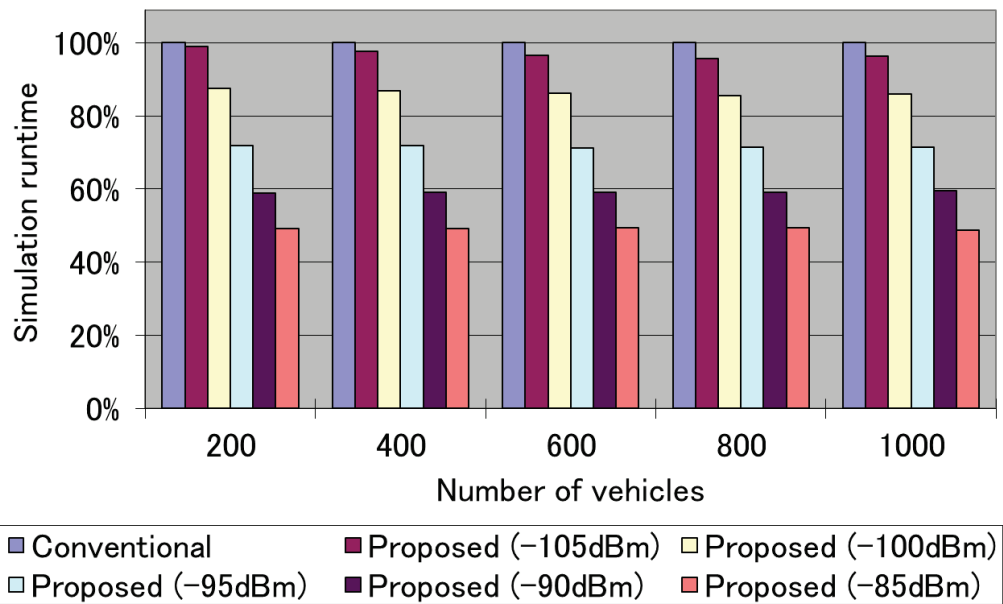


Figure 6-8. Runtime performance with the fading calculation optimization (Two-ray ground reflection model).

Table 6-5. Average and variance of packet reception ratios (%) (Two-ray ground reflection model).

(1) 200 vehicles

	Conventional	Proposed (-105dBm)	Proposed (-100dBm)	Proposed (-95dBm)	Proposed (-90dBm)	Proposed (-85dBm)
Average	12.76	12.77	12.79	12.81	12.64	11.28
Variance	6.27	6.30	6.29	6.26	6.08	5.59

(2) 1000 vehicles

	Conventional	Proposed (-105dBm)	Proposed (-100dBm)	Proposed (-95dBm)	Proposed (-90dBm)	Proposed (-85dBm)
Average	2.60	2.60	2.61	2.60	2.57	2.47
Variance	0.39	0.40	0.40	0.39	0.37	0.35

Figure 6-9 and Table 6-6 show simulation results in the case where the ITU-R P.1411 model was used as a radio propagation model. Figure 6-9 shows that the

fading calculation optimization reduced simulation runtime by 10%. The number of fading calculations was reduced dramatically: by 90% (2.46 million calculations with 200 vehicles) in the case where the received power threshold was -105dBm, and by 97% (61.95 million calculations with 1,000 vehicles) in the case where the threshold was -85dBm. However, since fading calculations form a relatively small proportion in the entire simulation runtime, its impact on simulation runtime is not very large. Table 6-6 shows that the average and variance of packet reception ratios changed very little in the case where the received power threshold was -90 dBm or lower, indicating that the impact on simulation accuracy was small. However, in the case where the threshold was -85 dBm, the average packet reception ratio changed by 10%, showing that it had some impact on simulation accuracy. These results are similar to those for the case where the 2-ray model was used.

In summary, it was confirmed that, by applying the fading calculation optimization taking the proportion of the fading calculations in the entire simulation into consideration, it is possible to reduce simulation runtime by 10 to 40% with a minimum impact on simulation accuracy. As with the 2-ray model, the presence/absence of fading at received power of -85dBm had a large effect on determining whether frames were received or not. Therefore, to reduce the number of fading calculations, it is important to set the received power threshold to -90dBm or lower.

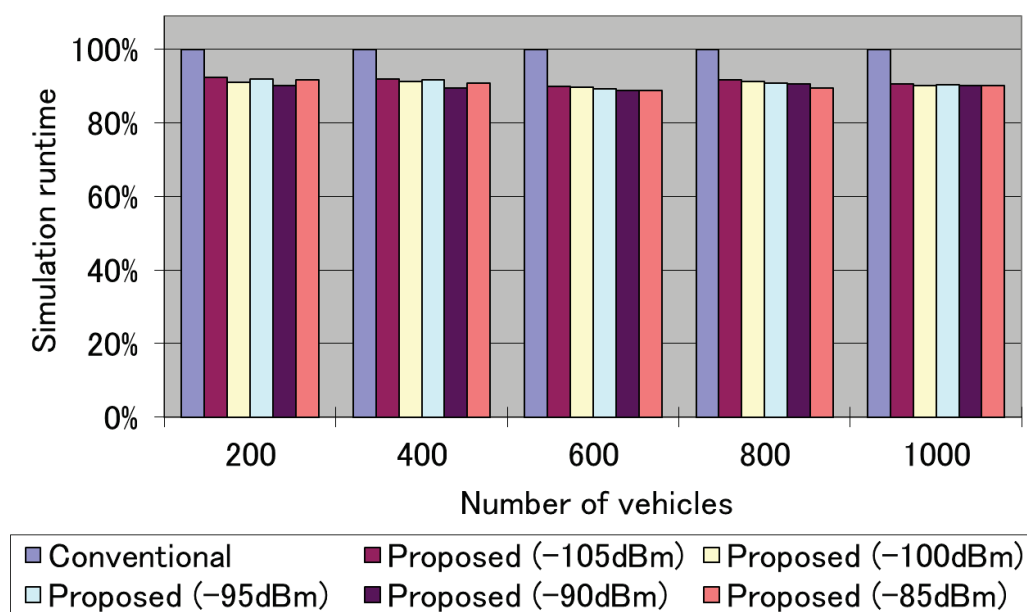


Figure 6-9. Runtime performance with the fading calculation optimization (ITU-R P.1411).

**Table 6-6. Average and variance of packet reception ratios (%) (ITU-R P.1411)**

(1) 200 vehicles

	Conventional	Proposed (-105dBm)	Proposed (-100dBm)	Proposed (-95dBm)	Proposed (-90dBm)	Proposed (-85dBm)
Average	1.80	1.80	1.80	1.80	1.79	1.67
Variance	0.54	0.54	0.54	0.54	0.54	0.51

(2) 1000 vehicles

	Conventional	Proposed (-105dBm)	Proposed (-100dBm)	Proposed (-95dBm)	Proposed (-90dBm)	Proposed (-85dBm)
Average	1.62	1.62	1.62	1.62	1.61	1.50
Variance	0.13	0.13	0.13	0.13	0.13	0.12

#### 6.4.4 Effects of applying both the pathloss calculation and fading calculation optimizations

This section describes the effects of applying both the pathloss calculation and fading calculation optimizations. Simulation results for the case of the 2-ray model are shown in Figure 6-10 and Table 6-7, and results for the case of the ITU-R P.1411 model are shown in Figure 6-11 and Table 6-8.

As shown in Figure 6-10 and Figure 6-11, the simulation runtime was reduced by up to 55% in the case of the 2-ray model, and by up to 70% in the case of the ITU-R P.1411 model. Table 6-7 and Table 6-8 **Error! Reference source not found.** show that it is necessary to set the received power threshold to -90 dBm or lower if we are to minimize the effect of the optimizations on simulation accuracy. Overall, taking the results described in Sections 6.4.2 and 6.4.3 into consideration, we can conclude that the pathloss calculation optimization and the fading calculation optimization improves runtime performance without affecting each other. In a radio propagation model in which the proportion of pathloss calculations is large, the pathloss calculation optimization makes a greater contribution while, in a radio propagation model in which the proportion of pathloss calculations is small, the fading calculation optimization is more effective in improving runtime performance.

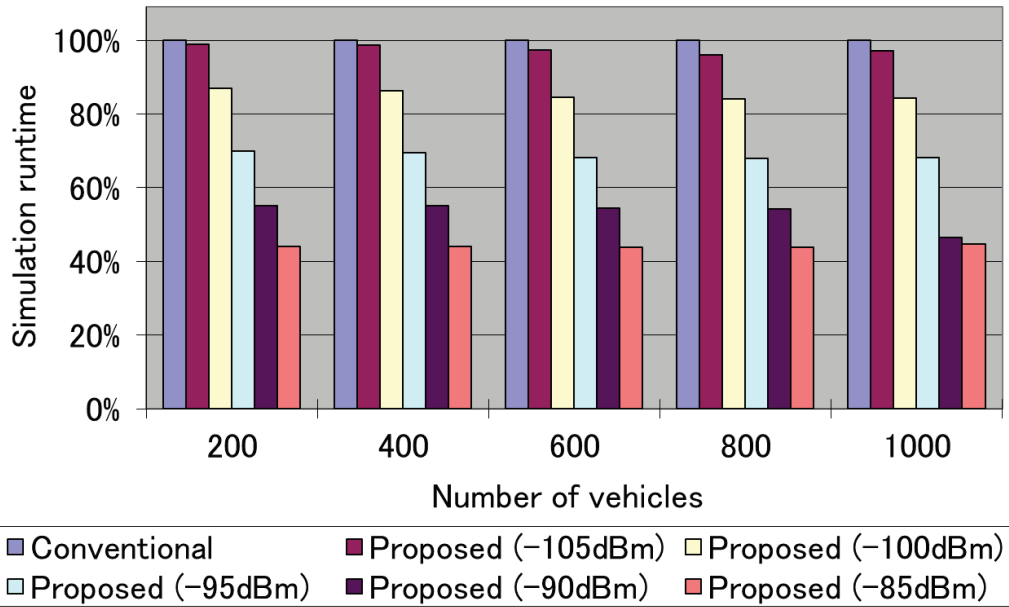


Figure 6-10. Runtime performance with the pathloss and fading calculation optimization (Two-ray ground reflection model).

Table 6-7. Average and variance of packet reception ratios (%) (Two-ray ground reflection model)

(1) 200 vehicles

	Conventional	Proposed (-105dBm)	Proposed (-100dBm)	Proposed (-95dBm)	Proposed (-90dBm)	Proposed (-85dBm)
Average	12.76	12.77	12.78	12.80	12.61	11.28
Variance	6.27	6.30	6.27	6.18	6.06	5.58

(2) 1000 vehicles

	Conventional	Proposed (-105dBm)	Proposed (-100dBm)	Proposed (-95dBm)	Proposed (-90dBm)	Proposed (-85dBm)
Average	2.60	2.61	2.61	2.60	2.58	2.47
Variance	0.39	0.39	0.39	0.40	0.38	0.35

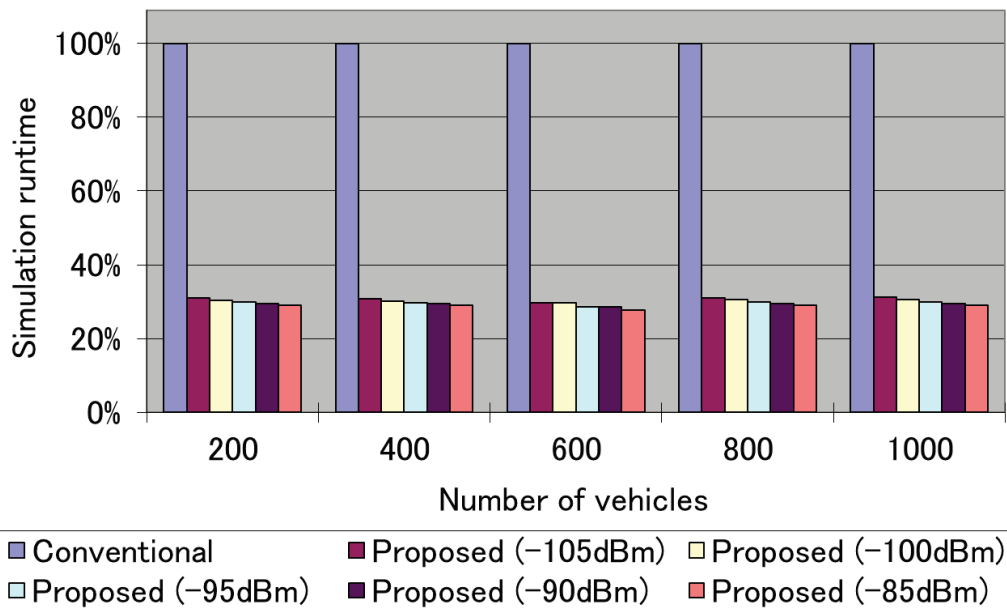


Figure 6-11. Runtime performance with the pathloss and fading calculation optimization (ITU-R P.1411).

Table 6-8. Average and variance of packet reception ratios (%) (ITU-R P.1411)

(1) 200 vehicles

	Conventional	Proposed (-105dBm)	Proposed (-100dBm)	Proposed (-95dBm)	Proposed (-90dBm)	Proposed (-85dBm)
Average	1.80	1.78	1.78	1.78	1.77	1.64
Variance	0.54	0.53	0.53	0.53	0.53	0.50

(2) 1000 vehicles

	Conventional	Proposed (-105dBm)	Proposed (-100dBm)	Proposed (-95dBm)	Proposed (-90dBm)	Proposed (-85dBm)
Average	1.62	1.61	1.61	1.61	1.60	1.49
Variance	0.13	0.13	0.13	0.13	0.13	0.12

Lastly, we examine cases where flooding is used. Flooding is a way of propagating messages by making a node that has received a broadcast message rebroadcast that message. It can be used in the ITS safe driving support system to notify

surrounding vehicles of urgent information, such as information about an accident. Let us consider the following scenario. Node 1 is a transmitting node. It sends a 128-byte message every 100 milliseconds. Other conditions of this scenario are the same as those of the scenario described in Section 6.4.1 and Table 6-2. We evaluated simulation results in terms of the message delivery ratio defined in Formula 6-5 and the message delivery delay defined in Formula 6-6. If a message transmitted is received by all the other nodes, the message delivery ratio is 100%. We use these two criteria because, even when the message delivery ratio is the same, the message delivery delay can vary depending on the number of hops each message experiences. The average and variance of message delivery ratios (or message delivery delays) are those of the packet delivery ratios at each node for all the nodes at when a certain initial location is given.

Message delivery ratio at node  $i$  = number of messages received at node  $i$   
divided by total number of messages transmitted

...Formula 6-5.

Message delivery delay at node  $i$  = average delay of all messages received by  
node  $i$

...Formula 6-6.

where the delay time of message  $m$  at node  $i$  is the period from the time when message  $m$  was transmitted to the time when it was received by node  $i$ . As in the previous sections, the two radio propagation models were used.

Figure 6-12, and Table 6-9 and Table 6-10 show simulation runtime, message delivery ratio, and message delivery delay, respectively, in the case where the 2-ray model was used. Figure 6-12 shows that the two optimizations reduced simulation runtime by up to 55% depending on the received power threshold, as in the case of applying CBR broadcast. Table 6-9 shows that the message delivery ratio was 100% in all cases. Table 6-10 indicates that the message delivery delay varied by only 1 to 2% when the received power threshold was -90 dBm or lower, but by several tens of percent when the received power threshold was -85 dBm. Since a message can reach some vehicles with one hop, the average message delivery delay was 30 milliseconds.

Figure 6-13 and Table 6-11 and Table 6-12 show simulation results in the case where the ITU-R P.1411 was used. It can be seen from Figure 6-13 that simulation runtime can be reduced by up to 70%, as was the case when CBR broadcast was used instead of flooding. Table 6-10 and Table 6-11 reveal that the message delivery delays and the message delivery ratios vary relatively significantly depending on the received power threshold when the number of vehicles involved was 200. In particular, in the case where the received power threshold was -85 dBm, both the average and variance of message delivery ratios differed from those of the conventional method by some 20%. Furthermore, even in the case where the received power threshold was -90 dBm or lower, the average message delivery ratio differed from that of the conventional method relatively greatly, specifically by several to 10 percent. This is because, when flooding is applied, whether a node has received a message successfully or not affects whether other nodes will receive that message successfully or not, and thus affects the message delivery ratio of the entire network especially when the number of vehicles involved is small. If, on the other hand, the number of vehicles involved is 1,000, there are many vehicles that receive the same message and transmit it successfully, and thus the message delivery ratio can reach 100% and the variation of the message delivery delay is relatively small.

From these simulation results, we can conclude that, by combining the two optimizations, it is possible to reduce simulation runtime greatly irrespective of the radio propagation model used. However, when flooding is used for message propagation, whether a single message is received successfully by a vehicle has a great impact on the reception of that message by other vehicles, and consequently on the average message delivery ratio and the average message delivery delay of the entire network.

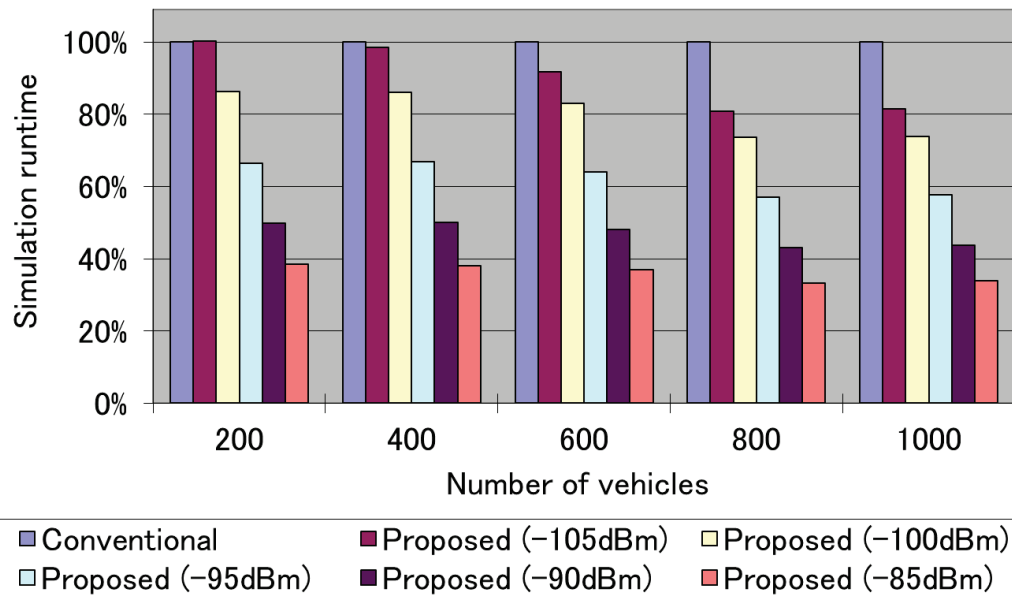


**Figure 6-12. Runtime performance with both pathloss and fading calculation optimizations (Flooding, two-ray ground reflection model).**

**Table 6-9. Average and variance of message delivery ratios (%) (Flooding, two-ray ground reflection model)**

(1) 200 vehicles

	Conventional	Proposed (-105dBm)	Proposed (-100dBm)	Proposed (-95dBm)	Proposed (-90dBm)	Proposed (-85dBm)
Average	100.00	100.00	100.00	100.00	100.00	100.00
Variance	0.00	0.00	0.00	0.00	0.00	0.00

(2) 1000 vehicles

	Conventional	Proposed (-105dBm)	Proposed (-100dBm)	Proposed (-95dBm)	Proposed (-90dBm)	Proposed (-85dBm)
Average	100.00	100.00	100.00	100.00	100.00	100.00
Variance	0.00	0.00	0.00	0.00	0.00	0.00

**Table 6-10. Average and variance of message delivery delays (sec) (Flooding, two-ray ground reflection model).**

(1) 200 vehicles

	Conventional	Proposed (-105dBm)	Proposed (-100dBm)	Proposed (-95dBm)	Proposed (-90dBm)	Proposed (-85dBm)
Average	0.026	0.026	0.026	0.027	0.027	0.033
Variance	0.000	0.000	0.000	0.000	0.000	0.000

(2) 1000 vehicles

	Conventional	Proposed (-105dBm)	Proposed (-100dBm)	Proposed (-95dBm)	Proposed (-90dBm)	Proposed (-85dBm)
Average	0.023	0.023	0.023	0.023	0.025	0.033
Variance	0.000	0.000	0.000	0.000	0.000	0.000

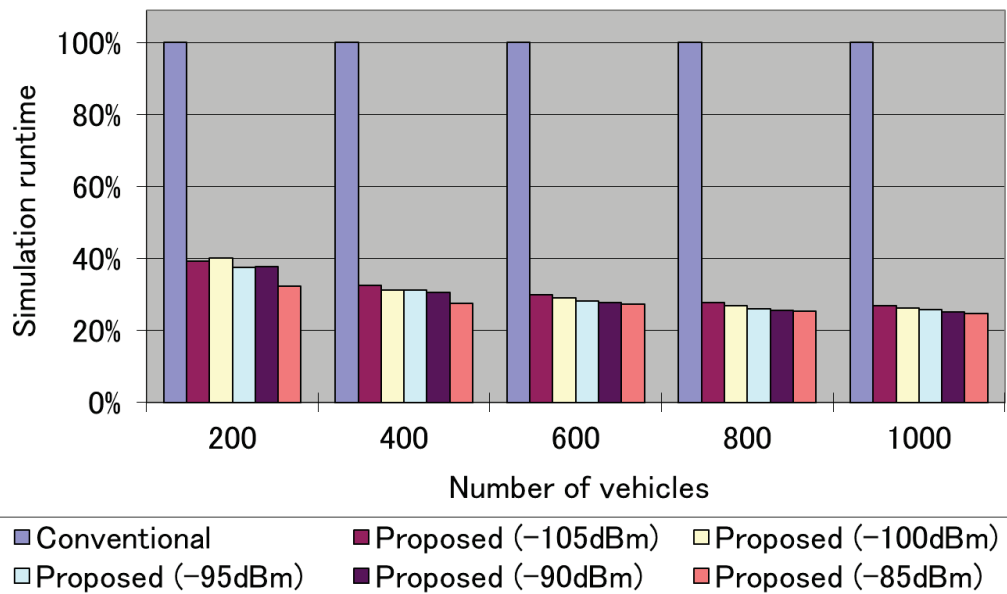


**Figure 6-13. Runtime performance with pathloss and fading calculation optimization (Flooding, ITU-R P.1411).**

**Table 6-11. Average and variance of message delivery ratios (%) (Flooding, ITU-R P.1411).**

(1) 200 vehicles

	Conventional	Proposed (-105dBm)	Proposed (-100dBm)	Proposed (-95dBm)	Proposed (-90dBm)	Proposed (-85dBm)
Average	40.53	37.49	37.89	35.43	36.11	30.97
Variance	144.04	133.07	146.89	149.70	153.55	152.48

(2) 1000 vehicles

	Conventional	Proposed (-105dBm)	Proposed (-100dBm)	Proposed (-95dBm)	Proposed (-90dBm)	Proposed (-85dBm)
Average	100.00	100.00	100.00	100.00	100.00	100.00
Variance	0.00	0.00	0.00	0.00	0.00	0.00

**Table 6-12. Average and variance of message delivery delays (sec) (Flooding, ITU-R P.1411).**

(1) 200 vehicles

	Conventional	Proposed (-105dBm)	Proposed (-100dBm)	Proposed (-95dBm)	Proposed (-90dBm)	Proposed (-85dBm)
Average	0.235	0.233	0.241	0.232	0.235	0.288
Variance	0.008	0.010	0.009	0.008	0.009	0.014

(2) 1000 vehicles

	Conventional	Proposed (-105dBm)	Proposed (-100dBm)	Proposed (-95dBm)	Proposed (-90dBm)	Proposed (-85dBm)
Average	0.112	0.113	0.113	0.113	0.114	0.133
Variance	0.002	0.002	0.002	0.002	0.002	0.003

## 6.5 Conclusion

In this chapter, we have proposed to speed up simulation of a large ITS wireless system by using an abstract model that is designed to reduce the number of pathloss and fading calculations required. Specifically, when the received power of a signal is below a specified threshold, the pathloss and fading calculations are omitted and substituted for by cached data. It has been confirmed that omission of some pathloss calculations achieved in this way can reduce simulation runtime by

up 8% when message propagation is represented by the 2-ray model, and by up to 60% when it is represented by the model defined in ITU-R P.1411. The impact of this omission on simulation accuracy was insignificant. The variation in the average message delivery ratio from that obtained using the conventional method (with no omissions) is only 1% at most. It has also been confirmed that ignoring the effect of fading, i.e., omitting fading calculations, when the received power of a signal is below a threshold can reduce simulation runtime by up to 50% in the case of the 2-ray model, and by up to 10% in the case of the ITU-R P.1411 model. Whether a signal experiences fading at the carrier sense level has a great impact on whether a frame can be received or not. It has been confirmed that it is necessary to set the received sensor threshold to -90 dBm or lower if we are to minimize the effect of the omission of calculations. Furthermore, by combining omissions of both the pathloss and fading calculations, simulation runtime can be reduced by up to 55% in the case of the 2-ray model, and by up to 70% in the case of the ITU-R P.1411 model. However, in cases where the number of vehicles involved is small and flooding is used for propagating messages, whether a message is received by a node or not affects message propagation in the entire network. As a result, omission of some calculations can reduce the message delivery ratio by up to 10%. By omitting some pathloss calculations and some fading calculations, it is possible to reduce simulation runtime dramatically irrespective of the proportion of pathloss calculations in the entire simulation runtime and irrespective of the particular radio propagation model used.

The proposed method can reduce simulation runtime dramatically with a minimal impact on simulation accuracy in the simulation of a wireless system, in particular, the ITS safe driving support system. Looking forward, we will study a threshold other than the received power used in this chapter, such as the SINR. We will also study how to reduce the impact of the proposed method on simulation accuracy by taking account of cases where pathloss values change significantly, such as when a vehicle moves from a site where it has a line of sight to another vehicle to a site where it does not or vice versa in the case of the ITU-R P.1411 model.

## 7 Conclusions

In this thesis, we describe network design and evaluation for photonic and mobile wireless networks. In Chapter 3, we propose network design algorithms that minimize the network cost for electrical and optical label switched multilayer Photonic IP networks. Using the developed algorithms, the cost-effectiveness of multilayered photonic IP networks has been evaluated. In fact, compared with LSP networks with point-to-point WDM transmission systems, the benefit of multilayer photonic IP networks is obtained even if the average LSP demand between pairs of nodes is less than the OLSP capacity. We have verified that most of the results obtained through the multiple different optimization procedures applying different scenarios and subcases converge to almost the same value. This implies that the heuristics developed here could effectively avoid the local minima, and the validity of the obtained results is very high. Each algorithm is based on heuristics and so the total calculation time required after multiple procedures is not excessively long.

In Chapter 4, we newly propose a network design algorithm that minimizes the network cost considering IP traffic growth for multi-layer photonic IP networks that consist of electrical LSPs and optical LSPs. We have evaluated the network cost obtained from the developed network design algorithm that considers different IP traffic growth patterns and volumes. The obtained results are compared with those obtained from the static zero-based algorithm that we proposed in Chapter 3. It is shown that the presented algorithm is effective; the cost increase from that cost obtained with the static algorithm is marginal. Furthermore, under various conditions (physical network topology, traffic demand, and the traffic increase rate), the proposed algorithm is confirmed to produce excellent results.

In Chapter 5, we have investigated the functional requirements for achieving an evaluation platform based on our proposed concept of a user and network integrated simulation which is able to represent individual user behavior in a realistic situation. We also have implemented a real map loading function, pedestrian mobility, and a user behavior model to meet the requirements. In addition, we have evaluated the simulator that includes the developed functions, and shown that differences in the mobility model and in the communication model definitely influence the simulation results. This means that in evaluations of the performance of mobile networks it is both important and effective to take realistic and detailed user mobility and communication behavior into consideration. To obtain more realistic simulation results, we plan to validate the simulation results using user behaviors through the developed simulator.

In Chapter 6, we have proposed to simulation optimization of a large ITS wireless system by using an abstract model that is designed to reduce the number of pathloss and fading calculations required. It has been confirmed that omission of some pathloss calculations achieved in this way can reduce simulation runtime by up to 8% when message propagation is represented by the 2-ray model and by up to 60% when it is represented by the model defined in ITU-R P.1411. The impact of this omission on simulation accuracy was insignificant. The variation in the average message delivery ratio from that obtained using the conventional method (with no omissions) is only 1% at most. It has also been confirmed that ignoring the effect of fading, i.e., omitting fading calculations, when the received power of a signal is below a threshold can reduce simulation runtime by up to 50% in the case of the 2-ray model, and by up to 10% in the case of the ITU-R P.1411 model. Whether a signal experiences fading at the carrier sense level has a great impact on whether a frame can be received or not. It has been confirmed that it is necessary to set the received sensor threshold to -90 dBm or lower if we are to minimize the effect of the omission of calculations. Furthermore, by combining omissions of both the pathloss and fading calculations, simulation runtime can be reduced by up to 55% in the case of the 2-ray model, and by up to 70% in the case of the ITU-R P.1411 model. As a result, omission of some calculations can reduce the message delivery ratio by up to 10%. By omitting some pathloss calculations and some fading calculations, it is possible to reduce simulation runtime dramatically irrespective of the proportion of pathloss calculations in the entire simulation runtime and irrespective of the particular radio propagation model used. The proposed method can reduce simulation runtime dramatically with a minimal impact on simulation accuracy in the simulation of a wireless system, in particular, the ITS safe driving support system.

In summary, we have proposed multi-layered photonic network design algorithms for a given traffic demand and a growing traffic demand. Also, we have proposed a mobile traffic control scheme and an evaluation and optimization methods. All proposed methods have been verified through simulation experiments with realistic scenarios. The obtained results show that our proposed methods contribute to design and evaluation for network systems and enrich our society through communication systems and services. In future work, we plan to modify our simulation model to represent real world more accurately and extend our simulation optimization method to expand simulation capability.

# Appendix

A network cost model was generated by reflecting node (OXC, IP router, and their interfaces) and link (optical fiber and repeaters) costs on the basis of state-of-the-art technologies. The given parameters, variables, and node/link costs are expressed as follows. A 16-wavelength multiplexing per fiber was assumed, where each wavelength provided 2.5-Gb/s capacity. Based on this assumption, the parameter values for the simulation were provided. Relative cost values used for the simulations are also indicated for given parameters.

## Given parameters:

$C_{NNI}$ : OXC NNI (Network Node Interface) port cost per wavelength

$C_{UNI}$ : OXC UNI (User Network Interface) port cost per wavelength

$C_{OXC}$ : OXC base cost

$C_{POS}$ : LSR interface cost (POS: Packet-Over-SONET/SDH basis)

$C_{LSR}$ : LSR switch cost per  $M$  (see below) Gb/s

$C_J$ : LSR junction cost (10 Gigabit Ethernet basis)

$C_F$ : Optical fiber cost per km

$C_{REP}$ : Repeater cost

$L$ : Repeater span (km)

$M$ : Maximum throughput of IP router (Gb/s)

$B_{LSP}$ : LSP bandwidth (Mb/s)

$B_{OLSP}$ : OLSP bandwidth (Gb/s)

$W$ : Maximum number of wavelengths per fiber

$N$ : Number of nodes in the network

$D_{ij}$ : Distance between node  $i$  and node  $j$ .  $D_{ij} = 0$  for node pair that is not physically adjacent to each other.

**Variables:**

$F_{ij}$ : Number of fibers between node  $i$  and node  $j$ .

$NNI_i$ : Number of NNI ports at node  $i$ .

$UNI_i$ : Number of UNI ports at node  $i$ .

$POS_i$ : Number of POS ports at node  $i$ .

$R_i$ : Number of IP routers at node  $i$  (no linear increase in component routers against handling IP traffic considering a cluster architecture).

**Node cost:** OXC, IP router, and their interfaces

$$\sum_{i=1}^N \left( C_{NNI} \times NNI_i + C_{UNI} \times UNI_i + C_{OXC} \right. \\ \left. + C_{POS} \times POS_i + C_{LSR} \times R_i + C_J \times R_i \times (R_i - 1) \right)$$

**Link cost:** optical fiber and repeaters

$$\sum_{i=1}^N \sum_{j=1}^N \left( C_F \times D_{ij} \times F_{ij} + C_{REP} \times \frac{D_{ij}}{L} \times F_{ij} \right)$$

# Acknowledgement

First of all, I would like to gratefully acknowledge the enthusiastic supervision of Professor Teruo Higashino during this research. I also express my appreciation for his great encouragement, support, and backup through trials and tribulations of this Ph.D thesis.

I am heartily grateful to Professor Toru Hasegawa, Professor Morito Matsuoka, Professor Masayuki Murata and Professor Takashi Watanabe for their invaluable comments and helpful suggestions concerning this thesis.

I am enormously grateful to Associate Professor Hirozumi Yamaguchi for the technical discussions and precious advices provided throughout the research. Also, I thank Associate Professor Takaaki Umedu from Shiga University, Assistant Professor Akihito Hiromori, and Assistant Professor Akira Uchiyama for their encouragement and support.

I would like to express my thanks to Professor Ken-chi Sato from Nagoya University and Professor Tomohiko Uyematsu from Tokyo Institute of Technology for their great encouragement and supports.

I also would like to thank to Naohide Nagatsu from NTT Corporation.

I would like to deeply appreciate Adjunct Associate Professor Mineo Takai for the insight full comments and suggestions. I also would like to thank to Dr. Sae Fujii.

Finally, I would like to thank my family, my friends, members of Higashino laboratory, and my colleagues from NTT DOCOMO Inc., Space-Time Engineering Japan Inc. and Space-Time Engineering, LLC. for their help and understanding.

# Bibliography

1. K. Sato, S. Okamoto, and H. Hadama, "Network performance and integrity enhancement with optical path layer technologies," *IEEE J. Select. Areas Commun.*, vol. 12, no. 1, pp. 159–170, Jan. 1994.
2. M. Murata, "Challenges for the next-generation Internet and the role of IP over photonic networks," *IEICE Trans. Commun.*, vol. 83-B, no. 10, pp. 2153-2165, Oct. 2000.
3. A. Rodriguez-Moral, P. Bonenfant, S. Baroni, and R. Wu, "Optical data networking: Protocols, technologies, and architectures for next generation optical transport networks and optical Internetworks," *J. Lightw. Technol.*, vol. 18, pp. 1855-1870, Dec. 2000.
4. K. Sato, "Recent developments in and challenges of photonic networking Technologies," *IEICE Trans. Commun.*, vol. E90-B, no.3 pp.454-467, 2007.
5. "PPP over SONET/SDH," IETF, RFC2615, 1999.
6. "Multiprotocol label switching architecture," IETF, RFC3031, 2001.
7. M. Koga, A. Watanabe, T. Kawai, K. Sato, and Y. Ohmori, "Large-capacity optical path cross-connect system for WDM photonic transport network," *IEEE J. Select. Areas Commun.*, vol. 16, no. 7, pp. 1260-1269, Sep. 1998.
8. E. Karasan and E. Ayanoglu, "Performance of WDM transport networks," *J. Lightw. Technol.*, vol. 16, no. 7, pp. 1081-1096, Sep. 1998.
9. IETF, RFC 3945, "Generalized multi-protocol label switching (GMPLS) architecture", Oct. 2004.
10. Y. Yamabayashi, M. Koga, and S. Okamoto, "Autonomously controlled multiprotocol wavelength switching network for Internet backbones," *IEICE Trans. Commun.*, vol. 83-B, no. 10, pp. 2210-2215, Oct. 2000.
11. N. Nagatsu, S. Okamoto, and K. Sato, "Optical path cross-connect system scale evaluation using path accommodation design for restricted wavelength multiplexing," *IEEE J. Select. Areas Commun.*, vol. 14, no. 5, pp. 893-902, Jun. 1996.

12. S. Binetti, A. Bragheri, E. Iannone, and F. Bontivoglio, "Mesh and multiring optical networks for long-haul applications," *J. Lightw. Technol.*, vol. 18, no. 12, pp. 1677-1684, Dec. 2000.
13. E. Modiano and A. Narula-Tam, "Survivable routing of logical topologies in WDM networks," in *Proc. INFOCOM 2001*, pp. 348-357, 2001.
14. N. Nagatsu, Y. Hamazumi, and K. Sato, "Optical path accommodation designs applicable to large scale networks," *IEICE Trans. Commun.*, vol. 78-B, no. 4, pp. 597-607, Apr. 1995.
15. H. Zang, J. P. Jue, and B. Mukherjee, "A review of routing and wavelength assignment approaches for wavelength-routed optical WDM networks," *Opt. Netw. Mag.*, vol. 1, no. 1, pp. 47-60, Jan. 2000.
16. K. Zhu and B. Mukherjee, "Traffic grooming in an optical WDM mesh network," *IEEE J. Select. Areas Commun.*, vol. 20, no. 1, pp. 122-133, Jan. 2002.
17. M. Lee, J. Yu, Y. Kim, C. Kang, and J. Park, "Design of hierarchical cross-connect WDM networks employing a two-stage multiplexing scheme of waveband and wavelength," *IEEE J. Select. Areas Commun.*, vol. 20, no. 1, pp. 166-171, Jan. 2002.
18. X. Cao, Y. Xiong, V. Anand, and C. Qiao, "Wavelength band switching in multigranular all-optical networks," in *Proc. OptiComm 2002*, pp. 198-210, Jul. 2002.
19. I. Chlamtac, A. Ganz, and G. Karmi, "An approach to high-bandwidth optical WANs," *IEEE Trans. Commun.*, vol. 40, pp. 1171-1182, Jul. 1992.
20. ITU, ITU-T recommendation G.803: Architecture of transport networks based on the SDH (03/00).
21. K. Sato and S. Okamoto, "Photonic transport technologies to create robust backbone networks," *IEEE Communications Magazine*, vol. 37, no. 8, pp. 78-87, Aug. 1999.
22. N. Nagatsu, "Photonic network design issues and applications to IP backbone," *J. Lightwave Technol.*, vol. 18, no. 12, pp. 2010-2018, Dec. 2000.
23. R. Ramamurthy, Z. Bogdanowicz, S. Samieian, D. Saha, B. Rajagopalan, S. Sengupta, S. Chaudhuri, and K. Bala, "Capacity performance of dynamic

- provisioning in optical networks,” *J. Lightwave Technol.*, vol. 19, no. 1, pp. 40-48, Jan. 2001.
24. M. Kodialam, T. V. Lakshman, “Dynamic routing of locally restorable bandwidth guaranteed tunnels using aggregated link usage information,” in *Proc. INFOCOM 2001*, pp. 376-385, 2001.
  25. S. Kaneda, T. Uyematsu, N. Nagatsu, and K. Sato, “Network dimensioning of electrical/optical label switched multi-layer photonic IP networks,” in *Proc. 7th European Conference on Network & Optical Communications*, pp. 14-21, June 2002.
  26. I. Yagyu, H. Hasegawa, and K. Sato, “An efficient hierarchical optical path network design algorithm based on a traffic demand expression in a cartesian product space,” *IEEE J. Select. Areas Commun.*, vol. 26, no. 6, pp. 22-31, Jan. 2008.
  27. P. Belottia, A. Caponeb, G. Carellob, and F. Malucellib, “Multi-layer MPLS network design: The impact of statistical multiplexing,” *ELSEVIER Computer Networks*, vol. 52, no. 6, pp. 1291-1307, 2008.
  28. H. Le, H. Hasegawa, and K. Sato, “Hierarchical optical path network design algorithm considering waveband add/drop ratio constraint,” *IEEE/OSA Journal of Optical Communications and Networking*, vol. 2, no. 10, pp. 872-882, 2010.
  29. K. Kanie, H. Hasegawa, and K. Sato, “Multi-layered photonic network design considering incremental traffic growth and different service contract terms,” in *Proc. 31st European Conference on Optical Communication 2005 (ECOC 2005)*, vol. 2, pp. 265-268, 2005.
  30. K. Kanie, H. Hasegawa, and K. Sato, “Quasi-dynamic network design considering different service holding/contract terms,” in *Proc. Optical Fiber Communication and the National Fiber Optic Engineers Conference 2007 (OFC/NFOEC 2007)*, pp. 1-3, 2007.
  31. K. Kanie, H. Hasegawa, and K. Sato, “Quasi-dynamic network design considering different service holding times,” *IEEE Journal on Selected Areas in Communications*, vol. 26, no. 3, pp. 47-53, 2008.
  32. Y. Yamada, H. Hasegawa, and K. Sato, “Evaluation of network parameter dependencies of hierarchical optical path network cost considering waveband protection,” in *Proc. IEEE 7th International Conference on Optical Internet 2008 (COIN 2008)*, 2008.

33. R. Sugiyama, T. Takeda, K. Shiimoto, "Performance of network design method considering path holding time under traffic growth," in *Proc. 7th International Conference on Optical Internet 2008 (COIN 2008)*, 2008.
34. Z. Shen, H. Hasegawa, and K. Sato, "Effectiveness of wavelength/waveband conversion and its allowable cost bound for hierarchical optical path networks," *Journal of Optical Communications and Networking*, vol. 5, no. 11, pp. 1262-1274, 2013.
35. M. Li, "Autonomous clustering-based heterogeneous waveband switching in WDM networks," in *Proc. IEEE International Conference on Communications 2006 (ICC 2006)*, vol. 6, pp. 2587-2592, 2006.
36. M. Li and B. Ramamurthy, "Heterogeneous waveband switching in wavelength division multiplexed networks based on autonomous clustering architecture," *Journal of Optical Networking*, vol. 5, no. 9, pp. 667-680, 2006.
37. H. Le, H. Hasegawa, and K. Sato, "Cost evaluation of hybrid-hierarchical optical cross-connects based optical path networks," in *Proc. Third International Conference on Communications and Electronics (ICCE)*, pp. 40-45, 2010.
38. B. Addisa, A. Caponea, G. Carelloa, F. Malucellia, M. Fumagallib, and E. Pedrinellib, "Designing two-layer optical networks with statistical multiplexing," *Fiber and Integrated Optics*, vol. 27, no. 4, pp. 249-255, 2008.
39. K. Sugimura, H. Hasegawa, and K. Sato, "Segmented network design and performance evaluation for large scale transparent OXC-based networks," in *Proc. SPIE 6012, Optical Transmission Systems and Equipment for WDM Networking IV*, 2005.
40. H. Le, H. Hasegawa, and K. Sato, "Hybrid-hierarchical optical path network design algorithms utilizing ILP optimization," *Optical Switching and Networking*, vol. 8, no. 4, pp. 226-234, 2011.
41. Z. Shen, H. Hasegawa, and K. Sato, "An efficient heuristic waveband assignment algorithm for hierarchical optical path networks utilizing wavelength converters," *Optical Switching and Networking*, vol. 10, no. 1, pp. 54-61, 2013.
42. F.R. Durand, Campo M. Abbade, F. Rudge, and E. Moschim, "Cost analysis in optical burst switching networks with optical label processing," *IEEE*

(Revista IEEE America Latina) Latin America Transactions, vol. 9 , no. 7, pp. 991-997, 2011.

43. K. Sato, and H. Hasegawa, "Optical networking technologies that will create future bandwidth-abundant networks," *IEEE/OSA Journal of Optical Communications and Networking*, vol. 1, no. 2, pp. 81-93, July 2009.
44. J. Guo, J. Wang, H. Li, and Y. J., "A new asymmetric spectrum assignment method to improve spectrum efficiency for spectrum-sliced optical network" *ELSEVIER Optical Fiber Technology*, vol. 19, no. 6, pp. 565-573, Dec. 2013.
45. S. Ferdousia, A. Naga, A. Reza, M. Tornatore, and B. Mukherjee, "Mixed-line-rate optical network design with wavebanding," *ELSEVIER Optical Switching and Networking*, vol. 9, no. 4, pp. 286-296, Nov. 2012.
46. T. Ogawa, H. Hasegawa, and K. Sato "Optical fast circuit switching networks employing dynamic waveband tunnel," *IEICE Trans. Commun.*, vol. E95-B, no.10, pp. 3139-3148, Oct. 2012.
47. K. Leung, W. Massey, and W. Whitte, "Traffic models for wireless communication networks," *IEEE J. Selected Areas in Comm.*, vol.12, no.8, pp. 1353-1364, Oct. 1994.
48. S. Choi, and K. Cho, "Traffic control schemes and performance analysis of multimedia service in cellular systems," *IEEE Trans. Vehicular Technology*, vol.52, no.6, pp. 1594-1602, Nov. 2003.
49. K. Tachikawa, "W-CDMA Mobile communication system," WILLY and MARUZEN, 2002.
50. Y. Hiehata, H. Koto, and H. Nakamura, "A proposal of a communication-broadcasting integrated system to support communication and navigation during disasters," in *Proc. 2010 Fifth International Conference on Internet Monitoring and Protection (ICIMP)*, pp. 110-116, 2010.
51. G. Motoyoshi, Y. Sudo, T. Murase, and T. Masuzawa, "Advantages of optimal longcut route for wireless mobile users," in *Proc. 2011 IEEE International Conference on Communications (ICC)*, pp. 1-6, 2011.
52. M. Yoshino, K. Sato, R. Shinkuma, and T. Takahashi, "Incentive-rewarding mechanism for user-position control in mobile services," *IEICE Transactions on Communications*, vol. E91-B, no. 10, pp. 3132-3140, 2008.

53. M. Yoshino, R. Shinkuma, and T. Takahashi, "Efficient radio-resource utilization by user position control with incentive rewards," in *Proc. 14th Asia-Pacific Conference on Communications 2008 (APCC 2008)*, pp. 1-5, 2008.
54. M. Yoshino, R. Shinkuma, and T. Takahashi, "Incentive-rewarding mechanism for radio resource control based on users' contributions," in *Proc. IEEE Global Telecommunications Conference 2008 (GLOBECOM 2008)*, pp. 1-5, 2008.
55. S. Kaneda, Y. Akinaga, N. Shinagawa, and A. Miura, "Traffic control by influencing users' behavior in mobile networks," in *Proc. 19th International Teletraffic Congress (ITC19)*, 6a, pp. 583-592, 2005.
56. S. Kaneda, Y. Akinaga, N. Shinagawa, A. Miura, and M. Takai, "Integrated user and network simulation for traffic control by influencing user behavior," in *Proc. second ACM International Workshop on Performance Evaluation of Wireless Ad Hoc, Sensor, and Ubiquitous Networks (PE-WASUN'05)*, pp. 99-105, 2005.
57. K. Maeda, K. Sato, K. Konishi, A. Yamasaki, A. Uchiyama, H. Yamaguchi, K. Yasumoto, and T. Higashino, "Getting urban pedestrian flow from simple observation: realistic mobility generation in wireless network simulation," In *Proc. 8th ACM/IEEE International Symposium on Modeling, Analysis and Simulation of Wireless and Mobile Systems (MSWiM2005)*, pp. 151-158, 2005.
58. J. Yoon, M. Liu, and B. Noble, "Random waypoint considered harmful," In *Proc. IEEE INFOCOM 2003*, vol. 2, pp. 1312-1321, 2003.
59. T. Camp, J. Boleng, and V. Davies, "A survey of mobility models for ad hoc network research," *Wireless Communication & Mobile Computing (WCMC): Special issue on Mobile Ad Hoc Networking: Research, Trends and Applications*, vol. 2, no. 5, pp. 483-502, 2002.
60. A. Rojas, P. Branch, and G. Armitage, "Experimental validation of the random waypoint mobility model through a real world mobility trace for large geographical areas," In *Proc. 8th ACM/IEEE International Symposium on Modeling, Analysis and Simulation of Wireless and Mobile Systems (MSWiM2005)*, pp. 174-177, 2005.
61. ns-2 the network simulator. URL <http://www.isi.edu/nsnam/ns/>.
62. Opnet technologies. URL <http://www.opnet.com/>.

63. QualNet from Scalable Network Technologies. URL <http://scalable-networks.com/>.
64. Y. Akinaga, S. Kaneda, N. Shinagawa, and A. Miura, "A proposal for a mobile communication traffic forecasting method using time-series analysis for multi-variate data," In *Proc. IEEE Global Telecommunications Conference 2005 (GLOBECOM 2005)*, vol. 2, pp. 1119-1124, 2005.
65. T. Heikkinen, "On the quality of service and pricing in a multiservice network," in *Proc. IEEE ICME 2000*, vol.3, pp. 1623-1626, Aug. 2000.
66. E. Viterbo, and C. Chiasserini, "Dynamic pricing for connection-oriented services in wireless networks," in *Proc. IEEE PIMRC 2001*, vol.1, pp. 68-72, Sept. 2001.
67. J. Hou, J. Yang, and S. Papavassiliou, "Integration of pricing with call admission control to meet QoS requirements in cellular networks," *IEEE Trans. Parallel and Distributed Systems*, vol.13, no.9, pp. 898-910, Sept. 2002.
68. D. Kotz, C. Newport, R. Gray, J. Liu, Y. Yuan, and C. Elliott, "Experimental evaluation of wireless simulation assumptions," in *Proc. 7th ACM international symposium on modeling, analysis and simulation of wireless and mobile systems (MSWiM2004)*, pp. 78-82, 2004.
69. G. Halkes, and K. Langendoen, "Experimental evaluation of simulation abstractions for wireless sensor network MAC protocols," *EURASIP Journal on Wireless Communications and Networking - Special issue on simulators and experimental testbeds design and development for wireless networks*, vol. 2010, no. 24, 2010.
70. E. Hamida, G. Chelius, and J. Gorce, "Impact of the physical layer modeling on the accuracy and scalability of wireless network simulation," *SIMULATION* 2009, vol. 85, no. 9, pp. 574-588, 2009.
71. M. Takai, J. Martin, and R. Bagrodia, "Effects of wireless physical layer modeling in mobile ad hoc networks," in *Proc. 2nd ACM international symposium on mobile ad hoc networking & computing (MobiHoc2001)*, pp. 87-94, 2001.
72. SAE J2735, "Dedicated Short Range Communications (DSRC) Message Set Dictionary," Nov. 2009.

73. J. Heidemann, N. Bulusu, J. Elson, C. Intanagonwiwat, K. Lan, Y. Xu, W. Ye, D. Estrin, and R. Govindan, "Effects of detail in wireless network simulation," in *Proc. SCS Multiconference on Distributed Simulation*, pp. 3-11, 2001.
74. E. Weingartner, H. Lehn, and K. Wehrle, "A performance comparison of recent network simulators," in *Proc. IEEE International Conference on Communications (ICC 2009)*, pp. 1-5, 2009.
75. M. Khan, B. Askwith, F. Bouhafs, and M. Asim, "Limitations of simulation tools for large-scale wireless sensor networks," in *Proc. 2011 IEEE Workshops of International Conference on Advanced Information Networking and Applications*, pp. 820-825, 2011.
76. M. Korkalainen, M. Sallinen, N. Kärkkäinen, and P. Tukeyva, "Survey of wireless sensor networks simulation tools for demanding applications," in *Proc. Fifth International Conference on Networking and Services (ICNS2009)*, pp. 102-106, 2009.
77. F. Roijers, H. Berg, and M. Mandjes, "Fluid-flow modeling of a relay node in an IEEE 802.11 wireless ad-hoc network," *Lecture Notes in Computer Science*, vol. 4516, pp. 321, 2007.
78. E. Egea-Lopez, J. Vales-Alonso, A. Martinez-Sala, P. avon-Marino, and J. Garcia-Haro, "Simulation scalability issues in wireless sensor networks," *IEEE Communications Magazine*, vol. 44, no. 7, pp. 64, 2006.
79. J. Liu, D. Nicol, L. Perrone, and M. Liljenstam, "Towards high performance modeling of the 802.11 wireless protocol", in *Proc. Winter Simulation Conference 2001*, pp. 1315-1320, 2001.
80. G. Monghal, I. Kov'acs, A. Pokhariyal, K. Pedersen, C. Rosa, and P. Mogensen, "Fast fading implementation optimization in an OFDMA system simulator," in *Proc. IEEE 65th Vehicular Technology Conference 2007 (VTC2007-Spring)*, pp. 1214-1218, April, 2007.
81. J. Ikuno, M. Wrulich, and M. Rupp, "System level simulation of LTE networks," in *Proc. IEEE 71st Vehicular Technology Conference 2010 (VTC 2010-Spring)*, pp. 1-5, May, 2010.
82. M. Takai, R. Bagrodia, A. Lee, and M. Gerla, "Impact of channel models on simulation of large scale wireless networks," in *Proc. 2nd ACM international workshop on modeling, analysis and simulation of wireless and mobile systems*, pp. 7-14, Aug. 1999.

83. S. Weber, V. Cahill, S. Clarke, and M. Haahr, "Wireless ad hoc network for Dublin: A large-scale ad hoc network test-bed," *ERCIM News*, vol. 54, 2003.
84. Z. Ji, J. Zhou, M. Takai, and R. Bagrodia, "Improving scalability of wireless network simulation with bounded inaccuracies," *ACM Transactions on Modeling and Computer Simulation*, vol. 16, no.4, pp. 329-356, Oct. 2006.
85. Scenargie, <http://www.spacetime-eng.com/>
86. T. Rappaport, "Wireless Communications, Principles, and Practice," 2002.
87. RECOMMENDATION ITU-R P.1411-6, "Propagation data and prediction methods for the planning of short-range outdoor radio communication systems and radio local area networks in the frequency range 300 MHz to 100 GHz," 2012.
88. S. Kaneda, T. Maeno, M. Takai, H. Yamaguchi, and T. Higashino, "Implementation of flat fading model for ITS communication system simulations," *IPJSJ DICOMO2011*, July, 2011. (in Japanese)